Understanding Adherent Cell Mechanics & The Influence of Substrate Rigidity

Ian Manifacier

Director: Professor Imad About

Co-director: Dr. Jean-Louis Milan

École Doctorale Sciences du Mouvement Humain

Aix-Marseille Université

Host Laboratory: Institut des Sciences du Mouvement Etienne-Jules Marey

UMR 7287 – AMU / CNRS

TABLE OF CONTENTS

PREFACE

Dear Reader,

I am pleased to share with you what I have learned during my doctoral studies about the mechanical behavior of adherent cells. I am an engineer by training, most definitely not a biologist. At the beginning of this research project, the realm of biology was thus a foreign domain to me. It is a source of wonder and fascination.

Human adherent cells use mechanical principles in ways that outstripped my personal expectations. In addition, this journey allowed me to formulate new hypotheses and therefore new goals. Interestingly, it also pushed me to formulate them differently. Whereas before, I was aiming for precision in formulating complicated models, I finally realized that such formulations brought fuzzier and less certain results that did not allow me to make significant conclusions. Therefore, as my knowledge in the domain started to grow, my strategy gradually began to shift toward the inclusion of simpler, yet fundamentally sounder models.

In the following introductory pages you will have an overview of the field of mechanobiology from my perspective, both based on my engineering background and the type of scientific questions that drove me. I take the time to say this, because, it is evident that a biologist would have structured his work differently and it may thus seem an awkward way to present biological phenomena. The parts that follow the introduction will be dedicated to answering the main problematic of this thesis, which is:

"Can we create a relevant mechanical model of adherent cells? And, what can we learn about the influence of substrate rigidity on the mechanical behavior of adherent cells?"

Knowing that this subject is at the interface of mechanics and biology, I have attempted to keep this manuscript assessable to members of both disciplines. Some parts may thus seem somewhat redundant, but that is to allow new concepts to take root in the minds of others.

I hope that this manuscript will bring a different, yet relevant perspective of the mechanical aspects of cellular adhesion.

GENERAL INTRODUCTION

1. General perspective: Why did we stick to cell adhesion?

Current medicine treats patients with the tools that are available today; the goal of research is to find new ways and new tools to better treat patients tomorrow and in the long run. Here we adopted a long run strategy that may be so far from its final goal that the objectives may be hard to understand without an introduction. Tissue engineering is a nascent field aimed at regenerating tissue, from hard bone to soft arterial epithelium, so that damaged organs or missing limbs may either be 3D printed or regrown. Yet this quests has been a challenging one, that will require years of additional research, first to understand how tissues and organs function and develop and then to recreate these tissues for patients. While the objective may be to obtain a macroscopic organ or limb, in reality everything happens at the microscopic or even nanoscopic level, as these processes involves the realm of living cells, protein interaction and gene activation. Therefore to either print a new organ or to attempt to regrow it requires adherent cells, as well as understanding how they will behave, especially when they first to adhere and spread within forming tissues to become an integrated part of it. While, these processes involve biochemical interactions, they equally require cells to move within, adhere to, pull on and remodel their environment. In other words adherent cells interact mechanically with their surroundings. This manuscript will consequently focus on understanding the mechanical concepts involved in the early phases of cell adhesion and spreading, which are directly related to the field of mechanobiology.

2. How to address the mechanobiological concepts behind cell adhesion?

Definition :

Mechanobiology *is the scientific field at the interface of biology and mechanical engineering. Its purpose is to understand how physical forces and changes contribute to development, physiology, and disease within cells and tissues.*

Cells are complex biochemical systems. In addition, human cells are also dynamic mechanical systems that interact mechanically with their surroundings. Moreover, cells are able to self-assemble their cytoskeletons, a filamentous and contractile mechanical structure that generates traction forces, provides structural integrity and enables cells to anchor themselves to their surroundings[1,2,3,4]. We can thus conclude that understanding how cells function not only requires an understanding of biochemistry, but of mechanics as well[5,6]. An often ignored fact is that cells

are also sensitive to mechanical stimuli[7]. In other words they can feel the mechanical properties of their surroundings among other mechanical cues[8,6]. For instance, mechanical substrate rigidity has been observed to influence events such as the way cells generate mechanical forces, the way they move and migrate[9]. Based on this knowledge, we can thus already expect a tight relationship between the way a cell generates forces and the way mechanical stimuli influence the cell (Figure 1). Mechanical stimuli, however, have an even more profound impact on cells due to the fact that they influence biochemical responses and gene activation[10,11]. Extracellular mechanical stimuli can consequently influence stem cell differentiation, as has factually been proven to be the case[7,12]. In the case of adherent cells, meaning cells that need to adhere to a substrate to function properly, experiments have shown that mechanical stimuli can even be a vital parameter for the cell that can dictate its survival or its death.

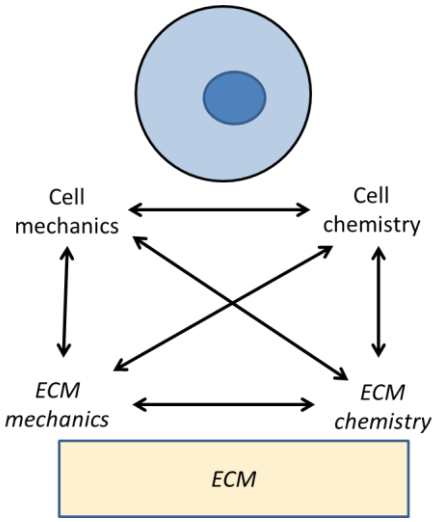

Figure 1: The cell is sensible to the mechanical properties of the extracellular matrix (ECM) and its chemical make-up. Interestingly, the cell can also change the mechanical and chemical properties of the ECM.

It is thus evident that mechanical forces can be transduced into a biological phenomenon and vis-versa. This transduction phenomenon has given rise to the term that we call mechanotransduction.

Definition :

Mechanotransduction *is the phenomenon by which mechanical forces can be transduced into a biological phenomenon and vice-versa.*

One of the main objectives of the field of mechanobiology is therefore to understand:

How are mechanical and biological events intertwined to form a coherent and well organized cellular system?

While answering this question is of the highest importance, understanding its full context is paramount. We will therefore take some time to ponder and ask ourselves three apparently

simple questions. I believe that these questions are worth asking, because they may bring forth valuable reasons to explore this subject with a new perspective.

2.1. Two basic questions to ask ourselves before we start:

- Why is mechanobiology an important phenomenon to study?
- How will this study influence our scientific views other than by directly answering a technical question?

2.1.1. Why is mechanobiology an important phenomenon to study?

Understanding mechanobiology is a quest for knowledge about how cells assemble and function. It is also about how they interact with their environment, both chemically and mechanically. It includes how their environment can influence them and how they can influence their environment in return. Understanding these basic concepts, may be a way to understand how cells migrate, replicate, and differentiate in respect to their environment, not only from a biochemical perspective, but from a mechanical perspective as well[9,7]. The understanding of such concepts would be invaluable to understand tissue formation and regeneration, as well as degeneration, such as aging and cancer. Cancer and mechanobiology are too often tied together, since mechanical cues and cytoskeletal properties are too often determinant factors to tumor growth, cancerous cell migration, and metastasis[13,14].

2.1.2. How can the study of mechanobiology influence our scientific views other than by directly answering a technical question?

Biomechanics is often considered as scientific field derived from Newtonian mechanics, which is meant to study the mechanical behavior, e.g., how physical forces interact within a living system and material properties of living systems based on theories generally used on nonliving systems.

On the contrary, mechanobiology is a scientific field that is supposed to derive from biology to explain how mechanical forces are transduced into biological phenomena.

We can then assume that both scientific fields are subtly different, in the sense that they are trying to approach similar problems from different, if not opposite, perspectives (Figure 2). Therefore, understanding cell mechanics will require conciliating mechanical models of the cell and the cellular structure as biologically described. Moreover, the structural backbone of the cell, the cytoskeleton, is a self-assembling structure. This is due to molecules interacting and regulating each other. The cytoskeleton of human adherent cells is capable of generating forces; it enables a cell to pull on its surroundings, spread, and move. In addition, it is not only capable of generating forces, for it can sense mechanical stimuli as well. For example, adherent cells are not only sensitive to mechanical cues, to regulate protein synthesis, cell division, migration or differentiation, but their very survival depends on it[7,11,15,16,17]. This type of dynamic structure is therefore complex and elusive; we may therefore wonder how they function, which will require understanding how mechanics and biology interact to form a coherent system (Figure 2).

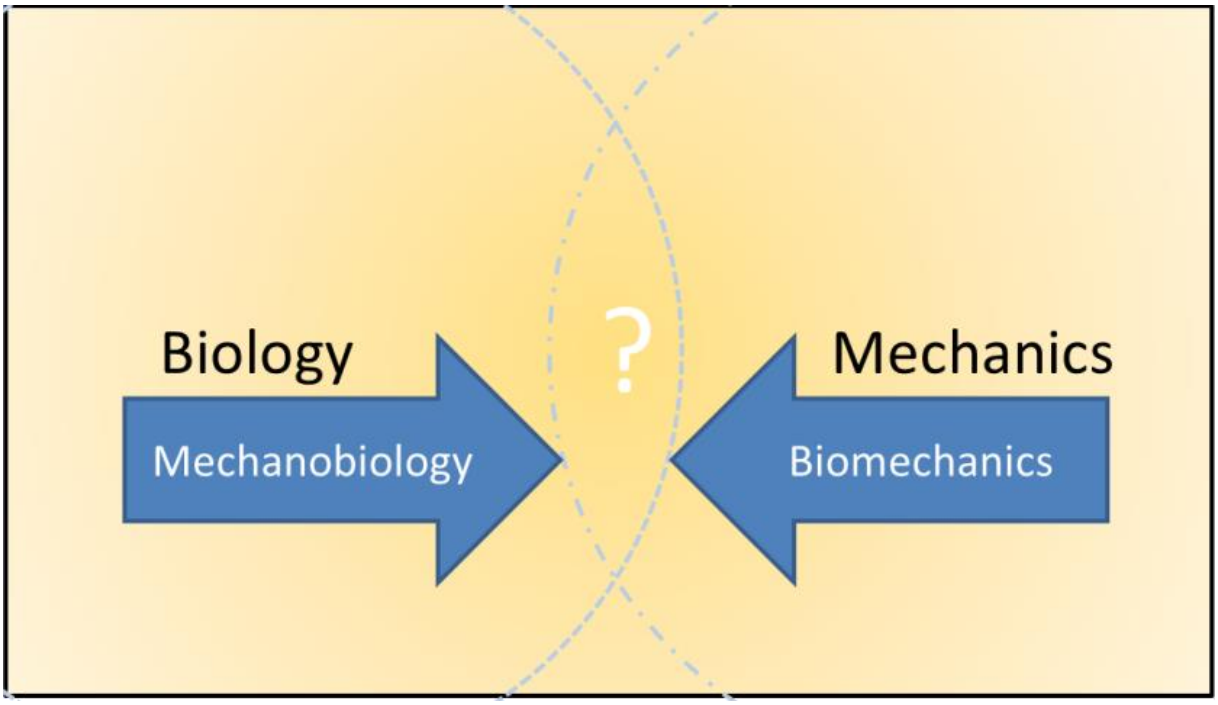

Figure 2: Mechanobiology and biomechanics are two sister fields with different approaches to problem solving.

2.2. The spreading process of human adherent cells and the mechanobiological phenomena resulting thereof will be the core focus of this thesis.

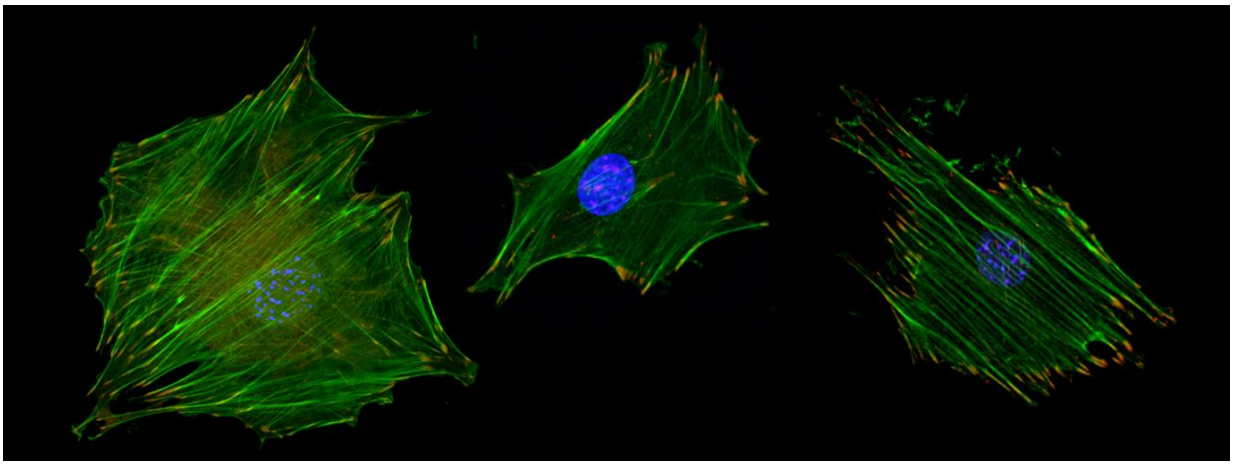

Figure 3: Photomontage showing the internal structure of three adherent cells between 50 to 130 μm in size. Actin (green), vinculin (red), nucleus (blue). (Source images: courtesy of Tatiana Bourgade)

One of the great challenges of the coming decades will be the development of new methods to heal and regenerate various types of tissues, such as arterial epithelium, so that patients with missing limbs or failing organs may have a chance for a normal life. Among other things, it will require us to understand how cells interact mechanically with their environment. Investigating how these interactions take place will hopefully allow us to formulate radically new strategies to take on tissue engineering.

More specifically, this will require us to understand how adherent cells (Figure 3) which compose living tissues can be influenced by the mechanical properties of their surroundings and vice-versa. The term 'adherent cell' does not denote any single cell type; instead it refers to a common property shared between several cell types. But, unlike motile cells that spend most of their time moving about within the human body, adherent cells have a general tendency to remain in one location as an integrated part of the tissue they constitute. Interestingly, some cell types are mostly bound to a non-cellular collagen based matrix called the extracellular matrix (ECM), while the others form cell to cell adhesions. Fibroblasts, for instance, favor ECM adhesions that form during the adhesion and spreading process as each cell becomes an integrated part of its tissue. Epithelial cells favor cell to cell junctions, thus creating epithelial tissues. But similar to fibroblasts, they can also generate ECM[18] adhesions. Understanding the adhesion and spreading process is therefore the main focus of this manuscript.

3. Bibliographic overview of the cellular structure

3.1. Notable facts about cell adhesion

When an adherent animal or human cell is not adhering it has a spherical morphology. This phenomenon, can for example happen during cell culture as cells are detached from one flask and plated into another, as this requires cells to be forcefully removed from their substrate. This process is called a cell passage. It is generally done by using trypsin, an enzyme that will chemically sever cell adhesions to the substrate. Doing so is a traumatic event that dissolves significant parts of the cytoskeleton which that is mediated by cell adhesions.

However, as surprising, as this may be, the cell is able to survive, reattach itself to a new substrate and respreads by regenerating its cytoskeleton (Figure 4). Interestingly, as it does so cell behavior can be influenced by the mechanical properties of the substrate[7,11,,16,19,20].

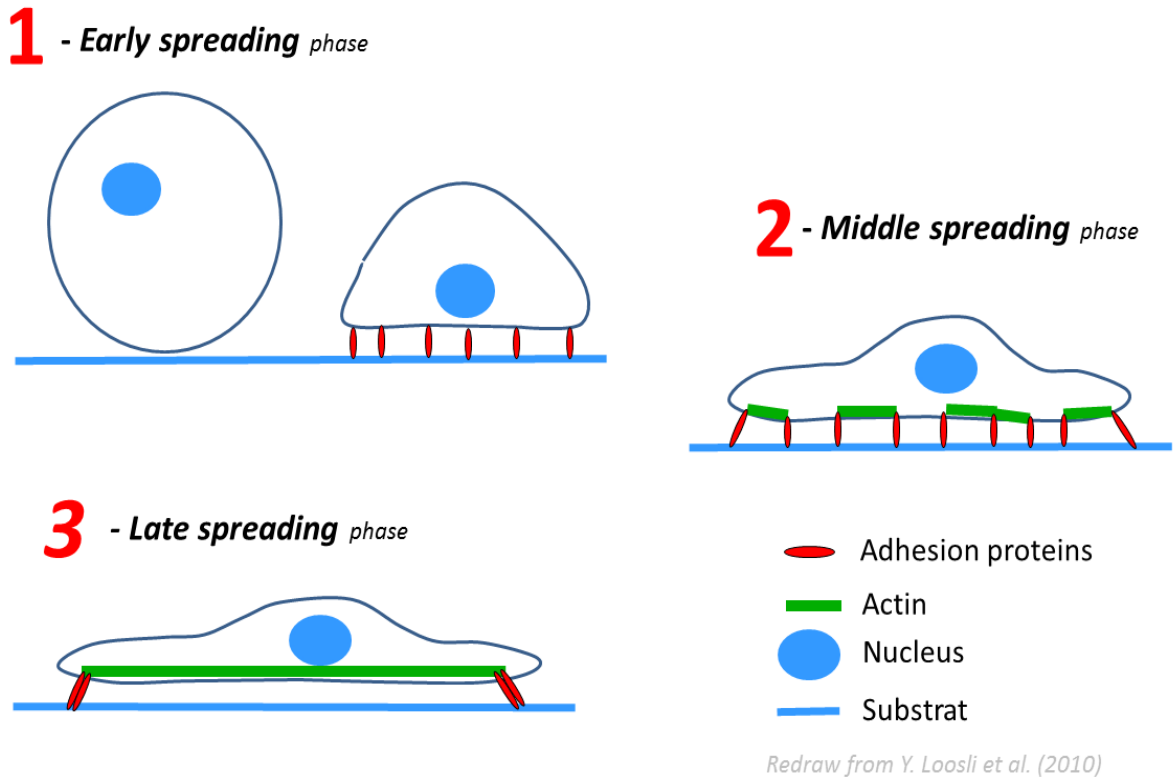

Figure 4 : A cartooned representation of the cell adhesion process in three stages. The cell is delimited by its outer cell membrane and the nucleus is contained within. (Redraw from Loosli et al. 2010)[21]

Stage 1) the cell becomes and remains round when it is mechanically unbound to its surrounding. As it makes contact with the substrate it forms primitive adhesions (red) and gradually flatten on the substrate, i.e., spreads.

Stage 2) the cell then forming contractile actomyosin connections (green) between its primitive adhesions.

Stage 3) once the adherent cell is fully spread, it is firmly anchored via its now mature focal adhesions (red) mechanically connected via tensile actomyosin rich stress fibers (green).

3.2. A quick introduction on how human adherent cells work.

The aim of this quick view of the cell is to present a few key concepts on how the cell works without being too exhaustive. We will use a fibroblast as an example.

The cytoskeleton is in constant interaction with the molecules contained in the cytoplasm. These molecules direct its assembly, disassembly, and the mechanical forces it generates. Most of these molecules are proteins. We can therefore ask: What makes proteins so special?

3.2.1. Proteins

Proteins are composed of amino acids that were assembled together by ribosomes which use RNA molecules as blueprints, themselves defined by segments of DNA, generally referred to as genes. Protein presence and concentrations are tightly regulated by interaction between DNA, RNA and proteins[11,22]. Protein regulation therefore largely controls the type of protein that can be present in the cell and at which time, as well as its concentration. Protein-RNA-DNA regulation is thus one of the major factors defining the cell behavior.

But what makes proteins special, is that they each have defined functions. They are advanced biomolecules with specific shapes and chemical properties. Their shape allows them to be structured systems, with often more than one reaction site. Changing their shape due to a chemical reaction or a mechanical force, may reveal, hide, enable, or disable a reaction site thus changing its chemical properties. A simpler way to see it, can be to consider that proteins are active or inactive, switched on or off. A common on/off switch mechanism is called phosphorylation, where one phosphate group is added to a protein. A few other types of post-translational modifications are acetylation, methylation, and proteolytic cleavage, each of which has potential to modulate the protein's action.

3.2.2. Biomolecular interactions form a coherent living system

Alone, a protein is not able to do much other than bind or chemically interact with other proteins and molecules. Within the well-regulated biochemical baths of the cell, however, proteins interact with each other and other types of molecules in a well ordered and regulated manner. The whole set of these ordered reactions between biomolecules form an interaction network called an interactome. The interactome, combined with other structuring parameters, allows the different components enclosed in the cell membrane to represent a well-defined and properly functioning system called a cell.

To create a functioning system, proteins interact with other biomolecules to act as logic gates that are able to switch chemical pathways on and off. These pathways can, for instance, activate a relevant gene, leading to RNA transcription and translation, and thus protein synthesis. If there were no proteins of the same type as the newly synthesized proteins within the chemical bath, it means that new proteins may form new interactions with the already present biomolecules. New chemical interactions imply an alteration of the chemical bath as a system.

The cellular, nuclear, and organelle membranes are the physical boundaries between the different chemical baths of the cell. They also regulate the interaction between these different domains. The cell can thus be viewed as a cluster of distinct chemical baths that can interact with one another to form a coherent system.

We will now consider the involvement of the cytoskeleton and its different functions, such as, it acting as a mechanical structure and how it interacts with the biochemical soup that surrounds it.

3.3. A bibliography sourced description of the cytoskeleton and adherent cell mechanics

The objective of this section will be to have a general understanding of the way the cell is structured based on an analysis of the bibliography. We will therefore review many sub-components of the cell that are deemed relevant to the cellular structure. We will also try to understand how all these different types of sub-components can interoperate to form a coherent mechanical system.

3.3.1. The cytoskeleton is a dynamic filamentous structure bathed in a biochemical solution

The cytoskeleton is primarily composed of filamentous network embedded in the cytoplasmic solution. The cytoskeleton acts as dynamic mechanical structure which enables the cell to control its shape and migrate. It is mostly composed of three filamentous components: actin, microtubules, and intermediate filaments. These filamentous components are bound together by different types of cross-link proteins such as alpha-actin, ACF7, and plectin, which respectively bind actin microfilaments together, microtubules to actin, and microtubules to intermediate filaments. Yet the dynamic of assembly is regulated by a large collection of accessory proteins as well, that will either promote assembly, contractility, and disassembly or prevent such phenomena from occurring[17,3]. Furthermore, cytoskeletal components have a dual role as structural components and chemical regulators[2,23]. At this point, it thus becomes very clear that mechanics and biochemistry are highly intertwined with each other to form a self-orchestrated ballet of molecules in constant interactions with each other.

3.3.2. The spreading process of adherent cells: a sequenced process

Cell spreading is the process by which a cell adheres to the ECM or substrate. It is thus named because cells flatten and spread when cultured on flat substrates. This process involves both cell adhesion and cytoskeletal formation i.e., self-organization. It should be noted that cells do not really spread when they are allowed to adhere in a three dimensional environment. Nonetheless, they still generate a cytoskeleton.

Cell spreading is a sequenced cellular process during which the cell will change shape and thus undergo several cytoskeletal transformations. It is important to note that the sequenced nature of the spreading process is regulated both at a local and global level. Therefore, at a given moment, the cytoskeleton may be at different stages of formation depending on the location within the cell.

The spreading process generally occurs after cell division and migration, or when the cell first makes contact with the substrate.

At first, before it makes contact with the substrate, the cell is completely round. Then integrin proteins imbedded in the cell membrane bind to the extracellular matrix (ECM) as it makes contact with it. The integrin proteins that are both latched on to the ECM and the cell membrane

then undergo a conformational change[24]. This conformational change enables a chain of events to occur.

- Lamellipodium formation
- Filopodium formation
- Lamellipodium advancement
- Focal adhesion and arc stress fiber formation
- Arc stress fiber retrograde flow and dorsal stress fiber formation
- Arc stress fiber maturation into-ventral stress fibers

3.3.3. The cell membrane

The plasma membrane is a 6-10 nm thick lipid bilayer that separates the cell from its environment (Figure 5). Interestingly, while membrane molecules have cohesive properties that prevent separation, they can nonetheless rearrange themselves relative to one another.[25] The cell membrane consequently does not transmit a significant amount of mechanical stress[6] instead superficial mechanical stresses are supported by the actin cortex (Figure 5).

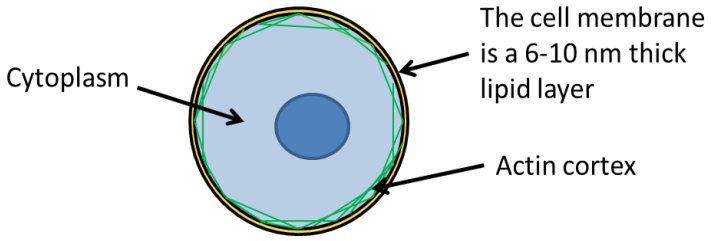

Figure 5: Cell - The cell membrane (black and yellow) defines the outer edge of the cell, it contains the cytoplasmic liquid. The actin cortex (green) is a meshed contractile network that is mechanically linked to the cell membrane. As the actin cortex contracts, it reduces the area of the cell membrane, consequently reducing the internal volume and creating internal pressure.

3.3.4. Integrin

The cell adheres to its environment (extracellular matrix, other cells, implants, culture flasks, slide) via adhesion proteins, which are often classified in two categories:

- calcium dependent
- calcium independent.

The calcium independent adhesion proteins include: IgSF, CAMs and lymphocyte homing receptors; calcium independent adhesion proteins are: integrins, cadherins, selectins.

Integrins are the most significant adhesion proteins that mechanically link the extracellular matrix and an intracellular protein called talin[4]. An integrin protein therefore has to traverse the cell membrane to protrude on both ends so as to bind to the cell's environment and to the cytoskeleton located inside the cell. Integrin molecules are therefore able to shield the cell membrane from mechanical stresses.

To create a new integrin adhesion, the integrin protein first binds itself to the cell's environment (ECM, substratum), at this point no mechanical stress is needed[26]. Once the integrin molecule is bound to the outside of the cell, it then undergoes a conformational change that will affect the behavior of its intracellular end.

At this point it is only a primitive form of adhesion, but it will activate Rac and Cdc42 proteins. Rac proteins lead to the formation of a lamellipodium and Cdc42 to the formation of filopodia (also called microspikes).

In addition, the conformational change of the integrin molecule also enables it to bind with free floating talin molecules. This consequently allows the talin molecule to form a weak mechanical bond with an actin microfilament that can later be reinforced by vinculin.

At this point we obtain successive bonding between the substrate, integrin, talin, and a microfilament belonging to the actin network; thus forming a weak mechanical bridge between the substrate and the cytoskeleton.

3.3.5. Actin Filament polymerization

Free floating globular actin monomers, G-actin, are the fundamental building blocks of an actin filament (Figure 6). Actin monomers polymerize to form long actin filaments. This process is regulated by several proteins: cofilin (severs), gCAP39 (caps positive end), severin (severs), capZ (caps positive end), tropomodulin (caps negative end). The proteins regulate actin filament assembly and disassembly by capping the growing end and the dissolving end respectively.

Profilin and capping protein prohibit uncontrolled assembly of actin in cells. Pure actin monomers combine to form a trimer, which can elongate rapidly from both its 'barbed' (+) and 'pointed' (-) ends. Capping protein bound to filaments prevents growth from the barbed end, while profilin bound to actin monomers inhibits both spontaneous nucleation and growth from the pointed end.

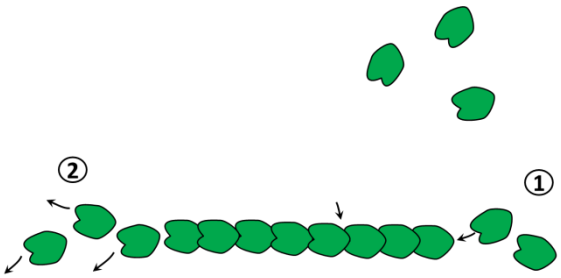

Figure 6: Cartoon illustration of actin filament assembly and disassembly[27].

3.3.6. Lamellipodium

The lamellipodium is a very dynamic structure composed actin filaments that branch outward to push the cell membrane as they grow (Figure 7). Several things set the lamellipodium apart from other types of actin networks.

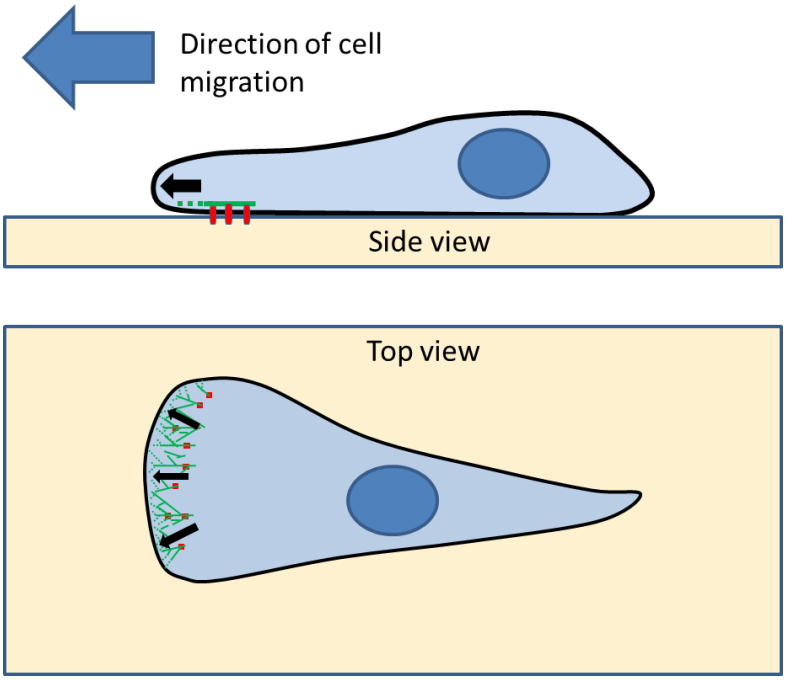

Figure 7: Lamellipodium pushes the cell membrane forward as it assembles[28,27].

For instance, the lamellipodium is a sub-actin network formed of dendritic actin filaments. These dendritic actin microfilaments are formed as the Arp2/3 protein complex[1] binds to microfilaments, allowing the nucleation of a new filament (Figure 8).

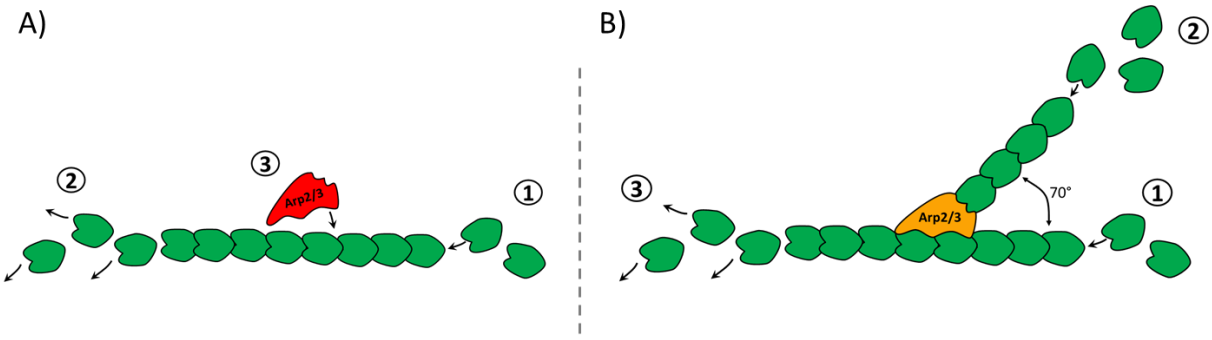

Figure 8: Arp2/3:

A) An Arp2/3 complex latches on an actin filament as it is assembling (1) on one end and disassembling (2) on the other[27].

[1] A protein complex (or multi protein complex) is a functional group of proteins that binds together. The Arp2/3 is composed the following proteins: p16, p21, p20, p34, p40, Arp2, Arp3.

B) Once the Arp2/3 complex is attached to the actin filament, it is able to nucleate a new actin filament that will also continue to assemble.

Therefore, microfilaments branch out laterally from one another at a 70 degree angle to form a dense network formed along the cell edge[28,27]. In addition, the lamellipodia network assembles in pulses at the leading edge and disassembles a couple micrometers behind. A portion of these micro-filaments are aimed towards the cell edge. Therefore, when a globular actin monomer polymerizes onto a filament, it shortens the gap between its filament and the cell edge. If there is no gap between the filament's growing end and the cell membrane, then the globular actin protein squeezes itself between the two. Some studies suggest that it is due to a Brownian ratchet, meaning that the actin monomer squeezes in, as Brownian movement separates the actin filament and the cell membrane[27]. Since the filament is more rigid then the cell wall, the cell membrane is thus pushed outward, i.e., towards the front. The lamellipodium is therefore very different from other sub-types of actin filament networks as it uses actin polymerization as its only motor, instead of using a separate protein motor such as myosin.

Interestingly during mesenchymal spreading and migration the lamellipodium both generates and uses filipodia to keep advancing.

3.3.7. Filopodium

Filipodia are spiky, actin rich linear sub-structures that protrude from the lamellipodia, i.e., the leading edge of the cell (Figure 9). Furthermore, they are short lived, dynamic structures that keep growing on one end as they dissolve on the other. Fillipodium elongation is regulated by the binding of a capping protein at their growing end, consequently preventing further growth. Active capping protein concentration can thus be viewed as a probabilistic determination factor of filopodia elongation. Interestingly, while the transient elongation process was faster than disassembly, the latter slower process continues, gradually dissolving from behind all actin filaments contained within the filipodium[29]. This ADF driven disassembly process, will ultimately lead to the dissolution of the filopodia[29].

Meanwhile, as each fillipodium protrudes out of the cell, it probes the surrounding environment, before being reabsorbed within the lamellipodia due to the disassembly process. Interestingly, based on the contact made by the tip of the filipodium, probing may favor filopodium advancement. In some ways filopodium formation may consequently be viewed as a sub-process of lamellipodium formation.

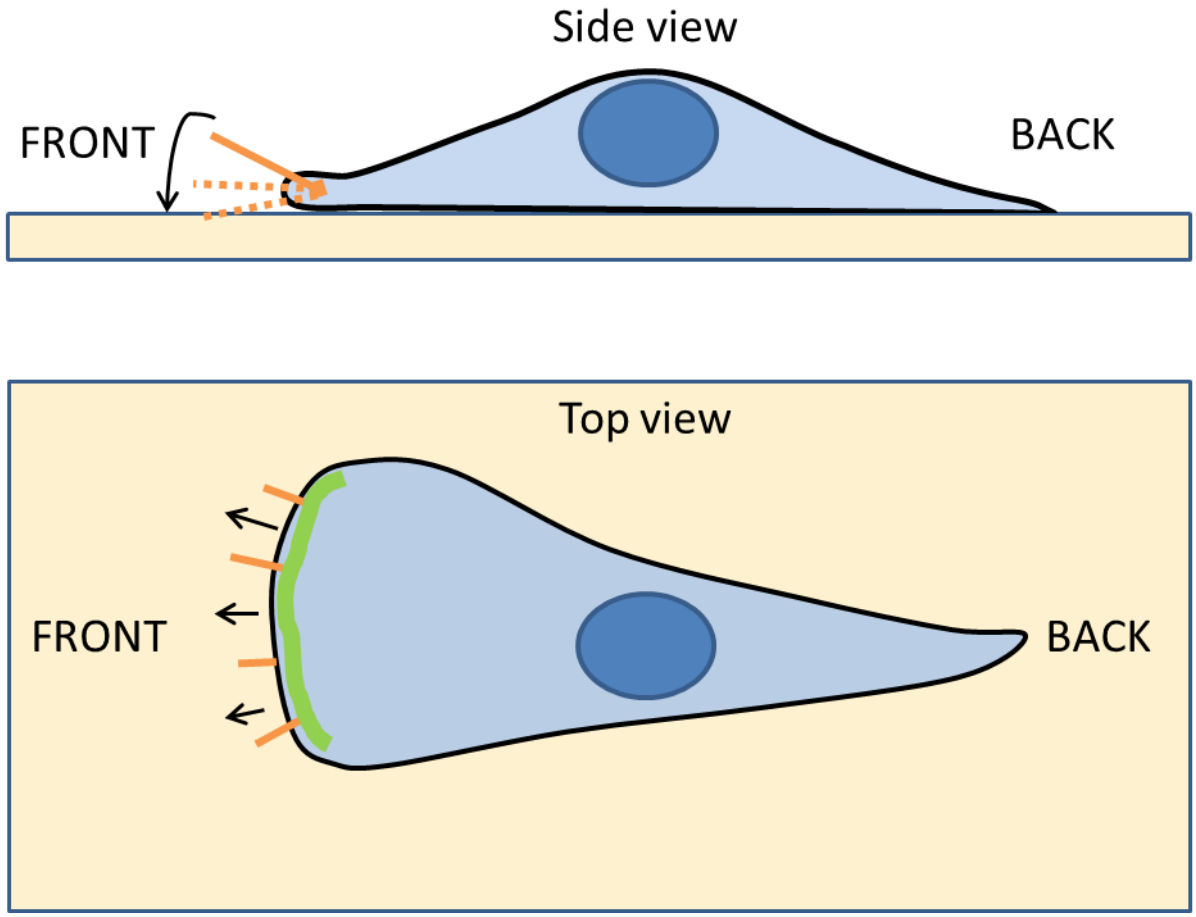

Figure 9: Fillipodia, also called microspikes are initiated within the lamellipodium and protrude from the cell membrane. They are used to probe the surface of the substrate in front of the cell, consequently influencing lamellipodium advancement.[29]

3.3.8. Lamellum

While the lamella and the lamellipodium have names that sound much the same, and are both composed of actin microfilaments, it should be clear to the reader that they are different from one another. The first obvious reason to make a distinction between the two, is that the lamellipodium is able to push the cell membrane, while the lamella have a contractile nature. Furthermore they do not have the same functions, nor are they similarly structured[17]. As we mentioned previously, the microfilaments within the lamellipodium are arranged in a dendritic fashion that is used by the cell to push its membrane outward. On the other hand, the lamella forms a contractile and tensile sub-actin network composed of microfilaments and myosin motor proteins[17].

Some studies[17,30,31] suggest that the lamella is composed of a network of contractile transverse arcs (page 25), although it still remains unclear[32,33]. Both arc stress fibers and the lamella are composed of thin Actomyosin filaments and undergo retrograde flow[30,34]. Furthermore, tropomyosin proteins are highly present in the lamella and in transverse arcs[35], while being almost inexistent in the lamellipodia[36]. Furthermore, arcs and the lamellum filaments are both formed via actin filaments nucleation within lamellipodia, form into arc-shaped Actomyosin filaments and run parallel to the leading edge[34,35,37].

Interestingly, the lamella has been observed to partially assemble and disassemble during retrograde flow. This dynamic assembly process is randomly distributed within the lamella network[30]. But overall, the lamella disassembles during retrograde flow[30]. Moreover, lamella and Arp2/3 have been found to be co-localized, suggesting a potential link between the two. However, Arp2/3's presence does not seem sufficient to generate lamella formation.[30]

3.3.9. Focal adhesions

While we have previously mentioned isolated integrin adhesions, we haven't really mentioned how several of these small adhesions can be grouped to form a much larger clusters called a focal adhesion domains[16,15,20]. Focal adhesions are at the center stage of many processes such as large force transmission between the substrate and the actin network[16,15]. In other terms, it is the cell's strong anchor point on to the substrate (Figure 10, page 22). In addition, it also contributes in accessing substrate rigidity and regulating actin network contractility[38,39]. Many of these processes involve different types of proteins, some of which take part in signaling transduction and others act primarily as structural components, or do both, such as alpha-actin[19].

Balaban et al. found a correlation between focal adhesion force and focal adhesion size[16]. Many other papers confirmed these findings and indicated that cell type was an influencing factor[15,20]. Later, Tan et al. noted that Balaban's relation does not apply to sub-micrometer squared focal adhesions[15]. Interestingly some of these small focal adhesions can withstand important adhesion forces sometimes larger then large focal adhesions may be supporting.

At the junction between focal adhesions and actin filaments, talin acts as a mechanosensing protein between integrin and actin. Alone, a talin-actin bond may slip repeatedly, and is not capable of resisting tension forces greater than ~2pN, such as can be generated by actin retrograde flow. The talin-actin bond, however, may be strengthened by the presence of several

vinculin proteins, so that the strengthened talin-actin bond may resist up to ~20pN.[38] Such tension may stretch talin by up to 350 nm[4,40].

As mentioned above, talin is capable of docking 11 vinculin protein heads in its rod domain[41], such docking sites are called Vinculin Binding Sites (VBSs). The Vinculin Binding Sites of the talin rod domain are only accessible when the tail domain is being stretched. Each vinculin protein resists to about 2.5 pN. [18]

3.3.10. The filamentous nature of the cytoskeleton

The cytoskeleton is the cell's structural backbone. It is composed of several types of filaments bathing in the cell's cytoplasmic solution. These different types of filaments are in continuous chemical interaction with the solution it is bathed in. These chemical interactions regulate assembly and disassembly of the different components that make up this filamentous network, thus controlling its structural nature. Interaction between the filaments and motor proteins can generate relative movement between filament and thus mechanical forces. The cytoplasmic solution is thus also known to influence the forces generated within and thus via the filamentous network.

This filamentous network is composed of several types of filaments (Figure 10) which fall in three main categories.

- The actin filament network
- Microtubules
- Intermediate filaments

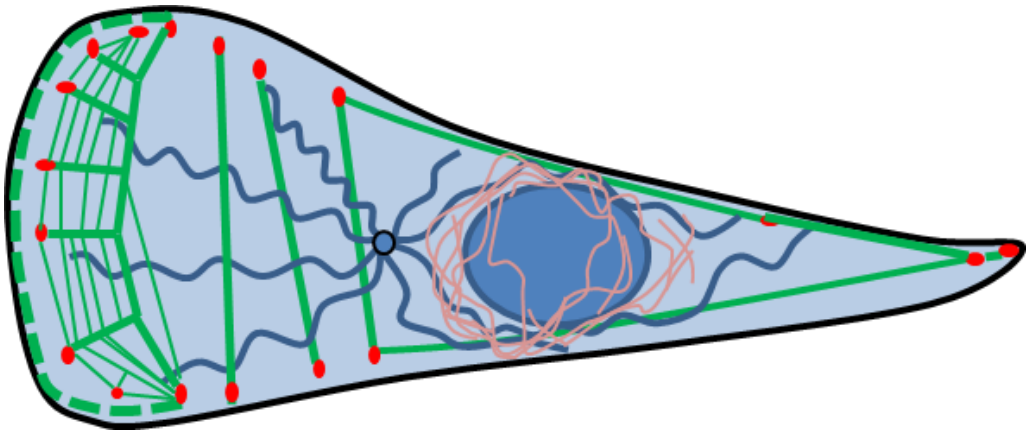

Figure 10: Cartooned illustration representing a cell with its filamentous cytoskeleton. Focal adhesions are in red, the actin network is in green, microtubules in blue and intermediate filaments in pink[2,17,42].

3.3.11. The microfilaments within the actin network

Actin filaments are considered as the predominant structural element of the cytoskeleton. Some experimental studies estimate that the actin network may be responsible for up to 90% of the cell's rigidity[43,44]. The actin network has a predominantly contractile nature[27], even if it isn't always so (page 17).

Actin filaments are composed of globular-actin monomers added one after the other in a head to tail fashion to form microfilaments[27]. Actin accessory proteins such as Arp2/3, alpha-actinin, actin cap, troponin… control the emergence of several different types of actin network motifs, each with a specific mechanical property and function[27].

Myosin motor protein and actomyosin contractility

Actin microfilaments are not contractile by themselves, but the association of actin and myosin motors allows for actomyosin fibers to be contractile. Actomyosin represents a functional group of actin microfilaments and myosin motors proteins. Myosin II proteins can generate relative movement between two actin filaments by hydrolyzing ATP molecules, as described in Figure 11.

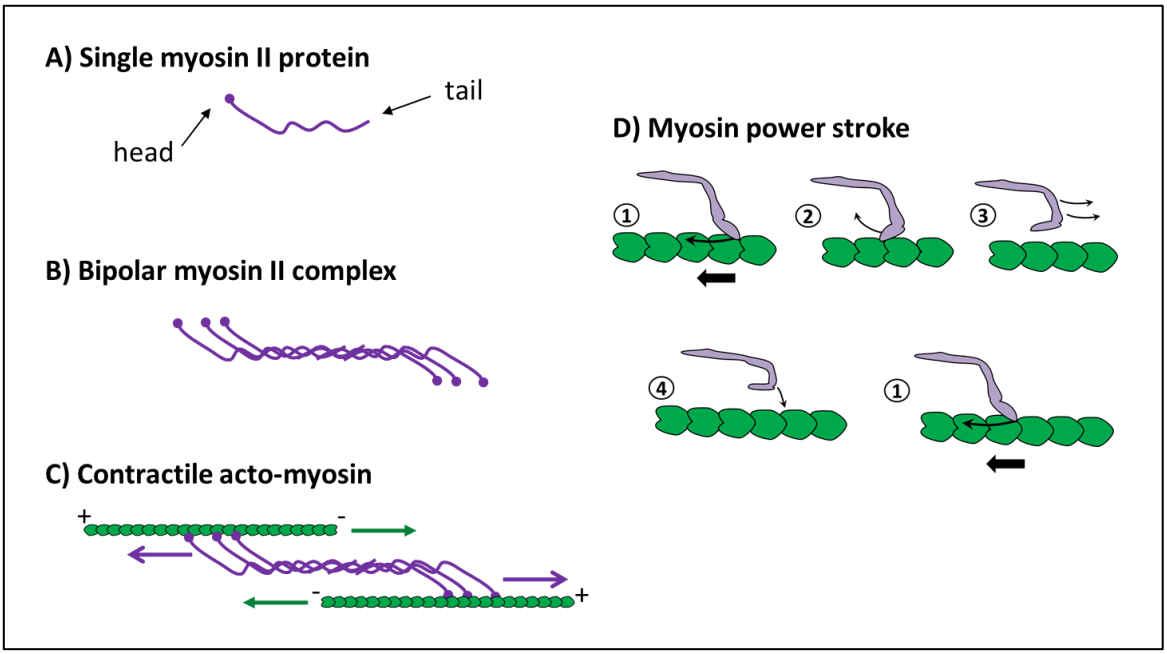

Figure 11: Myosin motor protein[45].

A) A myosin protein (purple) has a head and tail domain.

B) A bipolar myosin complex is composed of several myosin proteins connected by their tail domains.

C) The two polar actin filaments (green) are placed in an anti-parallel fashion. In addition, each end of the bipolar complex is connected to a different actin filament. Each myosin head is able to "walk" towards the positive end of the actin filament (green) it is connected to. A walking step is called a myosin power stroke.

D) Cartooned illustration of a myosin power stroke. (1) Myosin hydrolyzes ATP into ADP, consequently inducing a conformational change of the myosin protein, the myosin head is thrust backward, therefore pulling the actin filament it was latching on. (2-3-4). The myosin head releases the filament and reverts back to its initial shape, to only reattach itself further on.

3.3.12. Actin Cortex

In animal cells the plasma membrane is a highly flexible lipid bilayer that acts as a chemical boundary between the inside of the cell and its environment, while structural rigidity, comes from the actin cortex[46]. This contractile actin cortex is a structural layer composed of actin filaments, myosin II, and actin-binding proteins. It is located against the inner wall of the cell membrane and provides mechanical stiffness to the cell's edge (Figure 12A). It thickness generally varies between 50 nm to 2 μm[1,47].

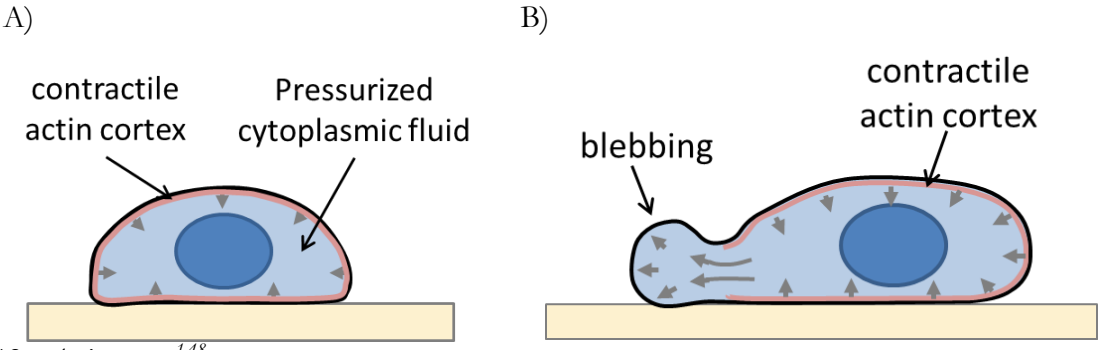

Figure 12 : Actin cortex[1,48]

A) the actin cortex pressurizes the cytoplasm

B) cell blebbing

As the actin cortex contracts, it pulls the cell membrane towards the middle of the cell consequently compressing the cytoplasmic fluid. However, since as a fluid, the cytoplasm is uncompressible and subsequently maintains its volume, it allows for a mechanical equilibrium to be reached. The cytoplasm therefore remains pressurized and press-stressed. In the case where the actin cortex is not sufficiently uniform, at the weakest point, the cytoplasmic pressure is able to push the highly flexible cell membrane out and it consequently forms a protrusion called a bleb (Figure 12B). Cell blebbing can consequently be in involved in cell shape and movement[48]. To conclude, the actin cortex is involved in cell morphogenesis and movement[1].

3.3.13. Actin Stress Fibers

When actin filaments are bundled up together in a more or less parallel fashion, myosin motors can be located in between them. Myosin motors generate relative motion between neighboring microfilaments that are bundled in parallel. These actin filaments are both polar, they consequently organize with myosin motors in such a way that the relative motion induced by the latter makes them move in opposite directions (Figure 11). This is what allows the actin filament bundle to shorten like and thus makes the cellular structure contractile (Figure 13). These contractile actin bundles are consequently referred to as actin stress fibers (Figure 13 & Figure 14). Alpha-actinin keeps actin microfilaments fibers together allowing several microfilaments to form a stress-fiber.

Arc Stress Fibers

Arc stress fibers assemble at, and parallel to, the leading edge of the cell (see Figure 13A)[17]. Since the leading edge is inwardly concave, the forming "arc stress fibers" are consequently arched when they form, thus their name. Furthermore arc stress fibers are contractile and gradually retract (Figure 13 B, C). As they do, they gradually become straighter between attachments (Figure 13 B, C). Yet arc stress fibers are not directly attached to focal adhesions, instead they are connected to dorsal stress fibers[17].

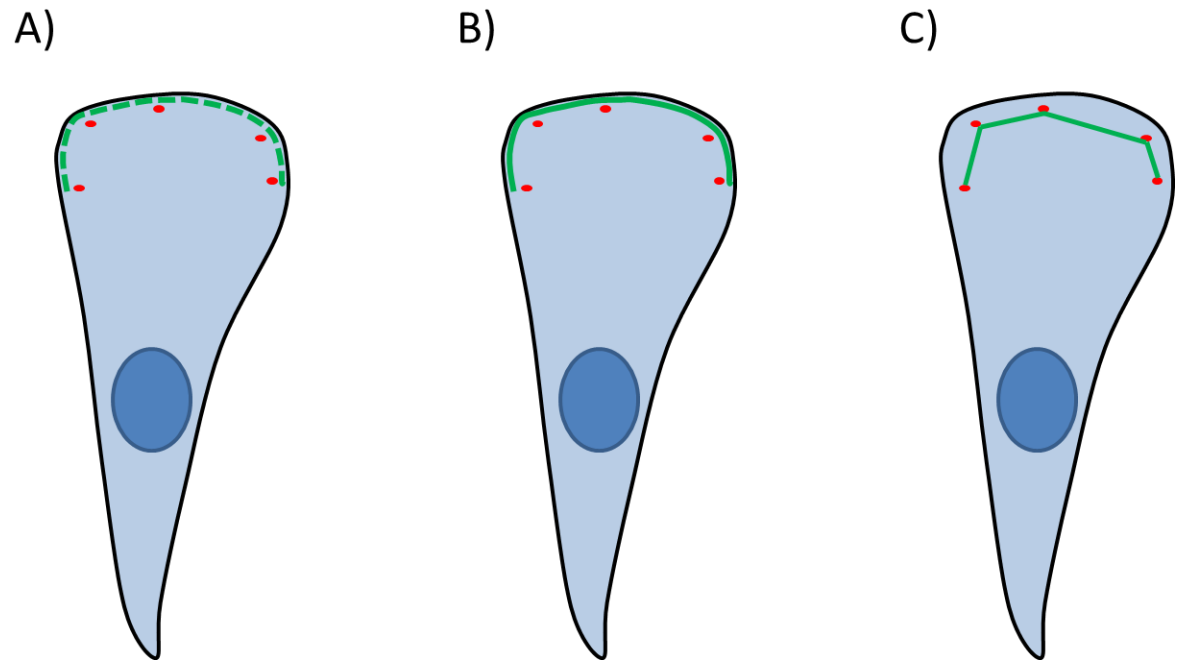

Figure 13: Arc stress fiber formation[17].

A) Arc stress fiber assembly at leading edge (green).

B) The assembled stress fiber is ready to start contracting.

C) Arc stress fiber contraction leads to a reduction of arc diameter, the stress consequently becomes "caught" by nearby focal adhesions (red). From this point on the arc stress fiber remains linked to focal adhesions via dorsal stress fibers (not shown here, seen next figure)

Dorsal Stress Fibers

Dorsal stress fibers are connected to focal adhesion and arc stress fibers(Figure 14A)[17]. As arc stress fibers retract, they pull on the passive, myosin deprived, dorsal stress they are connected to (Figure 14A-C). This pulling force therefore generates tension on focal adhesions and is consequently part of the reason why cells pull on their surroundings[17].

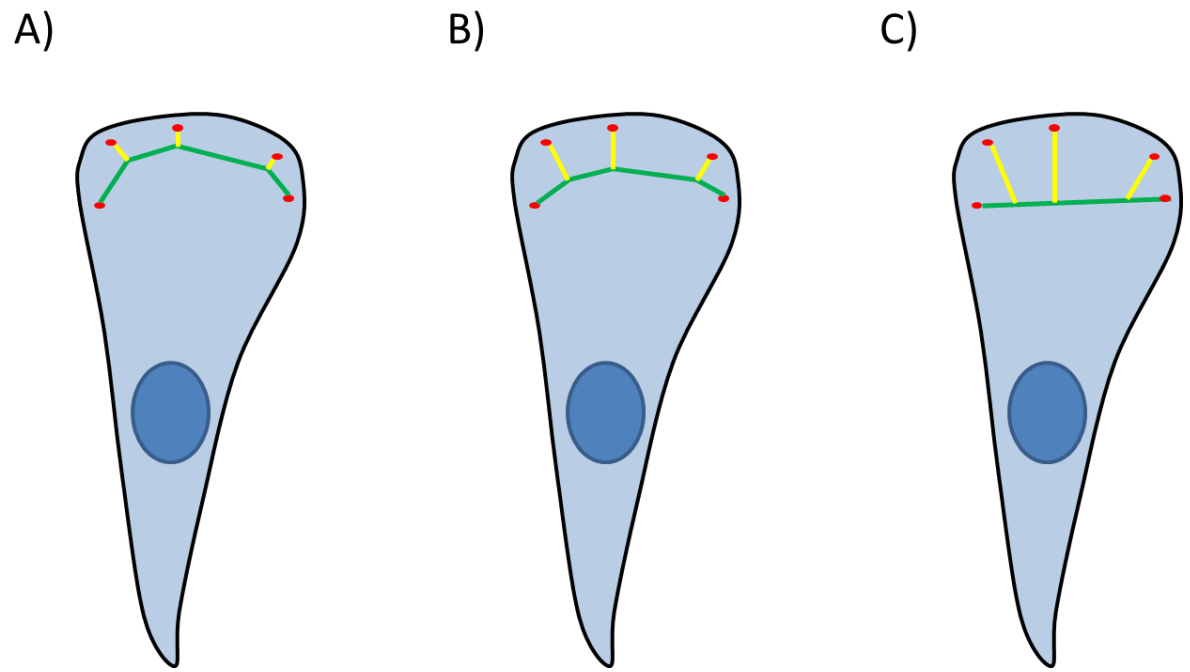

Figure 14: Dorsal stress fiber involvement in arc to ventral stress fiber transition[17].

A) As the arc stress fiber (green) contract, it attempts to get shorter, therefore straighter, consequently pulling on dorsal stress fibers (yellow) which are simultaneously being assembled (elongated) at focal adhesions (red)

B) The arc stress fiber keeps getting shorter due to actomyosin contraction, directly pulling on its simultaneously elongating dorsal stress fibers. The dorsal stress fibers are themselves that are connected to focal adhesions, consequently transmitting the tension force.

C) Once the arc stress fiber is straight, it cannot keep pulling on dorsal stress fibers anymore. The corresponding dorsal stress fibers are consequently assumed to slacken and dissolve. At this stage, the arc stress fiber is then referred to as a ventral stress fiber.

Dorsal stress fiber and focal adhesion interaction is governed by the following process. Dorsal stress fibers first form weak connections with focal adhesions via talin molecules. Yet as the dorsal stress fiber is being pulled on by its arc counterpart (Figure 14A, B), it consequently pulls on the talin molecule. At first the connection is too weak, so the dorsal stress fiber slips like a rope being held by the talin molecule. But as it is doing so, the remaining tension force gradually pulls on the corresponding talin protein, deforms it slightly and reveals one of its vinculin binding sites, as explained earlier[4,49,50]. Independently activated vinculin proteins are then able to bind to the talin molecule and the dorsal actin filament. This vinculin double binding consequently

reinforces the mechanical linkage between the dorsal stress fiber and the focal adhesion. While this talin and vinculin mechanism may seem simple, it is also in interaction with a multitude of other focal adhesion regulated pathways.

Ventral Stress Fibers

As arc stress fibers contract and become straighter and straighter, they finally converge to a more stable form (Figure 14A-C) and they finally end up only connected by their two extremities(Figure 15A)[17]. At this point, the arc stress fiber is referred to as a ventral stress fiber; because, as it is connected between two focal adhesions located on the cell's ventral side, the stress fiber takes the straightest and shortest way along the ventral (bottom) side of the cell.

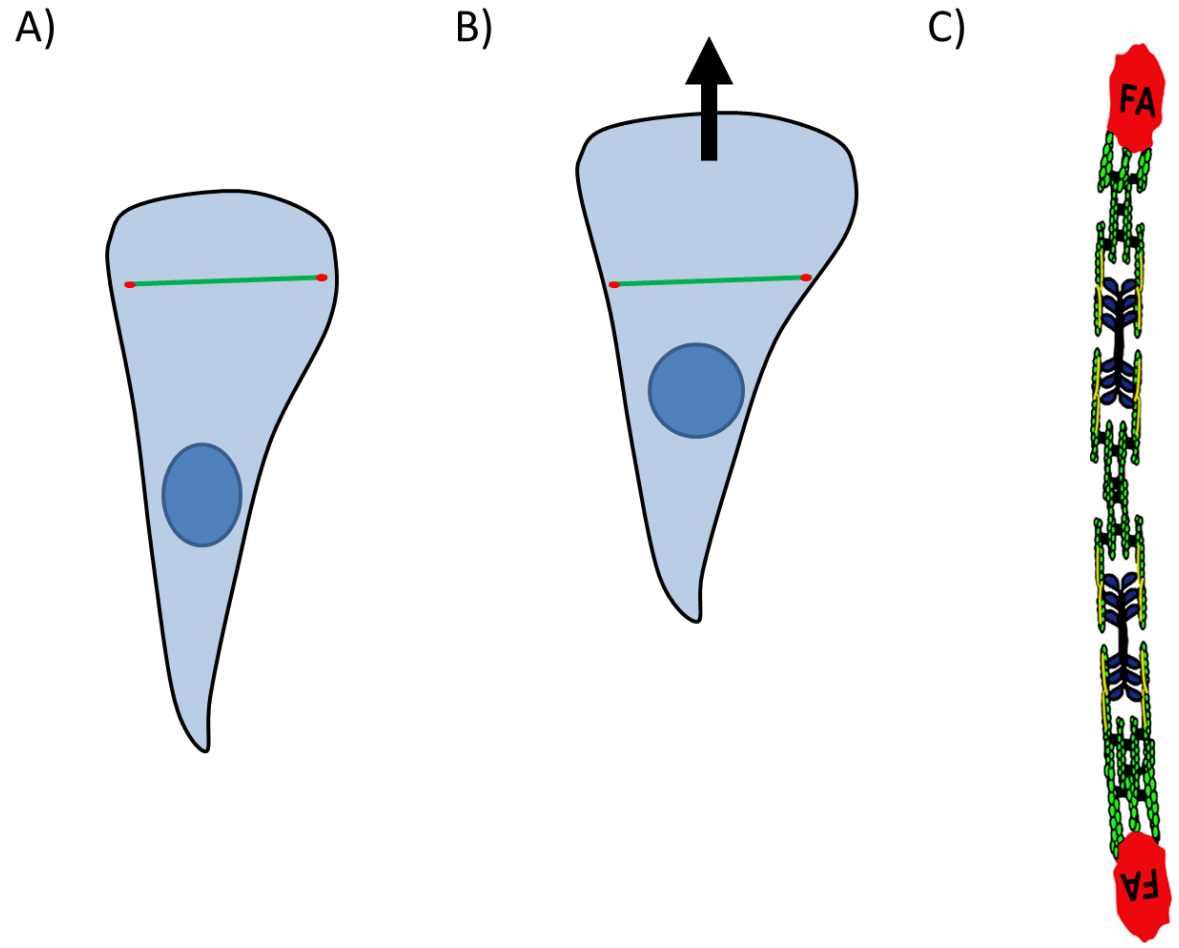

Figure 15: Ventral stress fibers[17].

A) The ventral stress fiber (green) is bound to focal adhesions at both ends.

B) The ventral stress fiber remains immobile, while the rest of cell moves forward.

C) Illustration of a stress ventral fiber: actin in green, myosin in dark blue and focal adhesions in red, tropomyosin in yellow (the exact spatial arrangement within a stress fiber structure is still unknown).

The ventral stress fiber then remains immobile, bound to the substrate by its focal adhesions, while the leading edge moves forward and the rest of the cell moves with it.

If a ventral stress fiber happens to be going over the nucleus it is often referred to as an actin cap[17].

Analogy:
The way ventral and arc stress fiber behave may be compared to a self-tightening belt.

3.3.14. Microtubules

Microtubules are long hollow tubular structures, that much like actin filaments, dynamically assemble and disassemble in the cytoplasm[51]. Similarly to actin microfilament, microtubules are polar, with a positive and negative end. This polar property implies that the two ends do not have the same chemical properties, consequently allowing free floating microtubules to be subject to tread milling, meaning that one end depolymerizes as the other end is being assembled[51]. But in adherent cells, microtubules mostly originate from the Microtubule Organizing Center (MTOC), i.e., centrosome (Figure 16). As one end of the microtubule is incased in the MTOCK and thus protected from disassembly, microtubule growth and disassembly happens at the peripheral end of the microtubule by a phenomenon known as dynamic instability[3]. By this process microtubules are able to rapidly grow and dissolve, respectively towards and from the cell edge.

Furthermore, it has been well established that microtubules grow toward focal adhesion sites to control their reinforcement or disassembly (Figure 16)[23,42]. Microtubule dynamics influences actin stress fiber contraction and focal adhesion dynamics[52]. Microtubule disassembly promotes actin stress fiber and focal adhesion assembly[52].

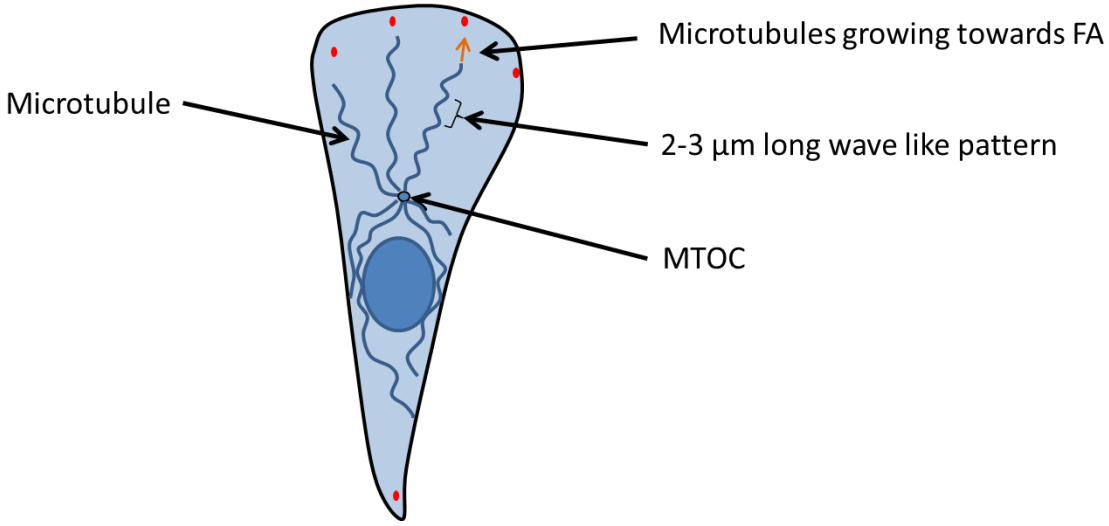

Figure 16: In adherent cells, microtubules grow from the centrosome, expand outward toward the edges and around the nucleus. Due to compression, microtubules buckle in wave like patterns. Furthermore microtubules have been shown to target focal adhesions.[42]

Interestingly microtubules often appear to have a wavy shape within the cytoplasm (Figure 16). This wavy pattern has been shown to be consistent with the mechanical behavior of a rod buckling in an elastic gel[53] (Figure 17 Right), also referred to as classical Euler buckling (Figure 17 Left)[54]. This can easily be understood in a macro scale environment, with an identical rod buckling under compression force in a water tank and another identical rod buckling inside an elastic gel (Figure 17). The typical observed buckling wave length is around 3 µm. Some studies

suggest that this wavelength may be used to measure the compression load transiting via a microtubule. The hollow tubular structure of microtubules and their width of 25 nm provides them with a higher second moment of area than actin or intermediate filaments. This feature make microtubules less prone to buckling as they bear compression forces within cells[55].

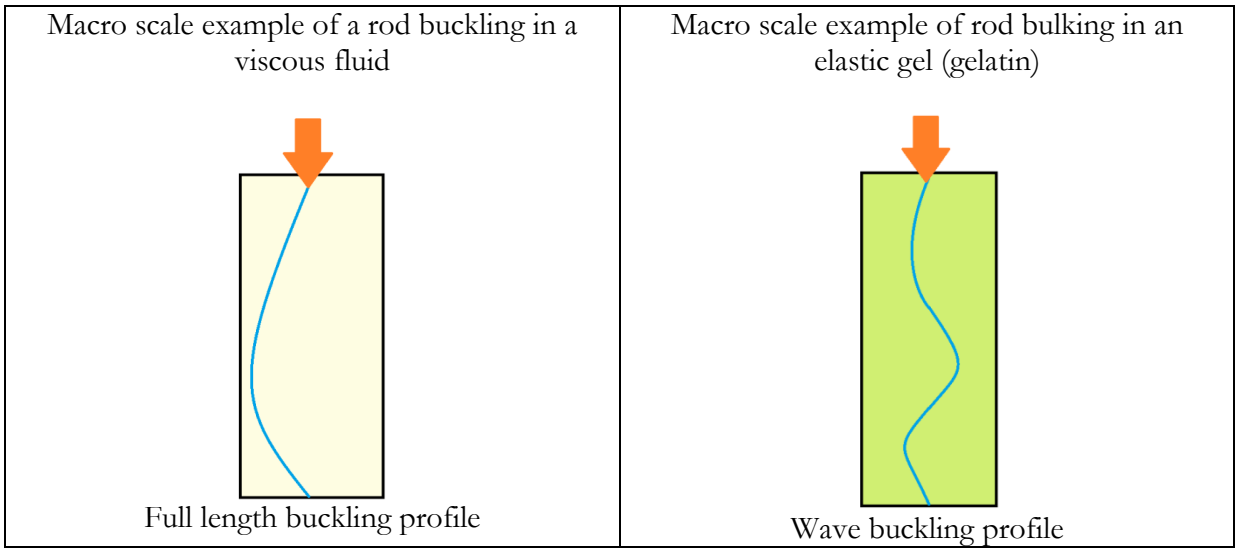

Figure 17: Illustration of buckling. Left) buckling in a viscous fluid creates a single bent shape. Right) buckling in a elastic gel creates a wavy pattern. Microtubules are believed to behave in this way due to the mechanical properties of the cytoplasm.

3.3.15. Intermediate Filaments

The name intermediate filament is due to their thickness which is between that of an individual actin filament and a microtubule. In reality, the intermediate filament family is composed of various types of filaments, among which are vimentin filaments. Intermediate filaments interact with other constituents of the cytoskeleton and especially with actin stress fibers[2]. In addition, the biochemical structure of vimentin and lamin are both very similar. In the nucleus, lamin filaments compose the lamina, a sub-nuclear membrane cortex that is the main structural component of the nucleoskeleton. Therefore, mechanical events involving intermediate filaments, such as mechanical interaction with stress fibers, can be transmitted to the nucleoskeleton and the nucleus. This now brings us to consider the nucleus and its nucleoskeleton.

3.4. Nucleus and nucleoskeleton

The nucleus is enclosed in the nuclear membrane, shielding it chemically from the rest of the cell. In addition, the nucleoskeleton provides mechanical structure to the nucleus, making it stiffer than the cytoplasm of the cell[56]. Yet, experiments show that the nucleus is deformed during spreading, since the nucleus is supposed to be much stiffer than the rest of the cell, we ask the following question:

Question for later:

"Since the nucleus is much stiffer than the cytoplasm:
are cytoskeletal forces able to deform the nucleus during spreading?"

The nucleoskeleton is largely composed of the nuclear lamina. It plays a role in chromatin organization and consequently in DNA storage and cell division. We may therefore wonder if mechanical stresses applied on the nucleoskeleton could influence gene activation. In other words:

Question for later:

"Can mechanical stimuli applied to the nucleoskeleton influence gene expression?"

Interestingly, the nucleoskeleton (i.e., nucleus) is also mechanically connected to the rest of the cell via SUN and nesprin connections, which are respectively linked to the lamellar network and actin. We can therefore suppose that the mechanical state of the cytoskeleton may affect gene expression.

Question for later:

"Can cytoskeletal tension influence gene expression?"

In this sense, Itano et al. showed that as cells spread and flatten on the substrate, the nucleus changes shape and nuclear calcium levels increased. Furthermore, they also recorded a change in myocyte enhancer factor 2 (MEF2) gene expression[11], a gene known to take part in cell differentiation and organogenesis[57]. In addition, they also found that cell spreading and osmotic stretching of isolated nuclei caused the release of perinuclear Ca^{2+} into the nucleus. They consequently proposed that the mechanically induced Ca^{2+} incorporation into the nucleus could directly be related to MEF2 gene expression[11].

In addition, Ihalainen et al., found that nuclear lamins behave differently depending on cellular contractility[58]. They showed that, as human mesenchymal stem cells were undergoing osteogenesis, lamins are less accessible on the ventral side of the nuclear envelope than on its apical side. Similar results were found with fibroblasts adhering to rigid hydrogels. It was interestingly not the case, when human mesenchymal stem cells were undergoing adipogenesis or when fibroblasts were adhering to a softer substrate[58].

They state that structural polarization of the lamina is promoted by compressive forces applied on the nucleus during spreading. It also requires lamins A & C as well as the presence of the LINK complex, which mechanically binds the nucleoskeleton and the cytoskeleton together via an cap-actin stress-fibers[59].

Moreover, the mechanical properties of the extracellular matrix have also been shown to influence cell behavior, nuclear deformation and gene expression[60,19,38].

3.5. Extra Cellular Matrix (ECM)

While cells are often considered as the basic unit of all biological processes (Cell Theory), they are in constant interaction with their surroundings, and in many cases this includes the Extra Cellular Matrix (ECM). In such case, the ECM acts as a mechanical scaffold for the cells that are enclosed within it. This scaffold is composed of a meshwork of macromolecules including collagen, fibronectin, elastin, and so forth.

Collagens are generally the dominant proteins that compose the ECM, consequently making it the most abundant protein in the human body[61]. The ECM will have different mechanical properties, depending upon the type of collagen, the degree of mineralization, collagen fiber orientation, and so on. As a matter of fact ECM collagen rich tissues, may have extremely different rigidity properties, ranging from hard bone to softer tissues, such as the skin, intestines, and blood vessels[62].

Elastin provides elasticity to the ECM, consequently allowing tissues to regain their shape after stretching or contracting. Patients with elastin mutations may in some instances show signs of accelerated aging, even at a young age. For instance, it may lead to an alternative aging process in the aorta[63,64], or cutis laxa[65] a disorder leading to loose and inelastic skin.

Fibronectin and other ECM proteins, have integrin binding site receptors, consequently connecting cells to the ECM[66]. Furthermore, the ECM is riddled with biochemical differentiation factors, helping cells to differentiate due to both chemical and mechanical cues. Interestingly, ECM protein synthesis is a cell mediated process, so a cells can consequently alter its mechanical properties and be influenced in return[60,19,38].

3.6. Contractile units located at focal adhesions allow cells to sense mechanical rigidity through a pinching mechanism

During the spreading phase, the leading edge repeats a protrusion-retraction cycle. Local contractile units, about 2 μm in size, assemble and disassemble along the cell edge to probe local rigidity.[19] The contractile units are known to allow cells to probe the rigidity of the surrounding substrate. Contractile units probe substrate rigidity by a process that resembles pinching. Both ends of a contractile unit (CU) are bound to the substrate, the contractile unit then contracts by applying a standard pick force of 60 pN. While the intensity of this pick force is not influenced by the rigidity of the substrate, it has been shown that the temporal response of the CU is affected, which therefore allows a "measurement" of local rigidity. Interestingly, knocking out alpha-actin, prevents the contractile unit assembly and allows the cell to spread on very soft substrates[39].

4. Bibliographic analysis of cell mechanics, from the "Why?" to the experimental tools

Adherent cells cultured on micropost substrates pull inward on the micropost on which they lay. Similar results were observed concerning adherent cells cultured on soft substrates. Adherent cells are thus generally found to pull on their environment, thus indicating that they have a contractile nature. Furthermore, the contractile nature of the cell is influenced by cell type.

Experimental results found in the literature indicate that adherent cells are indeed composed of a mechanical structure that is both capable of generating mechanical forces and sensible to many types of mechanical cues. The phenomenon by which mechanical cues induce a biological change is called mechanotransduction. In human adherent cells, mechanical cues such as substrate rigidity can influence cellular behaviors such as cell migration and its spreading process. Mechanical cues can thereby impact its size, morphology, as well as its mechanical properties. We can thus deduce that cells mechanically configure themselves in accordance to external mechanical cues. But mechanics can be the cause of more profound changes to the cell. In adherent cells, mechanotransduction phenomena are known throughout the literature to impact almost all major cellular processes such as, gene activation and protein secretion. It has also been shown to be a significant contributor to mesenchymal stem cell differentiation.

Several sets of questions thus arise from this brief analysis of the literature:

- Why is mechanotransduction so important to cell differentiation?
- How are cells structured to generate mechanical forces?
- How do mechanical cues influence the biological properties of an adherent cell as it spreads?

We will attempt to answer these questions based on the evidence found in the literature.

4.1. Why is mechanotransduction such an influential factor to adherent cells behavior?

While this question is very broad, our objective will not be to provide a full answer this question. Instead our aim is to grasp general ideas as to why cells would need to be mechanosensitive to differentiate. Having these notions in mind should in theory help us better analyze the biological system at hand.

One of the most obvious answers to this question is that the human body is composed of many different tissues, serving different mechanical purposes. This is why some such as bone may be hard, while other such as the lung may be much softer[67]. These tissues are in turn composed of many different cell types. Therefore, during embryological development, tissue maintenance or repair, cells need to assess their environment so as to take appropriate actions. Some of the ways cells can assess the environment is by communicating among themselves, responding according to chemical signals embedded in the extracellular matrix (ECM) and by sensing the mechanical properties of their environment.

If mechanical properties can be one of the indicators on how the cell should behave, it thus make sense that local mechanical properties can be an influential factor in cell differentiation.

Furthermore, cells are able to remodel their surroundings, including the ECM. It would thus make sense that the cell be able to mechanically analyze its surroundings in order to restructure it if needed.

The reasons and answers stated above are neither extensive, nor are they truly verifiable. They are nothing more than assumption and theories, which may be discredited at any time. That said they may help us know what we are looking for.

4.2. How are cells able to generate various types of mechanical forces?

As we observed previously, the cytoskeleton is composed of various types of filaments. These filaments can be used by the cell to form different types of structures (pages 22-29). The actin cortex, the lamella and stress fibers are contractile structures composed of microfilaments organized in different ways (pages 20 & 22-27). These micro-filaments are themselves composed of successive actin monomers linked in a head to tail manner (page 20). The head to tail manner allows this micro-filament to be polarized, which is why microfilaments are often described as having a positive and negative end. While the polarized nature of microfilaments is essential for the emergence of a contractile system, it also requires the involvement of a motor protein called myosin to do mechanical work. The polarity of the microfilament imposes the direction of the relative displacement generated by a myosin motor protein. With these ideas in mind, the way the myosin protein actually generates movement between two actin filaments becomes simple to understand. The myosin motor molecule can schematically be described as a linear molecule, with a tail domain on one end and one or more head domains on the opposite end. The myosin molecule is bound on one end to a polarized microfilament, while its head domain is temporarily attached to another actin microfilament polarized in the other way. The myosin motor protein will then be able to generate a relative movement between the two microfilaments which polarized in opposite direction. This relative movement is initiated by what is called a myosin power stroke, whereby the myosin head detaches from the microfilament, this myosin head then undergoes a conformational change allowing it to attach itself on further along this microfilament. The myosin head then reverts back to its previous shape without letting go of the microfilament, therefore moving the two microfilaments relative to one another. This relative motion between microfilaments coupled to an important relative length in respect to individual microfilaments stiffness in bending is what allows a microfilament network to acquire contractile nature.

At the leading edge of the cell, the lamellipodium is able to generate a force to push the cell membrane. This pushing force is generated by actin polymerization. When a globular actin monomer comes to bond at the extremity of its new microfilament, it squeezes itself between the extremity of the microfilament and cell membrane. By doing so the actin monomer therefore exerts an equal and opposite force that pushes the cell membrane forward and the microfilament backward.

We now understand how the actin network is able to generate pulling and pushing forces within the cytoskeleton. In addition, other elements of the cytoskeleton, such as kinesin motors are able

to generate mechanical forces within the cell. These cytoskeletal elements also play a secondary mechanical role within the cell in comparison to the already described actin network.

4.3. What is the influence of substrate rigidity on cell behavior?

While we have already mentioned the fact that adherent cells can be influenced by substrate rigidity, we still haven't mentioned any particular mechanism that would allow them to do so.

While some proteins, such as talin[49] and vinculin[16] have been shown to be mechanosensitive, cells have also been found to be equipped with a dedicated substrate rigidity sensing apparatus called contractile units[39] (CU). In addition, cells have been shown to have a greater projected area when cultured on stiffer substrates[18,7], while also pulling more on it[18] and becoming more stiff[8]. Surrounding tissue stiffness can also be a sign of illness, for instance, a fibrotic human liver is 2.5 times as stiff than a normal one[67]. Interestingly, cells also have a tendency to migrate towards stiffer area by a process known as durotaxis.

4.4. Measuring adhesion forces using micro-beads embedded in a deformable substrate

Deformable substrates may be used to cultivate cells or simply to allow them to spread. Markings or embedded micro-beads can be used to measure local substrate deformations[68]. The next phase is to calculate the possible forces that may be exerted on the substrate to create such deformation patterns.

The advantage of this technique is that it allows cells to spread on flat substrate without being affected by the measurement apparatus. Furthermore this technique has been enhanced to allow 3D forces force measurements(Figure 18 A).[68] Still, measuring adhesion forces may sometimes be challenging because micro-bead position has to be compared before and during adhesion. In addition it may be imprecise, as it does not necessarily clearly define the areas where the adhesion forces are being exerted.

A)

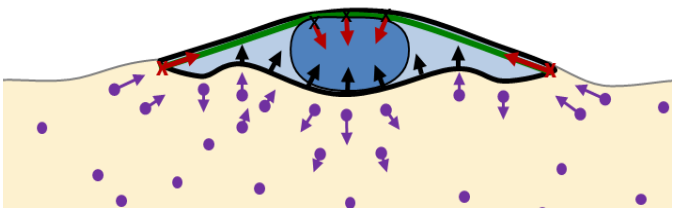

B)

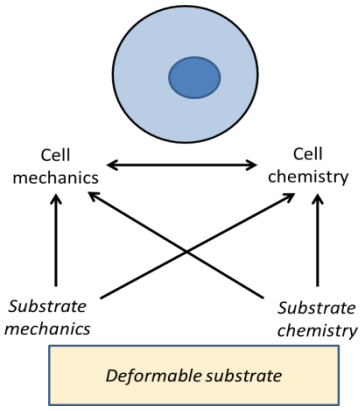

Figure 18: Deformable substrates

A) Embedded microbeads may be used to track the deformation of the substrate and measure forces applied by the cell on the substrate.

B) Changing the mechanical properties of deformable substrates requires a change in their chemical make-up, Therefore, deformable substrates can't be used in a parametric analysis to study the effect of mechanical properties on cell behavior without changing the way the cell is chemically influenced by the substrate.

But perhaps, for some studies, the most significant inconvenience is that changing the rigidity of the substrate will require a chemical alteration of the material (Figure 18 B). It thus raises the following question: Do cells act differently due to rigidity or due to the chemical change?

4.5. Micropost substrate

Mechanobiologists where initially wondering if substrate rigidity could impact cell behavior[18,69]. The problem was that changing a material's rigidity would also require changing its chemical makeup. Doing so consequently complicated the analysis because it was difficult to know whether the cells were behaving differently because of a change in the substrate's rigidity or because of its chemical make-up.

The solution was elegantly simple: Cells would be cultured on micropost substrates (Figure 19). The micropost substrates would all be made of the same material, the part of the microposts that would be in contact with the cell, namely the tops of micropost, would be identical. In fact the only difference between stiff versus a soft substrate would be the height of the micropost. Long microposts would thus be more flexible and shorter microposts would be harder to bend. Said differently, short microposts could mimic a stiff substrate and long microposts a soft substrate.

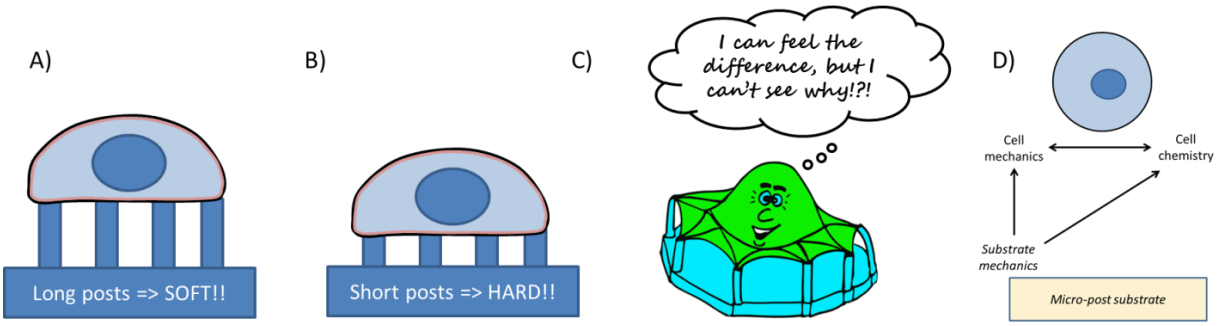

Figure 19: Micropost bending stiffness can be changed without influencing the chemical make-up.

A) Long posts mimic a soft substrate.

B) Short posts mimic a hard substrate.

C) Cartooned illustration of the fact that cells perceive no difference on the micropost chemical compound nor in the shape or size of their tops. Cells are therefore only influenced the bending stiffness of the microposts.

D) Influence of the substrate on the cell

Cell culture experiments using microposts showed that cells pull the post towards them. Furthermore, knowing how much force was needed to bend a micropost therefore indicated the pulling force exerted by the cell. The advantage of this technique is that it is precise to about 2-3 nano-newtons. In addition, it is very clear which post is being pulled on.[18] Yet this technique still has a few limitations. Force measurements are limited to the horizontal plain. Horizontal forces, measured at post located near the center of the cell may represent low force values. But this may be due to opposite horizontal pulling forces cancelling each other out. It is also important to notice that micropost adherence does not represent physiological conditions.

4.6. Fluorescence Resonance Energy Transfer tension sensors

Fluorescence Resonance Energy Transfer[70] (FRET) technology can be used to measure tension values transiting via individual molecules, such as vincluin[71]. Such constructs are called tension

sensor module (TSMod)[71]. This technique was originally used to measure distance between two molecules at the Nano-metric scale, by analyzing how the fluorophores from one type of molecule could excite the fluorophore from another type of molecule. This technique was later adapted to the needs of mechanobiology to measure the distance between fluorophores bound at each end of the same target molecule. Fluorophore excitation pattern then indicates if target molecules are under tension or not.

The advantage of FRET technology is that it reveals whether a specific type of molecule is under tension or not. It is even able to indicate how much tension is transmitted via each molecule. However, it is not able to indicate how many molecules are present, nor is it able to give stress or tension values outside of a molecules[18].

4.7. Measuring mechanical properties of the cell via Atomic Force Microscopy

Atomic Force Microscopy (AFM) can either be used to observe an object's topography down to a resolution of few nanometers or it can be used mechanically probe the surface of an object. The advantage of this method is that it can yield mechanical properties[44], such as stiffness, even for living cells[72]. The inconvenience is that these values are mostly superficial and the equipment is costly. AFM and many other techniques such as magnetic twisting devices[73] or magnetic pillars[74] have also been used to observe the effect of targeted mechanical stimuli on cells. Wang et al, found that pulling on integrin induced focal adhesion growth and induced a force dependent stiffening[73].

4.8. Observing the cell structure using Fluorescent Microscopy

Most cellular proteins and substructures are not visible without first being labeled. Fluorescent microscopy enables such labeling. Relevant proteins can for instance be indirectly observed using fluorescent antibodies or the cell can be forced to produce a modified fluorescent version of the protein of interest[43].
Fluorescent drugs such as green or red labeled phalloidin can also be used. Each labeling technique has its advantages and drawbacks. For instance, phalloidin is a toxic drug that stabilizes actin filament structures and can kill cells, it is therefore generally used to study fixed (preserved dead) cells. Furthermore, fluorescence microscopy is subject to photobleaching, meaning that the fluorophores (fluorescent labels) are degraded over time as they absorb and reemit light. Photobleaching can therefore be detrimental when continuous imaging is involved. On the other hand, this photobleaching can be useful to assess protein renewal rate. Resolution wise, when using a conventional microscope, the diffraction barrier generally prevents visual definition below 200 nm.

4.9. Confocal microscopy allowing a 3D view of the cell

Conventional microscopy offers a top view of the cell. It is a 2D perspective of a 3D world. So as to palliate this limitation confocal microscopy allows for a 3D acquisition of the cellular structure, by a slice by slice acquisition of the observed cell. The slices are numerically stacked on top of each other to form a 3D image. Image acquisition is achieved by reducing the diameter of the microscope pin hole, thus only preserving light belonging to the relevant plane. The inconvenience of this technique is that reducing pin hole diameter may reduce signal intensity.

4.10. Super resolution microscopy, allow visualization of individual actin filaments

Individual actin, microtubule and intermediate filaments have all have a thickness below 30 nm. Since the light diffraction barrier limits conventional microscopy to a resolution of 200 nm, all cytoskeletal images are consequently blurry. Large individual stress fibers seem clearly visible because they represent a collection of many actin filaments arranged in a parallel bundle, but the individual microfilaments contained within the stress fiber are not discernable from one another. Similarly, conventional microscopy may allow for a clear, yet blurred visualization of an isolated microtubule filament. On the other hand, two microtubules running in parallel at less 200 nm would appear as a single blurry filament.

Conventional microscopy is thus not able show the detail of individual filaments[75]. To do so would require the use of super resolution microscopy, so as to surpass the diffraction barrier. Several technologies exist, STED and STORM microscopes, even enabling 3D visualization[75,76,77].

4.11. Quantitative fluorescent speckle microscopy (qFSM)

Quantitative Fluorescent Speckle Microscopy (QFSM) is a live cell imaging method that allows high spatial and temporal resolution to analyze the dynamics of macromolecular assemblies with. QFSM's advantage compared to other methods is that it allows, across a large field of view, measurement of actin filament (F-actin) network movement and turnover kinetics with in living[78]. This technique requires fluorescent labeled monomers to be at a low ratio in comparison their similar to native counterparts. QFSM image analysis software is then used to track speckles dynamic so as to calculate polymeric network flow and map out assembly and disassembly rate[78].

4.12. Patterned substrate used to control cell shape:

Usually single adherent cell shape can vary significantly during free adhesions.[8] In vivo, the ECM and neighboring cells influence cell shape[19,38]. Similarly, in vitro, patterned substrates can be used to influence cell behavior. For instance by increasing by a factor of 50 fibronectin coating density, Wang and Ingber 1994 found that it promoted cell spreading by fivefold and more than doubled cytoskeleton stiffness and viscosity.[79] In addition to changing adhesion protein density, substrates which normally do not allow cell adhesion can be coated with micro-patterned shape motifs that do[60]. Such tools are useful to understand the influence of cell shape on other cellular properties[8,60]. With such tools cell shape has been found to influence cell stiffness[8].

In addition, deformable patterned substrates have also been used to measure adhesion forces. This lead to the finding that focal adhesion forces are proportional to focal adhesion size, but also depend on substrate stiffness and cell type[16,15].

5. State of the art concerning mechanical models of the cell

5.1. Tensegrity Theory

The tensegrity theory was proposed by Donald Inberg several decades ago to describe the internal structure of the cell. At that time, this theory described the cell as being mechanical structure that was shared similar characteristics to tensegrity structures[80,81].

Definition:

Tensegrity structure: *A tensegrity structure is composed of isolated compression bearing elements inside a net of counter actin tensile elements, in such a way that the compressed members (usually bars or struts) do not touch each other and the pre-stressed tensioned members (usually cables or tendons) delimit the system spatially.*[82]

In a self-testimony Donald Inberg explains the historical reasons why he proposed the tensegrity theory. He remarked that adherent cells would systematically become round when they were forced to let go of their substrate (Figure 20A). He therefore wondered what mechanism allowed cells to behave this way. This behavior reminded him of tensegrity structures (Figure 20 B &C). He then investigated this hypothesis and wrote several papers in support of this view[81,83,84,85].

One of the strong supporting elements of the tensegrity theory is that it seems to be the first conceptual model that could at the time explain how cells were able to round. Furthermore, Wang et al. have shown evident in to support the idea that the cell structure behaves as discrete network of interconnected elements, composed of interwoven actin and microtubules filaments which is in accord with the tensegrity theory[80]. In addition actomyosin filaments have been shown to bear tension while microtubules bear compression also supporting Inberg's theory[80]. In addition microtubules were shown to impact on cell shape[80].

Cells are able to spread and round without the involvement of microtubules. Moreover, several experimental studies have shown that microtubules only bear a marginal amount of the total compression load[44]. More importantly, stress fibers and microtubules have been shown to dissolve during cell rounding, which is not in accord with the initial tensegrity model. Additional research latter revealed that the cell forms new stress fibers as it reattaches to the substrate. Therefore, while the tensegrity theory is largely regarded as being a valuable model to understand how the cell is mechanically structured, evidence suggest that it is nonetheless an inexact representation of the true cellular structure.

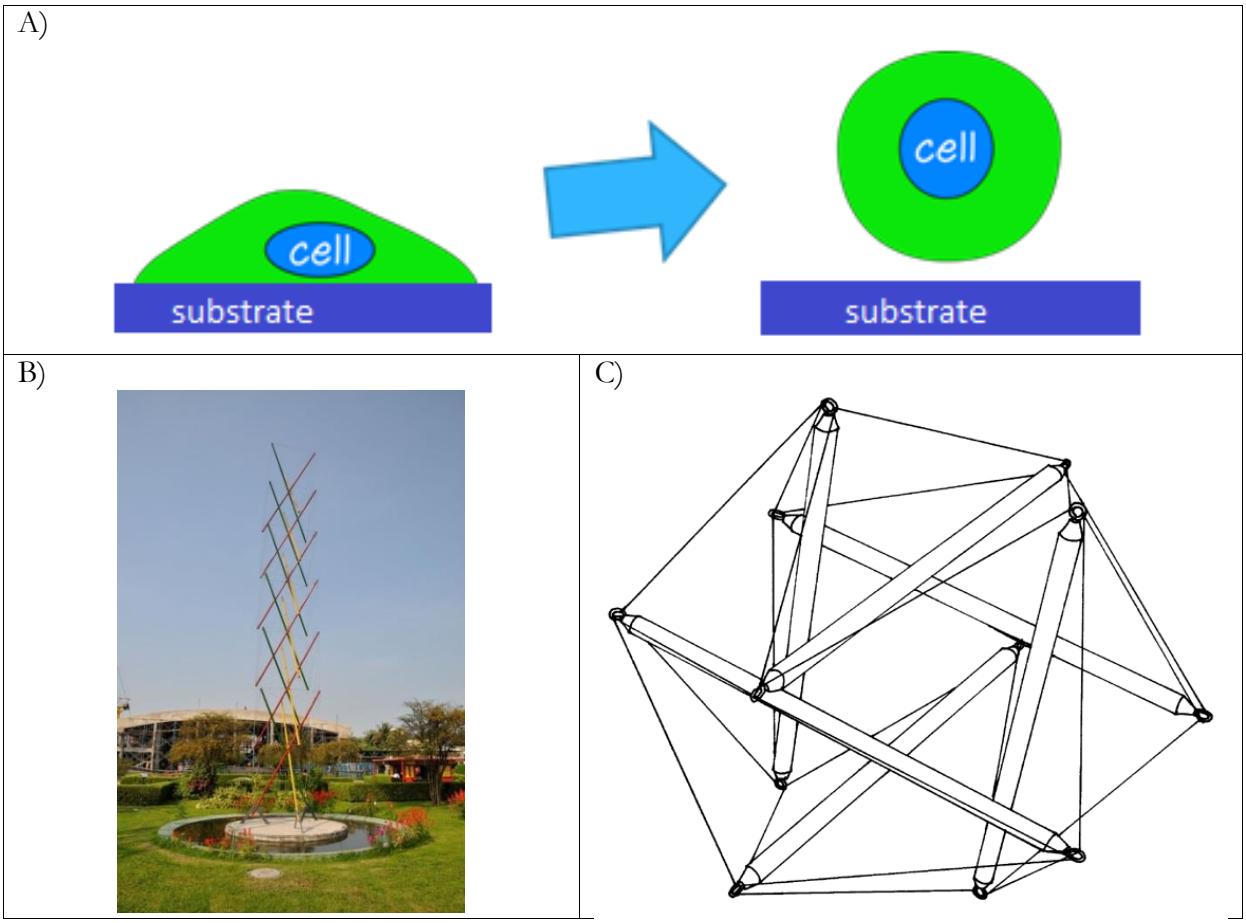

Figure 20 : Tensegrity structure examples

A) Cartooned illustration of cell rounding after letting go of its substrate

B) Tensegrity structure exhibit at the Science City, Kolkata (Calcutta), India.

C) Tensegrity Tetrahedron, Francesco Della Salla, 1952

5.2. Tensegrity models with fixed connectivity

Similarly to the tensegrity structure being illustrated in Figure 20C the first tensegrity cell models had a fixed number of connectivity. Based on Ingber's tensegrity theory, Stamenovic et al. 1997 realized a numerical tensegrity structure made of 6 rigid bars interconnected by 24 linearly elastic cables[81]. The bars boar compression loads and did not touch each other, while tension transited via the elastic cables. This tensegrity cell model was able to change shape by changing the length of its tension bearing elements and could therefore mimic spreading and rounding. Moreover, a similar tensegrity models were developed by Lauren et al 2002, their tensegrity model could explain experimentally observed low strain-hardening (in low strain domain) and pre-stress induced stiffening. Coupled with in vitro experiments, these models enabled a theoretical deduction between the equivalent cellular tension and the Young modulus of the cell[86].

5.3. Continuous mechanical models

Continuous mechanics represent an object as a continuous material. It has the advantage of representing the cellular medium by assigning it material like properties based on experimental findings[87,88,] such as viscosity and stiffness. For instance Vaziri and Mofrad measured the mechanical properties of cells using micropipette aspiration to latter develop a 3D model.

Inconveniently, however, it cannot represent the filamentous nature of the cytoskeleton, nor any of its subcomponents. A continuum approach therefore assumes that the smallest length scale of interest is greater than the dimensions of the microstructures that compose the medium[5]. Yet a continuous approach can provide information about mechanical strain and stress[87,88].

5.4. Hybrid tensegrity continuous model

McGarry and Prendergast developed a three-dimensional finite element model of an adherent cell[89]. They modeled membrane components, cytoskeletal pre-stress, cytoplasm and the nucleus. They wanted to determine the contribution of the various cellular components to cellular stability. The model was found to be sufficiently complex to behave non-linearly.

While these types of model were attempting to explain how cells could change shape while still preserving their structure, experimental evidence showed that the cellular structure was actually much more dynamic than what was previously anticipated, or at least what could be modeled at the time.

3D finite element models were used to model cells undergoing uniaxial stretched cells, yet the some of these earlier models were only composed of a soft cytoplasm and a harder nucleus[90]. Latter a more advanced models, was developed by Milner et al. to developed a viscoelastic finite-element model of an osteoblast cell under cyclic deformation. The model included actin stress fibers, an elastomeric membrane, a viscoelastic cytoplasm and a nucleus[91]. Interestingly, mechanical stresses intensity and their spatial distribution may differ depending on the frequency of the cyclic deformations. At 45 Hz cytoplasmic strain pick values were five times higher than at 1 Hz, and intra-nuclear peak values of Von Mises stress doubled. Yet the model was not based on the morphology of a real cell nor did it allow for dynamic connectivity.

5.5. Divided medium modeling allows abundant and dynamic connectivity

The divided medium mechanical models were an attempt to use tensegrity principles while allowing a dynamic rearrangement of the cellular structure[92,93,94,95]. This dynamic arrangement allows Milan et al. to generate models in accord with the morphology of the cells the observed[92]. They therefore provided an innovative approach that attempted to model the cell as a cluster of mechanically interacting elements (nodes and contactors). Similarly to previous tensegrity models, these models were able to represent the filamentous structural properties of the cytoskeleton. Actomyosin filaments were represented using tensile interactions which would connect mathematical nodes at a distance, while compression bearing elements, such as microtubules, where generally represented using sphere contactors, wrapped around the mathematical nodes (Figure 21). When two spherical contactors would come into contact, they would be both subject to a mechanical force that would prevent them from interpenetrating, therefore modeling a compression load between these two elements (Figure 21 C). From this perspective, the modeling strategy is therefore very different from purely tensegrity based models that instead represent compression bearing elements as beams (Figure 20 C).

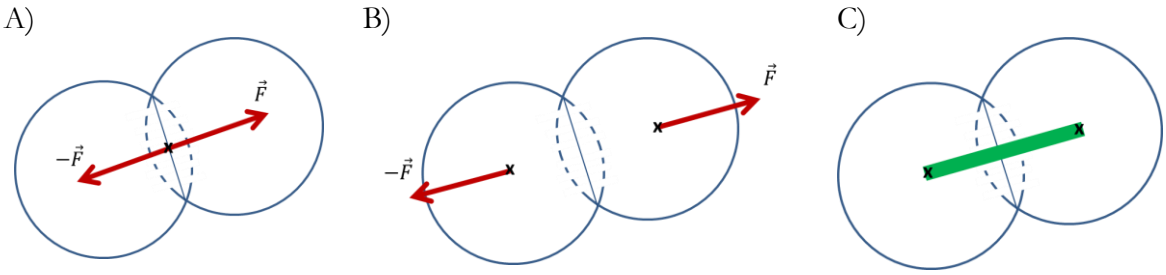

Figure 21 : Conceptual visualization of a sphere/sphere contact (NB: forces pushing the spherical contactors against each other not shown). Mechanical nodes are represented as small black crosses and spherical contactors as blue circles. The red arrows represent opposite and thus repulsive forces vectors formed between two interpenetrating mechanical contractors.

A) Represents the contact forces being applied where the contact occurs.

B) Represents a mechanically equivalent scenario, where the repelling contact forces are applied at the center of the each spherical contactor. This conceptual visualization allows better visualization of the fact that the contact generates forces that prevent the spherical contactors from running through each other

C) Center to center visual connections can be made to showcase the equivalent mechanical compression bearing element, i.e., microtubule.

In general, conventional divided medium mechanical models would represent real physical elements by utilizing elementary nodes and contactors, i.e., the spherical contactors themselves. Interestingly, this was not the case when it came to divided medium mechanical cell models which would instead represent the physical elements based on the interactions between nodes and contactors[92,93,94,95].

Furthermore, divided medium models had another critical advantage over conventional tensegrity based models, because they easily be composed of an elevated number of nodes, spherical contactors and interactions. CDM models would therefore be able to generate rich mechanical interaction networks, where each interaction could, for instance, represent an actomyosin fiber, microfilaments, or a microtubule depending on the type of interaction.

The CDM model[92,93] and other such models[94,95] were therefore a valuable evolutionary step from conventional tensegrity based models or any other previously presented computational modeling strategies.

Moreover, similarly to microtubule sprouting out of the centrosome, Maurin et al. attempted to recreate the compression network originating from a central location, bringing us closer to the actual cellular structure.

To estimate mechanical forces within the cell Milan et al. used a 3D version of the CDM model to measure the influence of cell shape on intracellular forces. To do so, starting from a round configuration, the model was gradually stretched to match the shape of an observed cell. Modeling results indicated that intracellular tonus, focal adhesion forces as well as nuclear deformation increased with cell spreading[92], which seems consistent with experimental observations[8,11,18]. Yet the study only relied on shape and did not use other experimental

parameters, such as experimentally adhesion forces. While consistent, the results of this study can therefore not be asserted as valid.

6. Conclusions concerning our bibliographic analysis

6.1. The lack of an appropriate conceptual mechanical model of adherent cells

The diversity of mechanical models based on various types of mechanical theories can in part be explained by the fact that each of these methods may have different scientific aims. Further, while the tools may differ, the conceptual basis of these various models differs as well[5,96,81].

Additionally, the assumption of mechanical cell models involving continuum media is to describe the cell at a sufficiently large scale to "average/smooth out" interactions between microstructures. It is however unclear, whether if this strategy is judicious, because, filamentous structures span and interconnect throughout the cell at length scales that equate cell size. Moreover, such techniques would neither be able to explain nor to estimate how forces transit within the filamentous structure, nor should they logically provide any type of information that may be relevant at a lower scale, e.g., to the mechanical stresses that may be applied to proteins. While, these models may provide mechanical stress values, we therefore ponder how relevant these values may be for a cellular system?

6.2. Substrate rigidity sensing, cell size and shape make a complicated system

Cells are clearly influenced by the rigidity of the substrate they adhere to, both biologically and mechanically, while still displaying signs of large variability[15,9,7]. In addition, when spreading freely in isolation, cells are also able to take very different shapes, while also being influenced by morphology and consequently, influencing mechanics[8]. Cell mechanics is thus a complex and intertwined system allowing for significant variability, understanding a system such as this one will consequently require an adapted research strategy.

6.3. The research strategy we implemented

The work done during the project will be presented in three chapters. The first chapter will involve the use of the CDM model to measure intracellular forces, such as forces applied to the nucleus and subsequent nucleus deformation. We will also see how the mechanical forces generated by the cytoskeleton can deform the nucleus. In the second chapter, we will discuss a new modeling approach developed during this thesis, aiming to increase modeling pertinence despite high cellular variability. The third chapter will use this new model to estimate intracellular force as cells adhere on substrates of different rigidities.

CHAPTER 1
THE INFLUENCE OF SUBSTRATE RIGIDITY ON CELL MECHANICS. AN IN SILICO MODEL BASED ON TENSEGRITY AND DIVIDED MEDIUM

NB: The following study presents work done during my thesis. It has already been published in the Journal of Biomechanics[97]*. A star symbol (*) at the beginning of a legend indicates that the figure or table has been published in the Journal of Biomechanics.*

1. Introduction

Substrate rigidity is known to critically affect adherent cell behavior. For example, it is known to affect cell shape, adhesion forces, nucleus nuclear shape, and gene expression. Furthermore, mechanosensitive molecules and contractile units located at FA are known to be influenced by substrate rigidity and consequently impact cellular behavior. Yet how these different molecular components and subsystems interact as a system to regulate or trigger these behavioral changes remains unclear. In addition, it is unclear how adherent cell mechanics is influenced by substrate rigidity. More specifically, how mechanical forces generated by the cytoskeleton mechanically affect the nucleus and, consequently, gene expression.

Problematic:

"How does substrate rigidity influence adherent cell mechanics?"

And more precisely:

"How is the nucleus mechanically affected?"

"Do cells pull more on their adhesions because they are larger,
or do they pull more because of higher tensile stresses within the actin network?"

"Will cellular tension be affected by substrate stiffness?"

We thus propose to use a numerical model to study how internal cell mechanics could be impacted by substrate rigidity. As was discussed previously in the general introduction, divided medium mechanics is better suited to represent a dynamically rearranging filamentous network than finite element, continuous medium, or regular tensegrity models. Its main advantage is that it is able to dynamically represent a tensegrity like structure, without being limited by fixed interactions. In other words, similarly to a real cell, the cytoskeletal structure of the model evolves over time as it spreads. We consequently decided to use the previously developed and published

Cytoskeleton Divided Medium (CDM) model. The CDM model was previously used to simulate cell adhesion, by allowing the modeled cell to either spread freely or by instructing it to spread so as to match the shape of the observed cell. Simulation results at the time showed that intracellular tonus and spread area lead to a non-linear increase of nuclear strain. Yet these studies were focused on cell morphology, thereby omitting the influence of substrate rigidity. We therefore developed a modified version of the CDM model to include it.

In addition, we formed a scientific partnership with Associate Professor Nathan Sniadecki and PhD candidate Kevin Beussman, two mechanobiologists from the University of Washington, USA. This partnership allowed us to include micropost substrates of different rigidities. For this study, we used two different apparent micropost rigidities, which we will refer to as the "Very Soft", "Hard" and "Hard+" conditions.

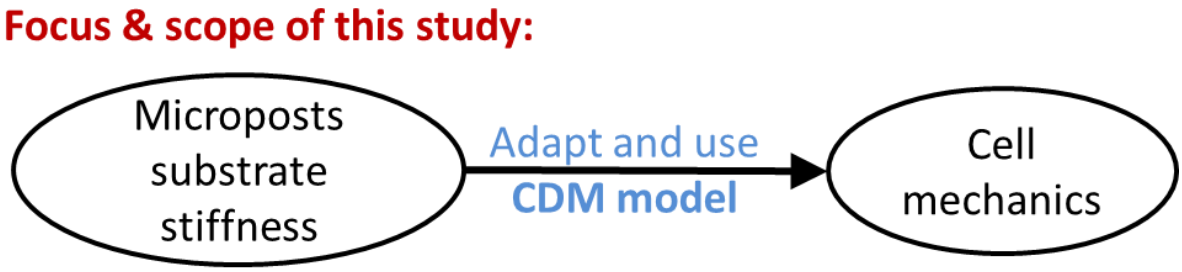

Figure 22: Scope and focus on this study.

The advantage of using micropost technology is twofold. First, cells are only able to perceive a difference in the bending stiffness of the post, which is can be assimilated to substrate rigidity (Figure 22). The way it is done is by changing the height of the microposts. Longer microposts bend more easily than shorter ones, therefore allowing us to have a "Very Soft", a "Hard" a "Hard+" substrate (see Figure 23). The material and the directly exposed geometry remains the same. Secondly, as cells adhere and tug on the microposts, it bends the microposts and displaces their top extremity. We can therefore measure the displacement, which can in turn be used to calculate the corresponding net vector force. In other words, micropost substrate enables us to measure net adhesion force applied to each post.

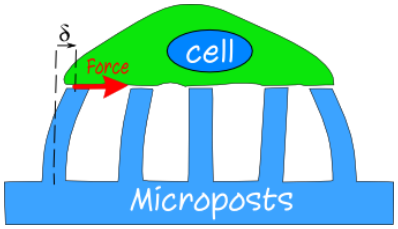

Substrates microposts bending stiffness:

- Very Soft: 11 nN/µm
- Hard: 31 nN/µm
- Hard+ 39 nN/µm

Figure 23 : Description of a micropost substrate

Left) Cartooned drawing of a cell bending microposts as it adheres. Individual post deflection is a direct quantitative indication of the force being applied to it by the cell.

Right) Microposts bending stiffness values used in the study

The CDM model was consequently modified to take into account adhesion forces in addition to previously considered parameters such as cell morphology. Our aim was to understand how substrate rigidity could have an impact on the mechanical state of the cell and its nucleus. The

experimental and modeling details are included in the next section, followed in two other sections by the results and a short discussion of these results.

2. Methods

2.1. Cell culture on "Very Soft", "Hard" & "Hard+" micropost substrates

Human pulmonary artery endothelial cells (HPAECs, Lonza) were cultured on silicone micropost substrates (Figure 23). Micropost deflection was used to measure local pulling force exerted by the cell (Lemmon 2005). To analyze the influence of substrate stiffness on cells, a Very Soft, Hard and Hard+ micropost arrays were considered. Very Soft substrate microposts, were 2.14μm in diameter and 8.96μm in height, leading to an average bending stiffness of 11nN/μm. Hard substrate microposts were 2.32μm in diameter and 6.95μm in height, leading to average bending stiffness of 31nN/μm. Both substrates (Very Soft & Hard) were made of the same PDMS with a Young's modulus of 2.5MPa measured according to ASTM standard D412. To extend the study, it also included 5 cells cultured on a "Hard+" substrate (39 nN/μm), the sample size was deemed insufficient to make conclusions about this group. Modeling results were nonetheless used to expand the overall sample size when deemed appropriate. Hard+ substrate specifications: substrate was made of PDMS material with a Young's modulus of 3.2 MPa. Microposts were 2.42 μm in diameter, microposts center to center spacing was 9 μm, 7.45 μm in height and bending stiffness equaled 39 nN/μm. For the 3 substrates, the spacing between microposts was 9 μm center to center. Master arrays were made with SU-8 photoresist. Silicone arrays were manufactured via replica molding of polydimethylsiloxane (PDMS) using a mixing ratio of 10:1 for the base and curing agent (Sylgard 184, Dow Corning). The silicone arrays were stamped with 50 μg/ml fibronectin (BD Biosciences) to enable the attachment of cells. After seeding the HPAECS onto the silicone arrays, they cells were cultured in F-12K Kaighn's modified media (Hyclone) containing 50 μg/ml ECGS (Biomedical Technologies, Inc), 100 μg/ml heparin (Sigma Aldrich), and 10% of fetal bovine serum (Gibco). After culturing for 14 hours on the arrays, the cells were permeabilized using Triton-extraction protocol and stained with Hoechst 33342 (Invitrogen), phalloidin (Invitrogen), IgG anti-vinculin (hVin1, Sigma Aldrich), and anti-IgG antibodies (Invitrogen). Images of the cells and microposts were obtained via fluorescence microscopy (Nikon TiE, 60× oil objective, 1.4 NA). The spread area of a cell on an array was measured from an outline of its actin image. Locations of focal adhesions were determined from vinculin immunofluorescence while traction forces were calculated from micropost deflections.

2.2. CDM model computation & improvements

2.2.1. A brief overview of the CDM modeling method

The CDM model is defined as a set of mechanically interacting nodes combined with sphere contactors. Before running the simulation, the model starts out in the shape of a round cell that includes a round nucleus at its center. Then, running the CDM model requieres two distinct steps, the second of which was developped for this study. The first step is intended to gradually deform the CDM model, so that it ultimately matches the shape of the observed cell. Yet morphological accordance does not imply mechanical accordance. It is at this point that the second step becomes important. The previously experimentally measured adhesion force magnitudes of each adhesion is entered in the model. The model then itteratively solves for a structural configuration that provides identical results. Once done, the results are then gathered and analysed.

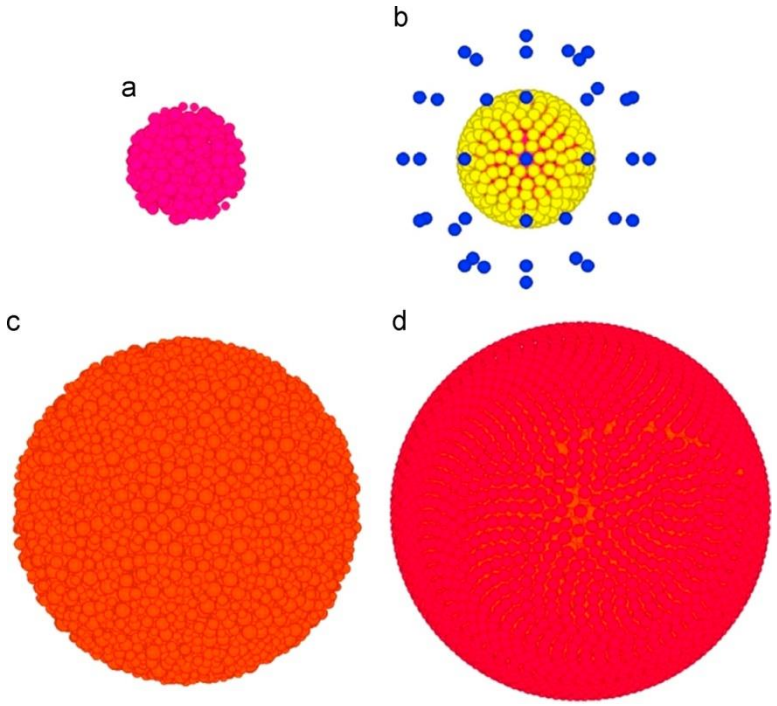

Figure 24: Three dimensional view of the model before spreading. At this stage the cell model is round with a diameter of 15 μm.*

a) nuclear core (pink)

b) nuclear membrane (yellow) and perinuclear nodes (blue)

c) cytoplasmic nodes (orange)

d) cell membrane and actin cortex (red)

2.2.2. Modeling tensile interactions

Tensile interactions were modeled using an elastic interaction law. It allows each interaction to behave as an initially pre-strained elastic rubber band, thus pulling the two connected nodes toward each other. In addition, similarly to an actual rubber band, each traction force was proportional to overall stretch (strain), which includes initial stretch (ε_0). Conversely, in the case of a slack interaction the tension force became null.

The tension force $\boldsymbol{T}$ is function of the distance between two nodes, generally termed gap value (see Figure 21 Figure 1page 42 & Figure 25), while $\boldsymbol{g_0}$ is the initial gap value. The stiffness $\boldsymbol{K}$ and the initial pre-strain ε_0 are both positive. So that interactions may only happen between direct neighbors, $\boldsymbol{g_v}$ is the highest initial gap value between two interacting nodes, beyond which no interaction would be generated.

Equation 1

$$\begin{cases} g \in \,](1-\varepsilon_0)g_0; g_v\,] \Rightarrow T = -K\,(\dfrac{g-g_0}{g_0} + \varepsilon_0) \\ g \in [0;(1-\varepsilon_0)g_0]\ \cup\,[\,g_v;\infty[\Rightarrow T = 0 \end{cases}$$

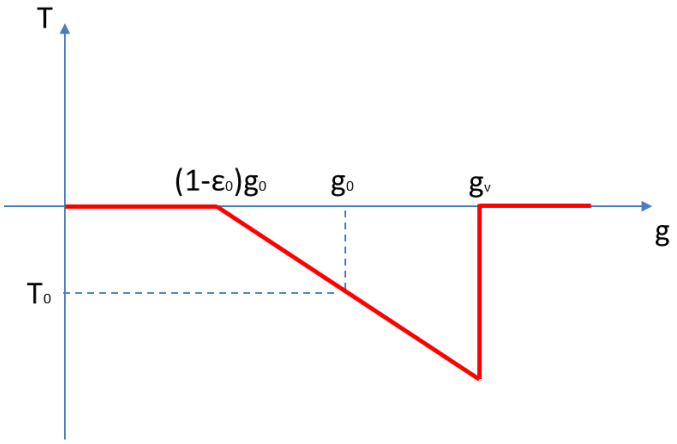

Figure 25: Elastic Wire interaction law. In the local system of reference the tension T is defined negative, because the compression forces that prevent interpenetration between contactor are defined positively.

The elastic rubber band like interaction law thus defined the tension force as linearly proportional to strain and stiffness. The initial pre-strain $\boldsymbol{\varepsilon_0}$ were defined positive for stress fibers, negative for cytoplasmic intermediate filaments, and null for nuclear filaments (Table 1).

2.2.3. Modeling microtubules and an intracellular compression network

While we have discussed how intracellular tension interactions were modeled, we will now consider how intracellular compressions are modeled. During cell spreading, microtubules have the tendency of bearing intracellular compression forces. Since microscope images were lacking for a direct representation of the microtubule network, this method consists of modeling the intracellular compression network by adding a single sphere around each mechanical node. The sphere acts as a rigid impenetrable contactor. When sphere contactors are brought in contact with one another, they come into contact and generate passive repulsion forces (Figure 21 page 42). As a whole these forces generate a passive contraction network. To accomplish this, we used a frictionless contact law (Figure 26 & Equation 2) that considers the gap (g) between the contactors and normal reaction force (RN).

Equation 2

$$g \geq 0\,;\; R_N \geq 0\,;\; g \cdot R_N = 0$$

Figure 26: Graphic representation of the frictionless contact law. In the local referential the compression force R_N is defined positive.

2.2.4. Numerical solver

The LMGC90 mechanical solver was used to run our model. This numerical solver relies on Non-Smooth Contact Dynamics to resolve the discrete forms of the dynamic equations involved in divided medium mechanics[98]:

Equation 3

$$M(q,t)\cdot\dot{V} = F_{ext}(t) + F_{int}(q,V,t) + R + T$$

- t is the time variable
- q is the vector of generalized degrees of freedom
- dV is the differential measure of the generalized velocities vector (V)
- M(q,t) the matrix of inertial mass
- R resultant vector of contact forces
- T is a vector which represents the resultant of the tensile interaction law
- F_{ext} (t) the external loads vector
- F_{int} (q, V;t) is the vectorial representation of the internal force (deformable bodies) and the nonlinear inertia terms (centrifugal and gyroscopic)

The generalized equation is adapted to describe collisions and other non-smooth phenomena via a differential formulation:

Equation 4

$$\mathrm{M}\cdot\mathrm{dV} = F_{int}(q,V^{+},t)\cdot\mathrm{dt} + F_{ext}(\mathrm{t})\cdot\mathrm{dt} + \mathrm{dI} + \mathrm{dT}$$

&

$$\mathrm{q(t)} = \mathrm{q(t_0)} + \int_{t_0}^{t} \mathrm{V^{+}}\cdot\mathrm{dt}$$

- dI contains, both the contribution of smooth contact (diffuse contribution of the resultant of contact forces Rdt) and the contribution of local impulsion densities exerted by shocks Pδ

Yet in our model F_{int} is null, we may therefore simplify the equation as follows:

Equation 5

$$\mathrm{M}\cdot\mathrm{dV} = F_{ext}(\mathrm{t})\cdot\mathrm{dt} + \mathrm{dI} + \mathrm{dT}$$

At any time during the simulation, the solver needs to define the contact interactions between mechanical bodies. Contact interactions can be described from a local reference point by designating one of the two interacting bodies as the candidate and the other as its antagonist. This local expression can then be expressed from a global stand point. A similar strategy is used to deal with tensile interactions between nodes.

The LMGC code resolves the dynamic equations for all nodes using an implicit non-linear Gauss-Seidel algorithm[99]. One of the specificities of this algorithm is that it locally considers one

contact at a time, freezing the contributions of other contacts. Over a time step, three important tasks take place. Firstly, the solver detects contacts between the different bodies, the contact problem is resolved allowing contact forces to be determined, and this allows the solver to determine the motion of the different elements of the media. The computation of the model was allowed to run until a mechanical equilibrium is reached.

To quantitatively assess the stability of the cell model (equilibrium), we used a divided medium stability criteria called free run length. The free run length represents the average node displacement per time step. A low value thus indicates a stable structure at rest, while a high value suggested internal movements. Furthermore, other criteria such as the evolution of the ratio between kinetic energy over potential energy were monitored to ensure proper convergence toward mechanical equilibrium.

2.2.5. Real adhesion forces are used to generate a valid CDM

We modeled 10 cells per substrate rigidity condition as a compromise between statistical relevance and computation time.

The computational process of the CDM model was individually and independently re-run for each cell. The full process was split in two successive steps. The first step is the "spreading phase" followed by the "optimization phase".

Spreading phase: Similarly to a real cell, the CDM model started at a round state. Outer edge nodes belonging to the cell model were selected to match a focal adhesion. The selection process was simple, the closest outer edge node to the focal adhesion of interest was chosen.

The CDM model was then iteratively strained by progressively pulling on all outer edge nodes to bring each of them closer to their corresponding FA. As described in Milan et al. 2013, this iterative process allowed the modeled cell to spread gradually onto the simulated substrate. This gradual process allowed nodes within the cell model to rearrange and form new connections based on the previously described interaction laws (see above, Table 1 & Table 2). After all selected outer edge nodes arrived at their corresponding focal adhesions, computation continued for several more steps so as to allow for stress relaxation within the simulated cell structure. These final steps are to prevent significant rearrangements during optimization. In other words, at this point, the cell model had reached its final spread shape and mechanical equilibrium.

Optimization phase: At this point, existing mechanical interactions (formed during the "spreading phase") represented the contractile cytoskeleton. This simulated cytoskeleton consequently pulled on its substrate adhesions. Yet at this point, nothing ensured the exactitude of these mechanical forces. So, since experimentally measured adhesion forces represent the external signature of the contractile cytoskeleton, we decided to optimize the CDM by taking experimentally measured adhesion forces into account. The modeled cytoskeleton would therefore be considered valid once the numerical and the experimental adhesion force signatures matched each other, i.e., the magnitude of the force exerted on each focal adhesion was the same. Doing this can be viewed as the resolution of an inversed mechanics problem. To numerically solve this inversed mechanics problem, we considered that the force exerted on each focal adhesion could be controlled independently, while other interactions would remain active. To control the tensile force exerted on the focal adhesion of interest, we assigned it an individual

identification number i (FAi) and a specific interaction law SFi between the perinuclear nodes and FAi.

Table 1: Parameter values of the various interaction laws used in the CDM*

Elastic Wire laws	**Rigidity K (nN/strain)**	**Prestrain ε_0**
short F-ACTIN (Actin filaments)	$3x10^{-4}$	$1x10^{-3}$
long F-ACTIN (Actin fil. in stress fibers)	$1x10^{-2}$	0.2 [24]
SF_i (stress fibers connecting FA_i)	To be computed	0.2 [24]
INTER.FIL (Intermediate filaments)	$2x10^{-2}$	-0.1
LAMIN (Nuclear lamina)	$4x10^{-2}$	0
INTRA-NSK (Intranuclear filaments)	$2x10^{-2}$	0
Contact laws	**Cohesion c (nN)**	**Rigidity S (nN/strain)**
CONTACT	0	/
MICROTUBULE (Microtubules)	0	1

Table 2: Table of interactions between the various node species represented in the CDM model the cytoskeleton substructures and the nucleoskeleton. For every law of interaction, the value of the maximum gap between nodes above which interaction vanishes is reported in μm in brackets. The interaction law SFi between Perinuclears and FAi was only activated in the cytoskeleton remodeling phase.

Nodes	**Nucleus core**	**Nucleus lamina**	**Perinuclears**	**Cell core**	**Cell membrane**	**FAs**
Nucleus core	INTRA-NSK (1) CONTACT (0.8)	INTRA-NSK (1) CONTACT (0.8)	CONTACT (0.8)	CONTACT (0.8)	CONTACT (0.8)	CONTACT (0.8)
Nucleus lamina		LAMIN (1) CONTACT (0.8)	INTER.FIL (20) CONTACT (0.8)	CONTACT (0.8)	CONTACT (0.8)	CONTACT (0.8)
Perinuclears			INTER.FIL (2) CONTACT (0.8)	short F-ACTIN (1) CONTACT (0.8)	INTER.FIL (3.5) CONTACT (0.8)	long F-ACTIN (35) CONTACT (0.8) SF_i (7.5)
Cell core				short F-ACTIN (1) MICROTUBULE (0.01)	short F-ACTIN (1) CONTACT (0.8)	short F-ACTIN (1) CONTACT (0.8)
Cell membrane					short F-ACTIN (1.5)	long F-ACTIN (3.5) CONTACT (0.8)
FAs						CONTACT (0.8) short F-ACTIN (1.5)
Substrate	CONTACT (0.8)	CONTACT (0.8)	CONTACT (0.8)	CONTACT (0.8)	CONTACT (0.8)	CONTACT (0.8)

Notably, as adhesion forces were readjusted, it consequently affected both force distributions within the CDM structure and the forces exerted on other FA. Adhesion forces were therefore adjusted iteratively, until adhesion force patterns were considered to match.

Initially, all SFi law rigidity properties Ki were set at a value of 1 N/strain. Then, for all succeeding optimization steps, Ki was multiplied by the ratio α. Such that:

$$\alpha = \frac{F_{FAi-calculated}}{F_{FAi-measured}}$$

At the end of each step, the relative error of measured and of calculated adhesion forces was assessed for each focal adhesion. When the relative error averaged less than 0.1% for all focal adhesions, the adhesion force patterns were considered to match.

2.2.6. Post-treatement

The mechanical index, "intracellular tension" latter referred to as T, was calculated as the sum of all Elastic Wire interaction forces traversing the transversal plane located in the middle of the cell and perpendicular to the direction of maximum tension. In addition, octahedral shear strain $\varepsilon_{nucleus\ shear}$ was calculated as the norm of nuclear strain differences in the 3 directions of space.

3. Results

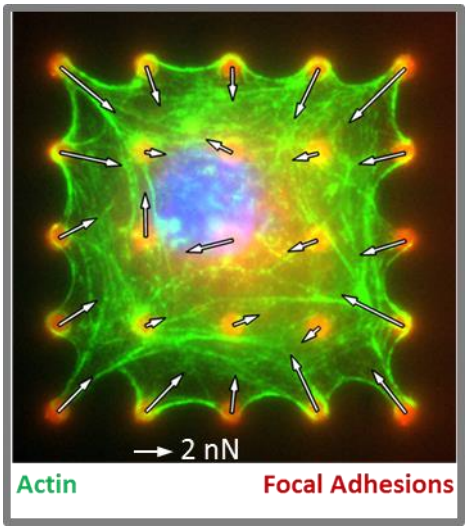

Figure 27: Microscope fluorescence image of cell on a bed of microposts.

The minimal distance between two microposts, i.e., focal adhesions, is 9μm from center to center. The actin network is labeled in green, focal adhesions in red, the nucleus in blue and adhesion forces represented as white arrows.

Experimental measurements show that the net adhesion force was higher on the Hard substrate than on its Very Soft counterpart (Figure 27, Figure 28 & Table 1). Nonetheless, substrate stiffness did not significantly affect projected cell area. In Figure 28 and Table 1, computation results indicate that intracellular tension increased in respect to higher substrate stiffness. The model infers similar conclusions in the case of the overall amount of tension transmitted to the nucleus and for nucleus strain.

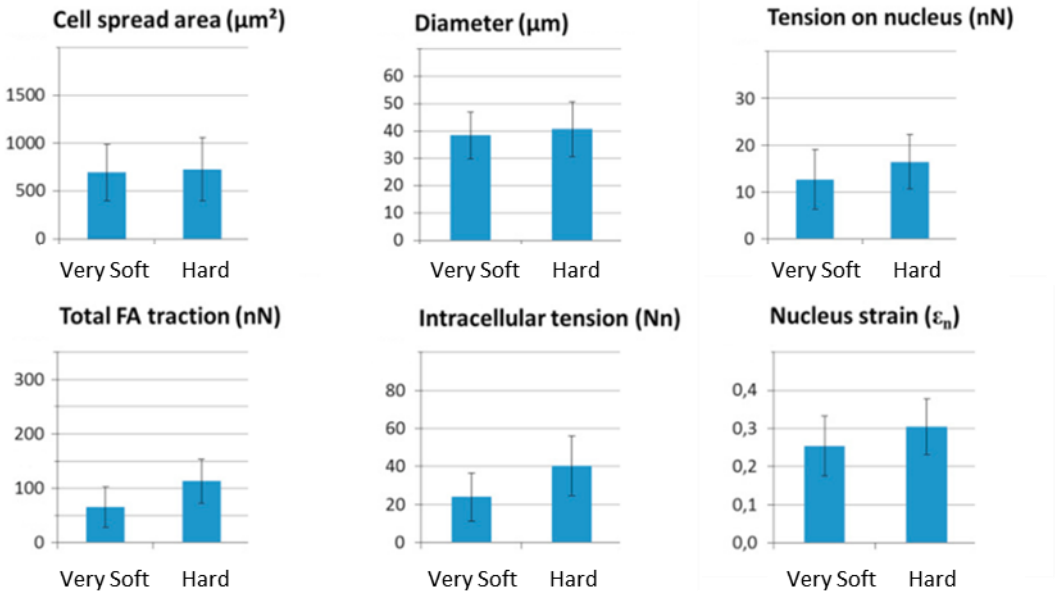

Figure 28: Evolution of mean values of cell spread area, cell diameter, total traction, nucleus strain in cells cultured on the Very Soft and Hard substrates.*

In, Figure 29 the CDM model is shown in typical specimens of cells adhering on Very Soft and Hard microposts. During the modeled spreading phase, the mechanical state of the CDM changed and the number of active interactions increased from 50,000 non-null force interactions, to 90,000 once the CDM had spread. When considering the whole cell sample (Very Soft, Hard, Hard+), the spread configurations had more tensile interactions (short and long F-ACTIN and INTER. FIL) and less compressive interactions (MICROTUBULE). While SF interactions (not stress fibers) reached forces of about 30–70 pN in average with a maximum of 150 pN, the magnitude of other tensile and compressive interactions were only about 0.1–1 pN. As substrate stiffness increased, stress fiber interactions were more numerous and more contracted. This indicates that substrate stiffness has a positive effect on cytoskeleton strengthening and stiffening (Figure 28). Furthermore, results showed an increase in stress fiber interaction rigidities (Ki) by an average factor of 50 and 70 times, on the Very Soft and Hard substrate respectively.

Table 3: Mean results*

In vitro cell measurements

	Microposts	
	Very Soft	**Hard**
Spread area (µm²)	694	729
Diameter (µm)	38	41
Aspect Ratio	1,02	1,1
FA number	16	18
Total FA traction (nN)	65	112
Mean traction on FA (nN)	4,4	6,5

Computational results

	Microposts	
	Very Soft	**Hard**
Cell strain ($\Delta D/D_0$)	1,56	1,72
Cell strain (D/d)	1,12	1,1
Intracellular Tension T (Nn)	24	40
$T/T_{initial}$	6,8	11,5
T/Total FA traction	0,4	0,4

Computation results on nucleus

		Microposts	
		Very Soft	**Hard**
Diameter (µm)		7,01	7,18
Strain	($\Delta dn/dn$ 0)	0,17	0,2
	Dn/dn	1,12	1,1
	ε_x	0,07	0,13
	ε_y	0,14	0,18
	ε_z	-0,43	-0,49
	$\varepsilon_{nuclear\ shear}$	0,25	0,3
Tension on nucleus (nN)		12,7	16,5
Tension on nucleus/T		0,56	0,41

The objective of iterative computation of cytoskeleton remodeling is to reduce the difference between the pulling force expressed by the model and the one measured experimentally for each

FA. Over the whole sample of cells, it only required 10 to 20 iterations to converge and to generate a contractile cytoskeleton that delivered a mean FA force error of less than 0.1% (Figure 30). Nevertheless, there were a very few FAs where the model was not able to yield results with such a high level of fidelity, which occasionally led to local errors lower than 10–30%. In these rare cases, additional iterations did not improve convergence. Between the round shaped CDMs to the end of the simulation, the intracellular tension increased by an average factor of 7 and 12 times in cells on Very Soft and Hard substrates respectively (Table 1). This increase in intracellular tension was partially transmitted to the nucleus via intermediate filaments (INTER.FILs). Initially slackened, INTER.FILs suddenly tightened under SFi tension, becoming active bonds between the stress fibers and the nucleus. The tension transmitted to the nucleus reached respective averages of 13 nN, 17 nN on the Very Soft and Hard substrates (Table 1). This consequently led to further nucleus deformation. As expected, nucleus deformation was higher on the Hard substrates compared to the Very Soft one (Figure 28). As expected, in the CDM model, intracellular tension correlated strongly (R=0.92) with total FA traction force (Figure 32) being equivalent to 35% of total FA traction (Table 1). While the nuclei strained linearly (R^2=0.86) due to the cytoskeletal tension, Figure 32 also shows that the cytoskeletal tension applied to the nucleus correlates with intracellular tension (R^2=0.74). Nonetheless, the shape of the cell also influences local distribution of intracellular tension forces and especially the tension transmitted to the nucleus. As matter of fact, Figure 32 also shows that nucleus deformation appears to be equally dependent on cell diameter (R^2=0.723) and intracellular tension (R^2=0.655). Since intracellular tension and net FA traction are related, from computations we were able to define the following equation as an approximate relationship linking the nucleus strain to the cell diameter (D) and the total FA traction.

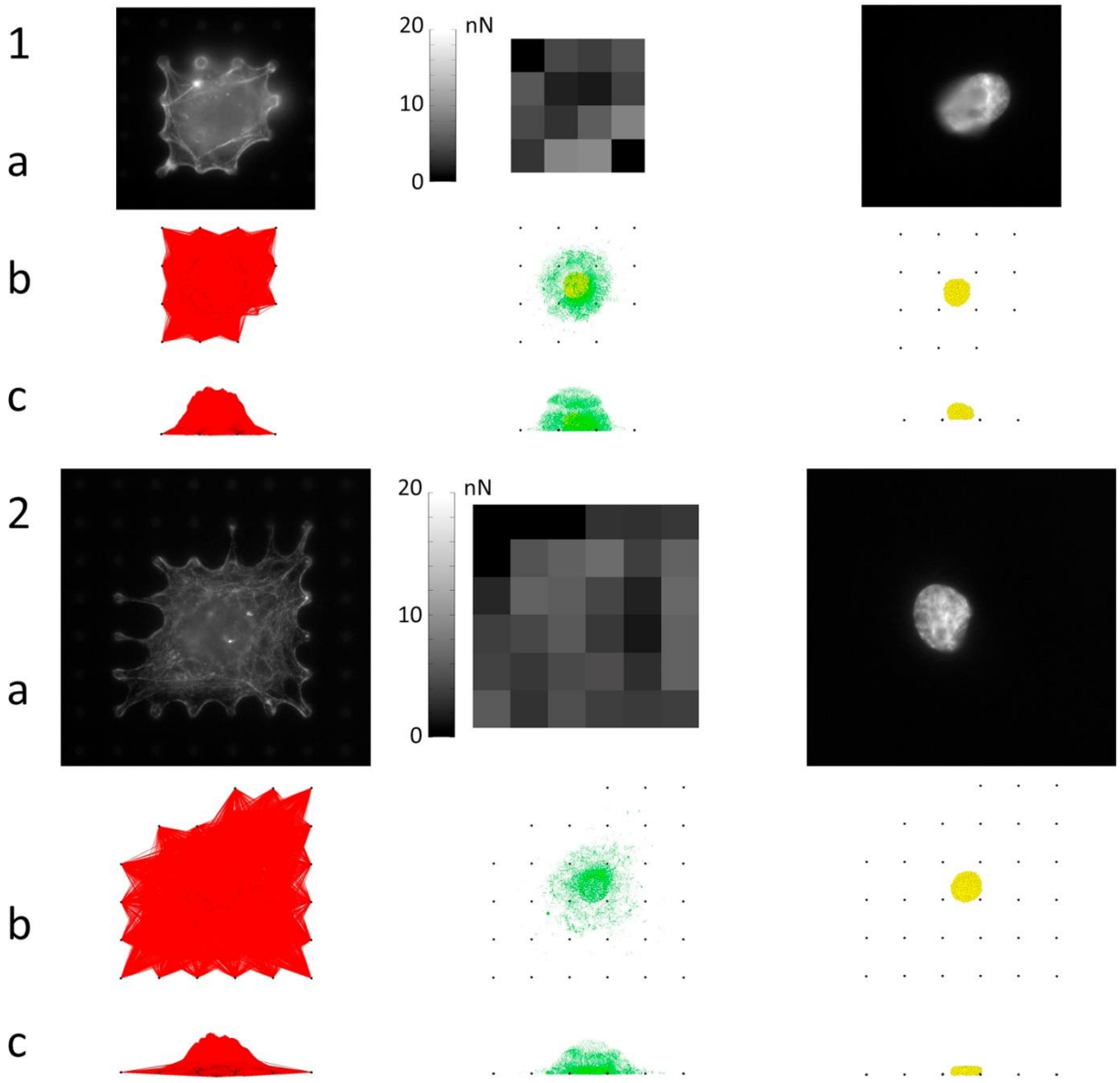

Figure 29: Computational results of cells 1 and 2 respectively cultured on Very Soft and Hard micropost arrays.*

a) Fluorescence actin network image (left), spatial distribution of experimentally measured adhesion force magnitudes (middle), nucleus (right).

b) Top view of fully spreading CDM model after matching experimental adhesion conditions, FA nodes in black, tensile interactions in red, compressive interaction in green; strained nucleus in yellow.

c) Side view of fully spreading CDM model after matching experimental adhesion conditions, FA nodes in black, tensile interactions in red, compressive interaction in green; strained nucleus in yellow. Space between microposts is 9 mm.

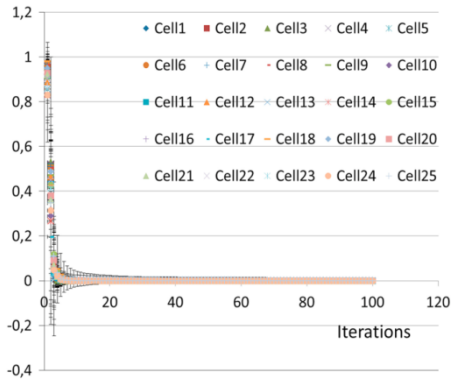

Figure 30: Evolution of mean relative error of CDM adhesion forces for each computational iteration. Results show convergence for all cells in less than 30 iterations.*

Equation 6

$$\varepsilon_{nucleusshear} = 0.0044\sqrt{totalFaforce * D}$$

Equation 6 allows us to estimate nucleus strain based on experimental measurements of cell diameter and total FA traction. Over the whole cell sample, this simple equation correlates well (R^2=0.85) to CDM nuclear strain. According to the model, these findings indicate that the cell shape has an influence on the distribution of intracellular forces. However, what may be more interesting is that the model indicates that the nucleus is not dissociated from this effect. Overall deformation of the nucleus may thus represent a mechanical signal during cell adhesion. Nuclear deformation, averaged 9 and 13% in cells respectively on both Very Soft and Hard microposts potentially inducing specific gene transcription[11].

Since substrate stiffness modulates net adhesion force (Figure 28), Eq. (1) may thus indicate the direct influence of substrate stiffness on nucleus strain.

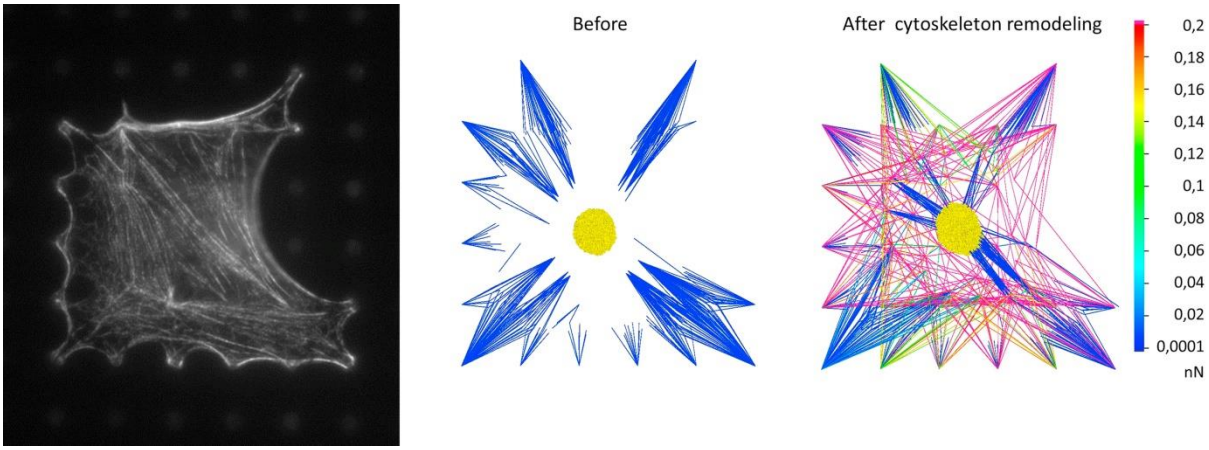

Figure 31: In vitro (left) vs in silico (right) cytoskeleton.*

The real cytoskeleton was imaged by immunofluorescence. The computed cytoskeleton is shown at the end of spreading phase, before and after cytoskeleton remodeling; only the sub-structures of the cytoskeleton corresponding to a range of force between 2 and 5 pN (B) are displayed.

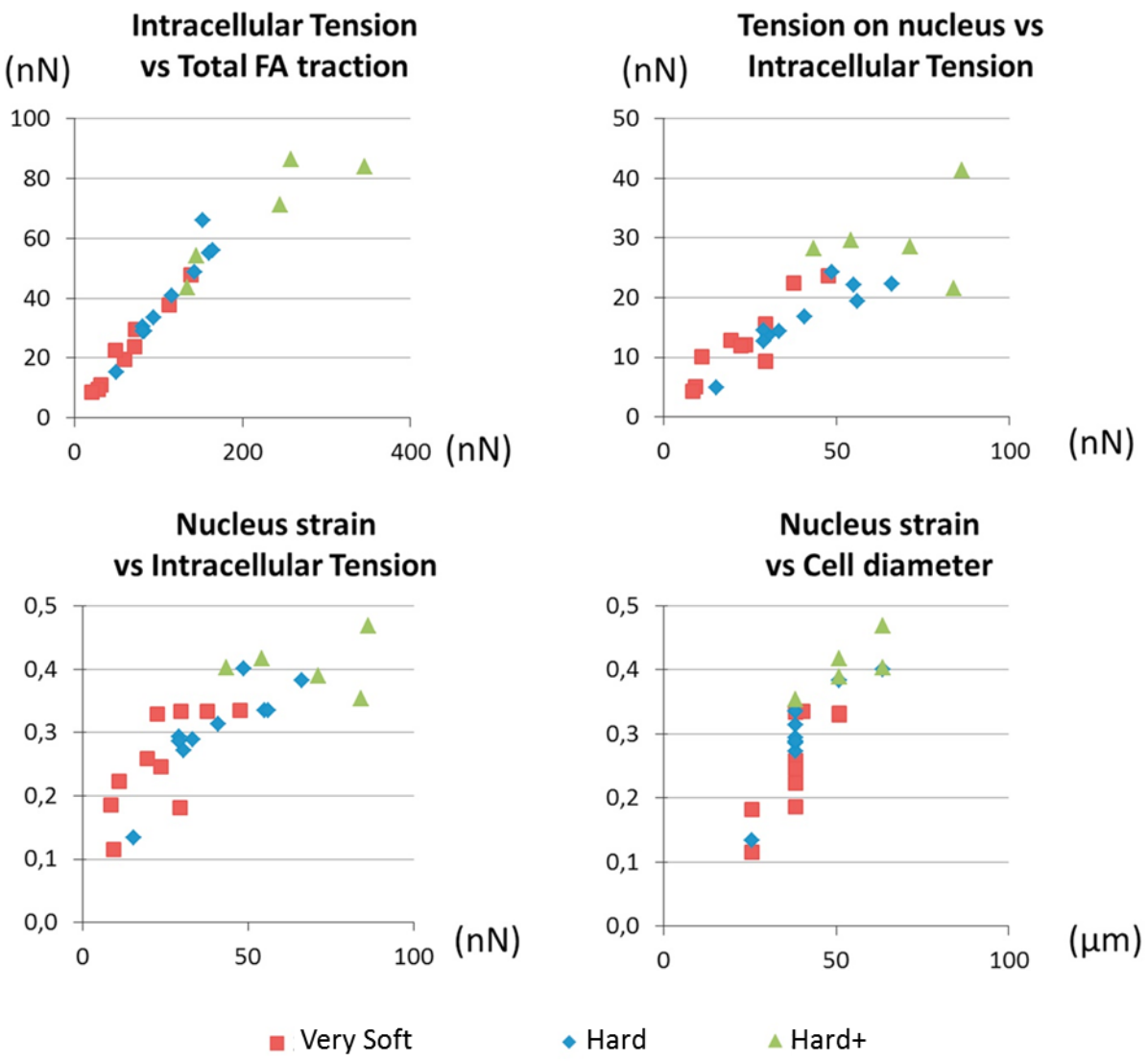

Figure 32:*

A) Evolution of intracellular tension vs total FA traction on Very Soft, Hard and Hard+ substrates with a strong positive correlation (R^2=0.92).

B) Evolution of tension transmitted to nucleus vs intracellular tension on Very Soft and Hard substrates (R^2=0.7434).

C) Evolution of nucleus strain vs intracellular tension (R^2¼0.655)

D) Evolution of nucleus strain vs cell diameter (R=0.723) on Very Soft and Hard substrates.

4. Discussion

4.1. Representation of the contractile cytoskeleton in the CDM model

This multi-interaction model is a way to represent the complex cytoskeletal network composed of intertwined filaments. Furthermore, it is a modeling attempt to represent the evolving mechanical structure of tensile and compressive forces found in the cell. For instance, one of the modeled cytoskeletons, was composed of 40,000 actin filaments, 1 μm in length, were diffused in a tensile network that also included 12,000 10 μm long actin filament forming long stress fibers and 7,000 1 μm-microtubules forming long chains of compression. In addition, 1,200 elastic filaments composed the nucleus lamina, each individually bearing forces generally between 1 and 10 pN.

In the CDM model, the distribution of stress fibers and their contractility are not initially imposed and result from the optimization process. Figure 31 displays the spatial arrangement of the stress fibers in one of the cells adhering on the Hard+ substrate. When it is compared to the actin image, the model shares similar principal orientation of stress fibers. Over the whole cell sample, model predictions of nucleus position differed by about only 5 μm in average from in vitro observations. The nuclear strain ratio (grand axis divided by the small axis) computed by the model only differed by about 25% in average.

4.2. Comparison between the present and previous version of the CDM model

In Figure 30, the first iteration corresponds to the model after spreading and before remodeling. This initial state corresponds to the previous configuration of the CDM model which was described and used in Milan et al.'s previous study[92]. This initial state is associated with an important error in FA traction forces of about 80–100% on average compared to their experimental values. This means that the past CDM model cannot compute a cytoskeleton that behaves as the real one does. On the contrary, as depicted by Figure 30, the iterative cytoskeleton remodeling process allows the CDM to closely mimic the pulling pattern of the observed cell. By incorporating in the model new conditions of cell-specific adhesion, we can safely assume that current results are more accurate than what we were able to present in our previous study.

4.3. CDM model and potential insights in cell mechanobiology

The CDM model is able to indicate how observable parameters such as nucleus strain, cell shape and FA forces interact, as experimentally observed[18,100]. Additionally, the CDM model is also able to take into account parameters that are currently unobservable, such as intracellular tension (Figure 33) and the amount of force transmitted to the nucleus. For instance, the present study reveals the positive effect of cell spreading on the increase of tension transmitted to the nucleus. Computed nuclear strain is equivalent to what has been experimentally observed as a possible factor modifying gene expression and inducing cell differentiation[11,101,102]. By analyzing how nucleus shape and cytoskeleton tension interact, our study proposes potential parameters which could be involved in mechanotransduction during cell adhesion. For instance, the CDM model may indicate the influence of spreading on force transmission to the nucleus. At the end of spreading and before remodeling, nucleus strain (*$\varepsilon_{nucleus\ shear}$*) respectively averaged average 14% and 18% in cells cultured on Very Soft, Hard, Hard+ microposts. We found that after the remodeling phase, nuclei strained further up to 25% (Very Soft), and 30% (Hard). Similarly, after remodeling, the tensile load carried by intermediate filaments increased by a factor of 4–5 to reach, −12.7 nN (Very Soft), −16.5 and nN (Hard).

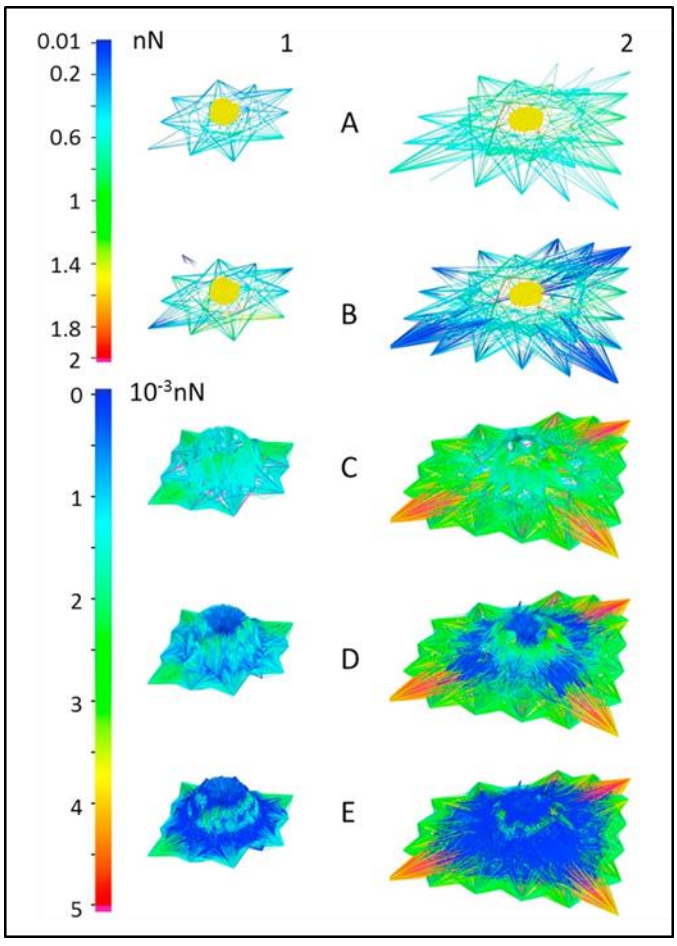

Figure 33: Contractile CDM substructures of typical cells on Very Soft (1) and Hard (2) substrates. A-E) Shown substructures belong to the following domains (A) 2-0.2 nN line; (B) 2 nN-5 pN; (C) 5 pN-0.1 pN; (D) 5 pN-0.01pN; (E) 5 pN-0.001 pN. Strained nucleus in yellow.*

Equation 6 relates the nucleus strain only with FA traction forces and cell diameter, some additional computations launched on few star-shape cells from Yang et al. (2011) showed that nucleus strain may also depend on cell aspect ratio[103]. The results are not shown because the size of the cell sample was not statistically significant[104].

5. Conclusion

Being able to mechanically represent the cytoskeleton and the nucleus with very limited information is an undeniable advantage provided by the CDM. The dynamically evolving tensegrity like structure of the CDM allows it to better represent the cellular structure than what is generally proposed by other tensegrity inspired models that rely on a fixed number of connectivity. Furthermore, micropost adhesion force measurement allowed us to numerically represent mechanical boundary conditions with a lot more accuracy, therefore leading to more pertinent computational results. In addition, the micropost arrays have the advantage of isolating the effect of micropost bending stiffness as being the exclusive varying between the Very Soft and Hard substrate.

This newly improved version of the CDM model therefore allowed us to show that substrate stiffness increases cell traction and that intracellular tension is neither directly, nor linearly transmitted to the nucleus. CDM model indicates the nucleus is more stimulated by tension forces in the case of highly spread cells, which in the case of stem cells is known to promote commitment into osteoblasts or fibroblasts[7].

On the other hand, the results provided by the CDM remain questionable and hard to interpret as the internal structure of the model lacks true resemblance with the original structure of the cell. In the next chapter, we will therefore discuss an image based modeling strategy.

CHAPTER 2
COMPUTATIONAL TENSION MAPPING IN ADHERENT CELLS. AN IMAGE BASED MODEL

NB: The following study presents work done during the thesis, it has is published in the online peer reviewed journal PLOS Ones[105].

1. Introduction

Since cells are sensitive to mechanical stimuli, we decided to develop a mechanical model that would be able to estimate and then map intracellular forces within human adherent cells. To do so we decided to create an image based mechanical model whose structure was defined based on microscope images of the observed cell. The objective was therefore to develop a modeling method and prototype so as to increase biofidelity in our analysis of cell mechanics (Figure 1).

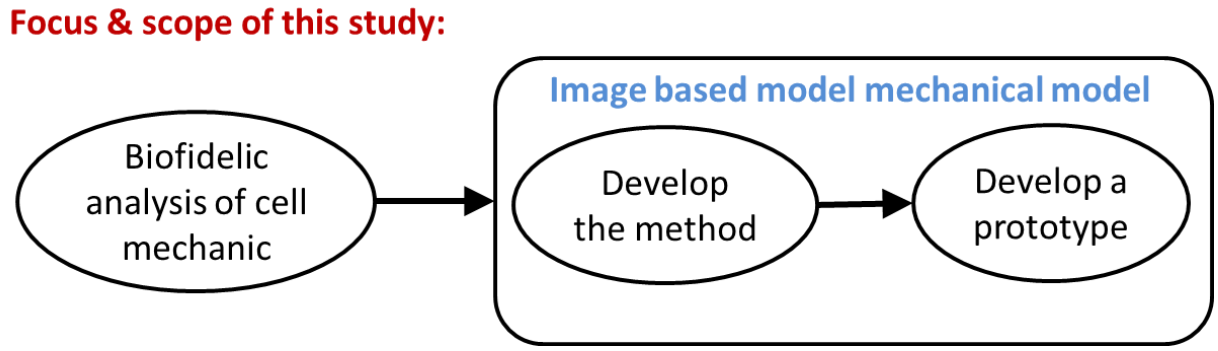

Figure 34: Scope and focus of this study

This goal raised the following question:

Problematic:

"How can we create an image based model that would allow us to measure tension forces within the actin network of an adherent cell?"

And more precisely:

"How can these mechanical results be analyzed to have relevant biomechanical meaning?"

To achieve this goal we decided to use three different superimposed images of the cell as input.

The first image is of the cell's focal adhesions, the second of the actin network, and the third is of the nucleus. At first we applied this method to study 8 different fibroblast cells that were allowed to adhere freely on a flat glass substrate. Pixels that represented the cell were converted into mechanical nodes. A label was given to each node based on its parent pixel: actin, vinculin or nucleus. Furthermore, actin labels were determined based on the brightness level of their parent pixels. The model was designed to generate a mechanical interaction between direct neighbor nodes. The intensity of each interaction was determined based on the weakest label contained within a pair of neighbor nodes.

The whole set of these neighbor to neighbor tensile interactions then formed a contractile network meant to represent the cell's actin network.

Vinculin labeled nodes were, however, fully constrained so as to represent the anchoring nature of focal adhesions. Tensile interactions between direct actin and vinculin neighbors allowed the contractile actin network to pull on focal adhesion. This method therefore allowed the modeled cells to have similar mechanical properties to those of their original counterparts. In addition, cell imaging allowed a more coherent representation of local mechanical properties as it determined node positions and the intensity of the interactions between these nodes.

2. Methods

In order to estimate intracellular tension forces transiting throughout the actin network, we developed a mechanical model of the cell. The mechanical structure of the model is generated based on microscope images of an actual adherent cell. The model therefore uses three different superimposed fluorescence microscope images of the cell to self-generate. Each image respectively represents focal adhesions, the actin network, and the nucleus.

The real objective of this initial study was to serve as a proof of concept of this modeling method. To do so we used this modeling method to study 8 dental pulp fibroblasts cells cultured in adhesion on a flat glass substrate. The model converted the set of images into a mechanical model by converting pixels mechanically representing the stained cell that were converted into mechanical nodes. A label was attributed to each node depending on what it represented: vinculin, actin, and its level of expression or the nucleus. Vinculin labelled nodes were fully constrained to serve as anchor points for the cell. Vinculin labeled nodes were also connected to actin labeled nodes by tensile interactions, so as to simulate the actin network's pulling effect onto the surrounding substrate. In addition the model also generates tensile interaction between each actin labeled nodes so as to present internal stresses. But the intensity of each tensile interaction between direct actin neighbor nodes is governed by the labels themselves, so that parts of the network representing more actin may generate more tensile stress and vice versa.

2.1. Biological protocol

2.1.1. Cell culture:

Human pulp fibroblasts were prepared from immature third molars. Briefly, the teeth were obtained from subjects between the age of 16–21 years old in compliance with French legislation.

After extraction, the teeth were washed and the apical portions removed. The extirpated dental pulp was minced, and explants were cultured in 100-mm-diameter culture dishes containing minimum essential medium (MEM) supplemented with 10% fetal bovine serum, 100 UI mL−1 penicillin, 100 µg mL−1 streptomycin and 0.25 µg mL−1 amphotericin B and placed at 37°C into a humid incubator with an atmosphere of 5% CO2. Cells from confluent cultures were collected by trypsinization and sub-cultured in T75 flasks.

2.1.2. Cell imaging by immunofluorescence double-staining:

Pulp fibroblasts cells were allowed to spread for a period of time of 24h in 8-well glass culture chambers. Isolated cells were fixed with 4% paraformaldehyde for 20 min at 37°C. After washing with phosphate buffered saline (PBS), cells in the chambers were incubated in blocking/permeabilization buffer (3% BSA, 0.3% Triton X100 in PBS) for 45min at room temperature an incubated overnight at 4°C with mouse anti-human vinculin IgG (1/100), diluted in PBS containing 1% BSA and 0.3% TritonX100. After washing with PBS 0.1% bovine serum albumin (BSA), cells were incubated for 45 min with the fluorescent secondary antibodies Alexa Fluor-594 goat anti-mouse IgG (1/400), phalloidin conjugated with Alexa Fluor-488 (1/2000) for actin staining, and DAPI (1µg/ml) for nuclear counterstaining, all diluted in PBS containing 1% BSA and 0.3% TritonX100.

After washing with PBS, the slides were mounted with Glycergel, kept at 4°C and visualized with fluorescence equipped light microscope (Axio Observer.A1, Carl Zeiss Microscopy, Jena, Germany). Phalloidin stained actin, vinculin, and DAPI were respectively captured on three different color channels (RGB) so as to observe each cellular component separately. 3 images of the same size and resolution were obtained, one representing actin, another vinculin and the last one the nucleus. Each image was treated separately. The image representing vinculin was treated to increase contrast on focal adhesions. Once extracted from the image, the cell is 62 µm in length, 35 µm across and is defined by about 35 000 pixels. Images were stored using the TIFF format to avoid information loss.

2.1.3. Estimating focal adhesion forces:

A linear relationship has been reported between the area covered by vinculin in focal adhesions and the value of traction forces magnitudes transiting through focal adhesions[16]. The expressed relationship is 5.5 nN/µm2. Other studies confirmed the existence of a linear relationship between focal adhesion size and force intensity[15, 20]. One study argued that this relationship only applies to focal adhesions larger than 1 micrometer squared[20]. Thus, in this study, we only considered focal adhesions larger than 1 µm2.

2.2. Constitutive equations behind the mechanical model of the cell

As previously stated, the main idea behind the numerical method was to convert pixels into mechanical nodes, so as to generate a mechanical model of the cell. Focal adhesions were fully constrained so as to mimic their anchoring properties, while actin network nodes and nucleus nodes were not. Instead the actin network and nucleus nodes were mechanically connected to their direct neighbors by tensile interaction. So as to work around computational limitations, the number maximum of nodes was limited to 10 000. In general, it led to the conversion of a group of 4 pixels into a connected node. Respecting physical scales and dimensions led to the definition of a distance of 0.58 µm between direct neighboring nodes (4/8). Tensile elastic interactions

would then be generated between actin nodes. The interactions were pre-stressed, so as to mimic the contractile properties of the simulated actin network. The laws used to define these tensile interactions are identical to the inter-tension law used in the CDM model (page 50.)[93, 92] .

As a simplification the initial pre-strain value was the same for all interactions. Its value was set to 20%, in accordance with the mean experimental value found by Deguchi et al. [106].

To restrain tensile interactions between direct neighbors, the visibility threshold gap gv was given a value greater than g0 and lower than $\sqrt{2}g_0$ so that diagonal neighbors would not be allowed to interact. We thus set g_v equal to $1.1g_0$.

The whole set of these tensile interactions composed a pre-strained tensile network that was spatially organized in accordance with the microscope images of the observed cell. All actin and nucleus nodes, were mechanically unconstrained during computation. The model ran until mechanical equilibrium, this led to local tensile forces adjustments.

The same modeling strategy was used to model microtubules and an intracellular compression network, as described in Chapter 1 page 51 and in the introduction Figure 21 page 42. We defined spherical contactor diameter equal to 0.58 µm.

2.3. Converting Nucleus & Focal Adhesions pixels into mechanical nodes

Custom noise removing filters were applied on nucleus and vinculin images and then binarized for object extraction. Corresponding nucleus and vinculin nodes were then generated at the same node density as that of the actin network. Focal adhesions were automatically identified by using NHI's ImageJ software[107,108].

Focal adhesion areas were used to estimate the net adhesion forces generated by the cell. Actin-vinculin and actin-nucleus node interactions were the same mechanical interaction laws than the ones we used for the actin network. The only technical difference is that interactions stiffness between nucleus nodes were all 10 times larger than their strongest actin network counterpart.

2.4. Parametric analysis to determine intracellular forces

Earlier we made the simplification that local actin density was proportional to local actin stiffness. To include this simple idea in the model we increased interaction stiffness proportionally to the observed actin density observed on the image. This simple principle allowed us to take into account the heterogeneous distribution of an actin filament in the model and its effect on cellular mechanics. However, the proportionality coefficient linking actin pixel gray values to interaction stiffness was still missing at this point. To solve for this missing coefficient we used inverse mechanics principles, in other words we did a simple parametric analysis to find the appropriate coefficient value so that the net adhesion forces generated by the cell model and the real cell would be of equal value.

We first normalized the image so that actin gray values, noted c ranged between 0 and 1. The value 0 implies a dark area with no actin; while a value of 1 represents a white area, with the highest amount of actin.

Pixels from actin images were split into 10 different labels ranging from I_1 to I_{10} each corresponding to an equal sized gray value domain. With I_1 being the label representing the lowest actin densities, while highest actin density was referenced by label I_{10} , such that:

Equation 7

$$\forall c \in]0;1\,] \Rightarrow \exists!\ i\ \in [\![1;10]\!]\ such\ that\ \ c \in C_i =]0.1 \cdot (i-1)\,;0.1 \cdot i]\ \Rightarrow\ l_i$$

This denomination allowed our custom built program to automatically convert pixels into corresponding labeled nodes. The stiffness value K_i of each of the interaction laws was defined by the node label I_i that represented the lowest actin value li value. For instance, for a given label valued i, the stiffness K_i is given by the following equation:

Equation 8

$$K_i\ =\ a * c_{i\,max}$$

where $c_{i\,max} = 0.1 \cdot i$, is the highest gray value contained within C_i. Interactions between nodes with two different labels interacted as if they were both from the weakest label. The method we developed to calculate the value of the coefficient a, linking stiffness to actin density, will be the topic of the next sub-section.

2.5. Solving the equation between model stiffness and actin density

The pre-stressed nature of the modeled actin network consequently led to spontaneous intracellular tensile force generation. The imbalance of intracellular forces consequently made the cell model pull on its focal adhesions. Based on the interaction laws we chose to model the contractile actin network, we can conclude that adjusting that overall interaction stiffness will modify intracellular forces and thus consequently impact how the modeled cell pulls on its surroundings. We thus decided to use the external pulling forces generated by the cell model as our analysis criterion. We compared the net pulling force generated by the model with the one exerted by the cell on its surroundings. To do this, we did a parametric analysis by either proportionally increasing or reducing overall interaction stiffness within the cell (Equation 8). Meanwhile, our model kept comparing the net adhesion force generated by the model to the one that had previously been experimentally observed. Once the external forces generated by the model were deemed equivalent to the ones generated by the cell, we considered that the modeled actin network was a mechanical equivalent to that of the cell.

The methodology used to converge toward the solution is straightforward. Increasing a would increase the sum of pulling force on focal adhesions, or pull less if a decreased. Finding the solution was thus an iterative process governed by a simple gradient based solving algorithm. The number of necessary iterations was kept to a minimum by interpolation to converge faster to the desired solution.

2.6. Additional computational parameters

Nodes masses were set to equivalent water density in respect to the apparent free volume between nodes. As a result node masses were all equal to 0.8pg. The model was allowed to rearrange during computation. Tensile interaction strains were nonetheless hypothesized to relatively constant along the stress fibers. In other words, tension forces were to remain the same along stress fibers throughout the computation, thus implying that the force between two nodes was mostly determined by the weakest label i of the two. The configuration of the mechanical system therefore implied a stiffness of value K_i and a constant pre-strain ε_0 of 20%. Yet since the stiffness K_i depends on the corresponding pixel gray value c_i, we can argue that the force intensity is proportional to visual actin density. We named this proportionality coefficient a.

In other words we can use the results of the parametric analysis to solve (Equation 9) for the value of a that links visually actin density to local intracellular tension T. We used the LMGC90 as a numerical solver. The model was computed for 600 time steps of 300 µs each.

Equation 9

$$g \approx g_0 \Rightarrow T \approx -K_i \,.\, \varepsilon_0 \approx -a * c_{i\,max} \,.\, \varepsilon_0$$

Once the value of coefficient a was acquired, we were able to exploit the image directly by converting pixel gray values into intracellular tensions.

To illustrate, a low resolution model would be represented by a proportionally low number of interactions, thus implying elevated force magnitudes per interaction, while a higher resolution model would be represented by a higher number of interactions, leading to low force magnitudes per interaction. We can, however, divide T by the minimal spacing between two nodes to reduce the influence of nodal density. At this point we obtain T_{cl} which represents the density of force transiting through a segment crossing the 2D model of the cell. T_{cl} is thus expressed in nN/µm as a cross-linear tension.

By analogy, T_{cl} represents a density of force that is the 2D equivalent to a stress tensor expressed in 3D. Therefore, in 2D to estimate the intra-cellular density of tension within the model, while remaining independent of the resolution of the model, i.e., the mesh size, requires the use of T_{cl}, the cross-linear tension (or cross-linear density of tension) defined as:

Equation 10

$$T_{cl} = \frac{T}{d_0} \approx -a * c_{i\,max} \,.\, \frac{\varepsilon_0}{d_0}$$

As a consequence we could define $T_{cl\text{-}max}$ as the cross linear density of force corresponding to the highest value of actin density, i.e., which relates to the highest actin concentration represented by label number 10 ($c_{10\,max} = 1$).

Equation 11

$$T_{cl-max} \approx -a * c_{10\,max} \,.\, \frac{\varepsilon_0}{d_0} = -a \,.\, \frac{\varepsilon_0}{d_0}$$

We then used all inter-tensions generated by the model to calculate the mean tension value of all actin interactions that we named $\boldsymbol{T_{mean}}$. This allowed us to introduce $\boldsymbol{T_{mean\text{-}cl}}$ the cross linear mean inter-tension defined as:

Equation 12

$$T_{mean-cl} = \frac{T_{mean}}{d_0}$$

Since $\boldsymbol{T_{mean}}$ is based on the averaged tension value of all the interactions within the cell it can therefore be considered as whole cell mechanical index.

2.7. Estimating tension transiting via parallel actin fibers

We will now see how we can use the image of the actin network to measure tension within parallel actin filaments. But first we need to consider that the gray values of an image can be readjusted to range between 0 (dark) and 1 (white). A fluorescent image of the actin network with an appropriate contrast would thus expressed areas with no actin as dark (0) and areas with the highest actin density as white (1). At this point, the model enabled to define $\boldsymbol{T_{max-cl}}$ as the cross-linear tension value of the brightest pixel within the image. In perspective we can express a local cross-linear value as:

Equation 13

$$T_{cl} = T_{max-cl} * c$$

We can thus conclude that the tension transiting via a stress fiber can be expressed as:

Equation 14

$$T = \int_0^L T_{cl} \cdot dl \text{ with L being the width of the stress fiber.}$$

To estimate tension transiting through the target filaments we need:

- $\boldsymbol{T_{max\text{-}cl}}$, cross-linear tension corresponding to the highest actin density
- $\boldsymbol{\bar{c}_{cross}}$, measure the gray values along our target filament's cross section ($[0; 1]$)
- $\boldsymbol{\emptyset_{SF}}$, the diameter of the cross section

But, instead of calculating the integral, it is equivalent and simpler to measure the average gray value and multiply it by the width of the target filaments.

Which then enabled us to calculate the amount of tension transiting through the given a stress fiber ($\boldsymbol{T_{SF}}$) with the following equations:

Equation 15

$$T_{SF} = T_{cl-max} \cdot \bar{c}_{cross} \cdot \emptyset_{SF}$$

3. Results

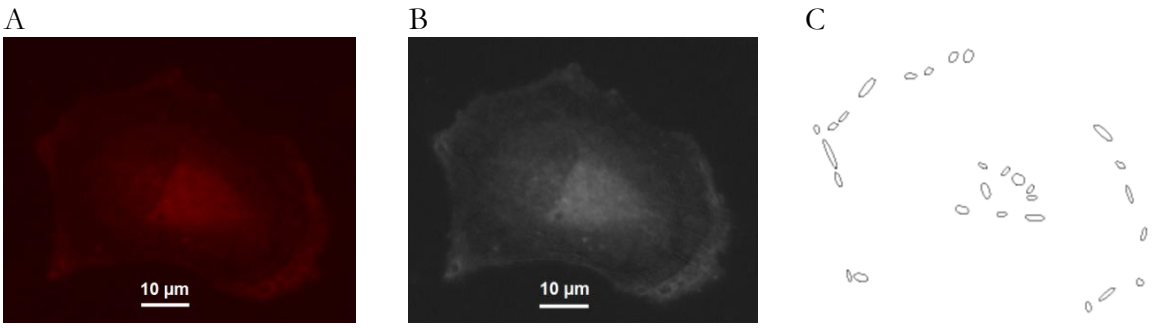

Figure 35: Images of the example cell

A) vinculin staining

B) vinculin staining & view of focal adhesions

C) focal adhesions larger than 1 µm² detected by ImageJ after image treatment.

3.1. From focal adhesion size to cytoskeleton pulling force

We used vinculin stained focal adhesion size to roughly estimate the sum of pulling force magnitudes exerted by each cell (Figure 35). Focal adhesions smaller than 1 µm² were ignored in our estimation since their size is not proportional to the amount of tensile force transiting through them (Figure 36).

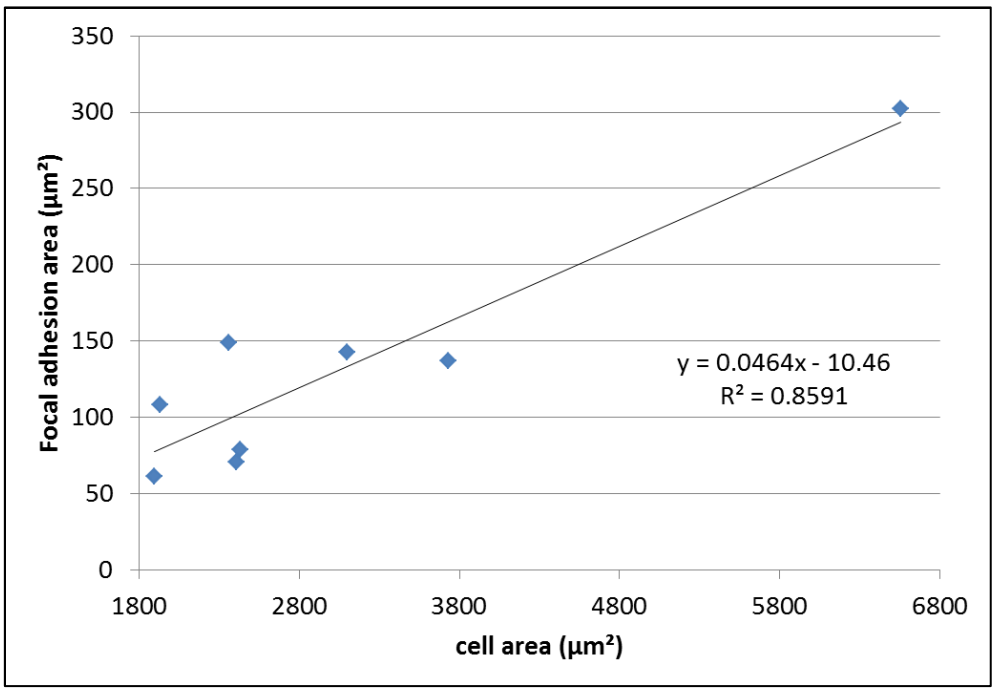

Figure 36: Focal adhesions area vs cell area. We notice a linear relationship between focal adhesion area (μm^2) and cell size (μm^2) for 8 cells.

3.2. From cell imaging to a biofidelic reconstruction of the contractile actin network

Actin expression of our Cell Example is shown in (Figure 35). To constitute the contractile system representing the actin network, pixels of the image were transformed into interacting nodes labelled according to actin density. Interactions between nodes acted as pre-strained elastic rubber bands whose stiffness was proportional to local actin density (Figure 37). Yet at this point, the coefficient of proportionality ***a***, of each cell, remained unknown.

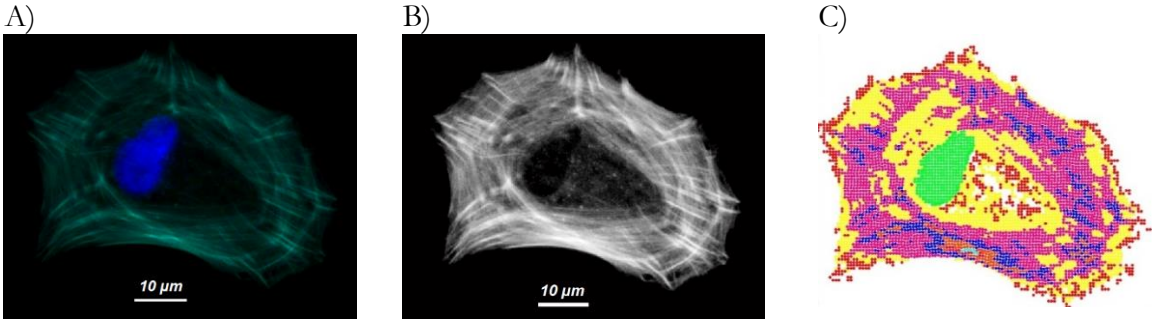

Figure 37: Actin and model images of the cell example:

A) Superposition of actin in green and nucleus (DAPI) in blue

B) Image of actin network after refinement treatment.

C) Pixels were transformed into labelled nodes using a custom built Matlab™ script. Nodes mechanically interacted between each other according to their respective labels.

3.3. Finding the missing link between actin density and stiffness

In the method we presented ***a*** as the coefficient links interaction stiffness and actin density. A parametric analysis of coefficient ***a*** showed that tension within the model and the magnitudes of the pulling forces exerted by the modeled cell's surroundings increased when coefficient ***a*** increased and vice versa. An automated parametric analysis of coefficient ***a***'s therefore allowed us to compared the sum of adhesion force generated by the model with what was estimated based on focal adhesion size. When both numerical and experimental adhesion forces were equivalent, the value of a was considered to have been found.

This parametric analysis enabled us to evaluate the coherence of the model and its potential variations. To access the influence of internal compression bearing elements such as microtubules, we thus decided to test two scenarios: one where passive internal compression forces were enabled and another one without any.

- Scenario MT^{+}: internal compression force enabled (with microtubules) (Figure 1 a1, b1 and c1)

- Scenario MT^{-}: internal compression force disabled (without microtubules) (Figure 1 a2, b2 & c2)

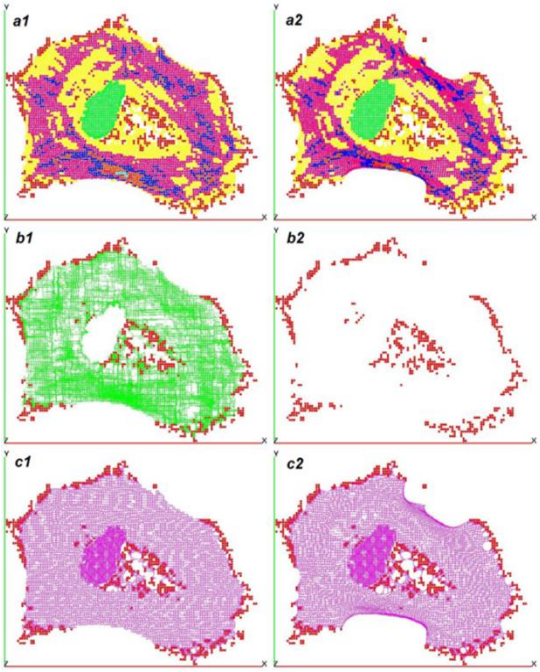

Figure 38: Model images.

Cell Example: Left: scenario with microtubules (MT+); right scenario without microtubules (MT-). A) Interaction nodes and spherical contactors, network of B) compressions, C) tensions. Model MT+ was able to retain its initial shape contrary to model MT-. This seems to indicate that the intracellular compression network contributes to cell morphology.

A parametric analysis of coefficient ***a*** was conducted for both scenarios. The shape of one of the modeled cells can be observed in Figure 38. Both columns show the modeled cell after 600 calculation steps of 300 μs each, for a = 4.

The first column shows the modeled cell capable of generating passive compression forces, while the second column shows the computation results when passive internal compression forces are disabled. A visual comparison clearly reveals that passive internal compression forces play a role in overall morphology. The shape of the modeled cell is preserved when intracellular compression is enabled. When internal compression forces are disabled, the cell model changes shape during computation. We can observe in this case that the modeled cellular edge retracts inward due to internal contraction in areas that are not firmly anchored by adhesion nodes. Similar results were observed for the other cells (results not shown), although retractions were less noticeable when adhesion nodes were uniformly distributed at cell edge. Based on the results expressed by the model we can assume that internal compression forces are necessary to maintain cellular shape.

After a few calculation steps the MT+ cell model were able to spontaneously generate compression forces. As internal compression would therefore counter balance internal tension, for a given value of a, each MT+ cell model consequently pulled less on its focal adhesions than its respective MT- counterpart. Furthermore, some simulated cells required intracellular compression to maintain their initial shape.

For both types of scenario (MT+ & MT-), the sum of adhesion force magnitudes generated by the model was almost linearly proportional to the value of coefficient a (Figure 39: Sum of FA forces.). Such that:

$$\mathrm{F}_{measured} = \propto \cdot a - \beta \quad \text{with} \quad \begin{cases} \mathrm{F}_{measured} \\ \propto : slope\ coefficent \\ \beta : constant \end{cases}$$

In the case of our modeled cell:

Equation 16

- Scenario MT^{+}: $y = 72.8 \cdot \mathrm{a} - 18.2$; R^2=0.99

Equation 17

- Scenario MT⁻: $y = 77.0 \cdot a - 19.9$; R^2=0.95

The R^2 value varied between cell to cell, while still remaining close to a value of 1. In addition, in all cases when trying to linearly express y as a linear function of ***a***, increasing time step resolution brought the value of R^2 closer to 1 and that of β closer to 0. These results indicated that y is linearly proportional to ***a***. We therefore used this reasoning to justify the fact that we could linearly interpolate the ideal solution.

On the other hand, the value varied quite significantly for each modeled cell, which can be explained by the following reasons:

- focal adhesion force values varied from cell to cell
- each cell is structured differently
- fluorescence intensity may vary from cell to cell

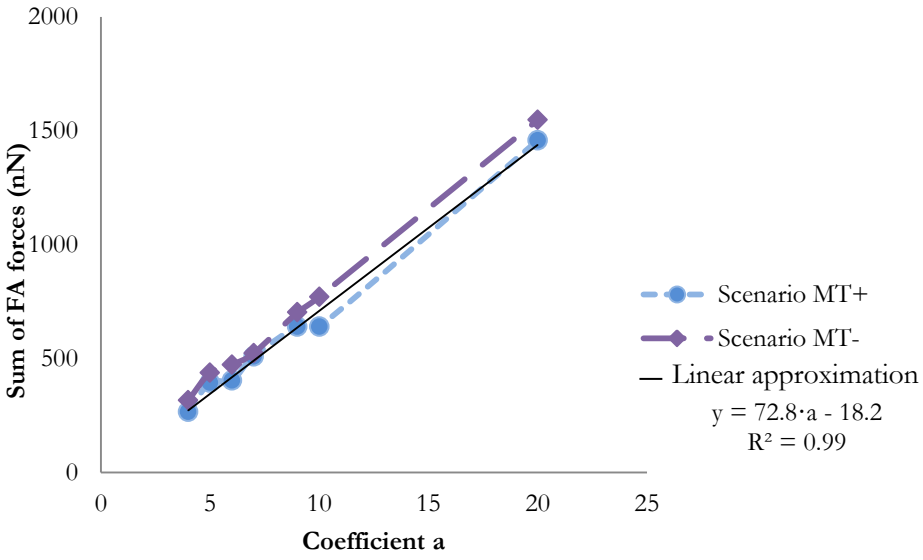

Figure 39: Sum of FA forces.

For each simulation of scenario MT+ we made coefficient ***a*** *vary between 1 to 15, the sum of focal adhesion forces output by the model ranged from* $F_{a=1}$ *to* $F_{a=15}$*, which included the value. Knowing that the sum of focal adhesion force magnitudes was* $F_{measured}$*, we used the linear interpolation from Scenario MT+ (Equation 16) to solve for a.*

3.4. Stability and computation quality

To quantitatively assess the stability of the cell model, we used free run length. We compared overall model stability between MT+ & MT- at the end of computation. Free run length was lower when microtubules where enabled (MT+) then when they weren't (MT-). We can thus conclude that the counter balancing of internal tension by spontaneous compression forces allowed the MT+ scenario to be more stable. These results thus indicate that internal compression forces contribute to the stability of the model.

A parametric analysis (not shown) indicated that the free run length value negatively proportional to the value of coefficient a. In both scenarios, MT+ & MT-, stability increased as the value of ***a*** decreased.

In addition, mechanical nodes were attributed a mass so that the enclosed volume designated by the corresponding spherical contactor would be equivalent to the density of water. Since the aim of the simulation was to model static or quasi-static phenomena and because local accelerations remained negligible with respect to external applied forces we therefore came to the conclusion that node masses were sufficiently well chosen to meet the criteria of this study.

3.5. How do forces balance out within the cell model?

Here we will analyze how tension and compression forces interact with each other within the model. If we sum all tensile force magnitudes generated by the model on one side and sum all compression force magnitudes on the other, we notice that total tension forces increase linearly with coefficient ***a***, while that is not the case for the amount of total compression forces. Furthermore, the sum of all tensile force magnitude generated within the modeled cell is significantly higher than that of the sum of all compression magnitudes also contained within the modeled cell. By considering the grid like connectivity of the cell model, we therefore suppose that the cell structure cannot reach mechanical equilibrium by itself. This claim is supported by the fact that the cell model mostly pulls inward on its surroundings. In all MT+ modeled cells the mechanical load that counteracted actin filament tension transited for the most part through the substrate instead of transiting via a spontaneous network of sphere/sphere contact interactions. From our analysis we can thus deduce that the substrate is the key structural element that enables the cell model to mechanically support itself. On the other hand, some cells may require intracellular compression bearing elements to maintain their shape and for this reason we will now try to assess the role of passive compression network.

Comparison of the MT+ & MT- clearly showed that intracellular compression forces could contribute to preserving the shape of the model while analysis of the cell model showed that there were about half as many compression interactions compared to tensile ones. This may be a clear indication that the cell model did not collapse on itself due to an important mechanical imbalance. Otherwise, if the morphological change between scenarios MT+ & MT- were to be due to a structural collapse of the tensile network, we would have observed an overwhelming majority of nodes packed against each other. Such a scenario would have resulted in an almost equal number of tension forces and compression forces, which is not the case. We can thus assume at this point that the passive compression network may have a secondary role meant to readjust local mechanical imbalance within the tensile network. This view is therefore quite different what would normally be expected within a tensegrity structure where compression networks are supposed to counter balance the effect of tensile interactions. We may therefore suppose that we are studying a tensile structure rather than a true structure of tensegrity.

In support to this claim, results indicate that the sum of internal tension force magnitudes predominates that of internal compression forces (Figure 40). Furthermore, in the case of scenario MT+, as coefficient ***a*** increases, consequently increasing the magnitude of every tensile interaction. We noticed that the net intensity of compression forces does not increase significantly or proportionally. The number of tension interactions varies between scenarios, but

remains the same independently of the slope to rigidity gradient. These additional results therefore clearly support the idea that compression forces have a secondary mechanical role meant to cancel minor imbalances within the actin network instead of counter acting it altogether. System equilibrium is thus primarily reached by a balance between intracellular contractile forces and the passive forces arising from the substrate, while intracellular compression forces seem to have a secondary role in that matter. When comparing the relevance of different modeling criteria, we may therefore make the assumption modeling intracellular forces with fidelity may be of lesser importance than observing the actin network or measuring adhesion forces accurately. This does not mean that modeling a passive compression network is unnecessary. On the contrary, in some cases modeling intracellular compression is required to preserve cell shape and thus avoid additional strain on tensile interactions.

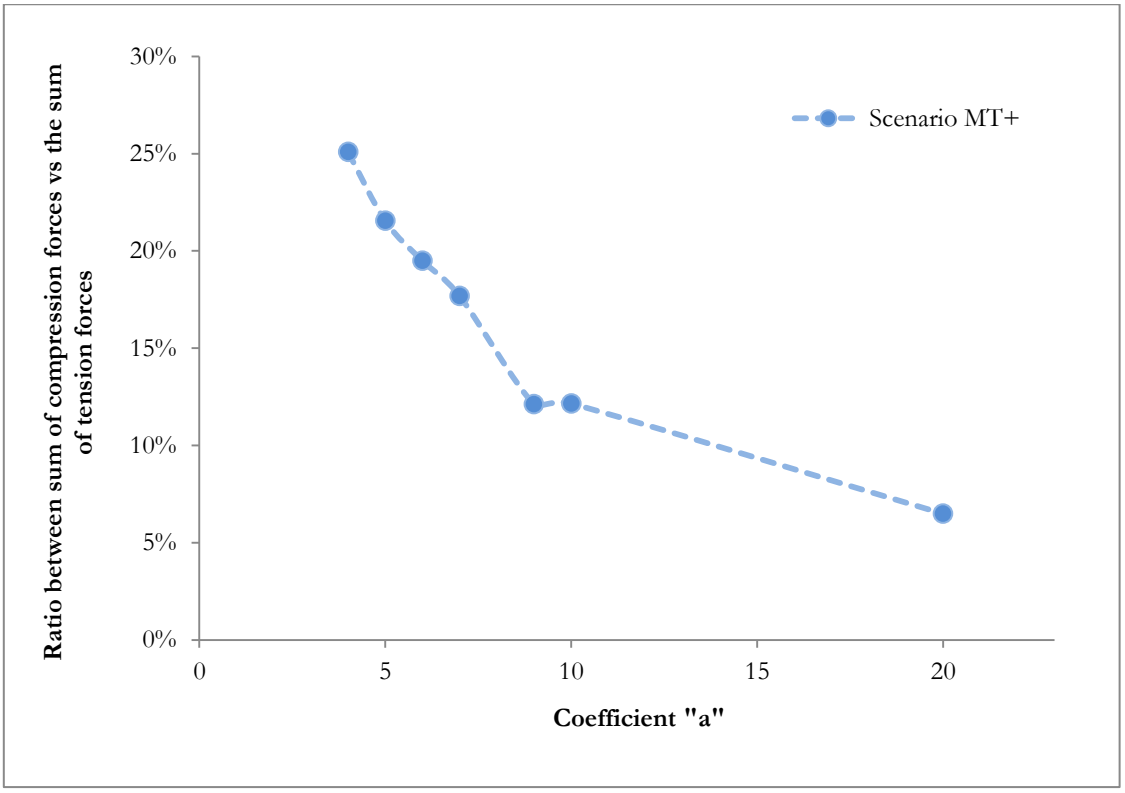

Figure 40: Ratio between the sum of compression forces vs the sum of tension forces.

*Cell Example: ratio between the sum of all inter-compression magnitudes over the sum of all inter-tension magnitudes decreases, as "**a**" increases. This implies that an increase of tension does not significantly increase compression.*

3.6. A parametric analysis of the model shows that mean tension is linearly proportional to the value of *a*

By testing evenly distributed values of coefficient a ranging between 4 to 20 nN, the MT+ model of the Example Cell outputted sums of focal adhesion forces that ranged from 266 nN to 1458 nN. Furthermore, post processing analysis allowed calculation of the mean magnitude of all tension interaction, which we called Tmean. These results allowed us to correlate relation linking mean inter-tension Tmean and the sum of focal adhesion force magnitudes "x" for the Cell Example:

$$T_{mean} = 0.0035\ x\ + 0.1594 \quad \text{(Cell Example)}$$

$$R^2 = 0.9912$$

Thus by inputting the sum of focal adhesion force magnitudes "x" into this function, we obtained the mean inter-tension value "y". While this linear mathematical function only applies to the model and not to the cell itself, it has the advantage of allowing us to save time by using interpolation and solving methods to find a desired solution. For a value of x equal to 336 nN we thus obtain a mean inter-tension values of 1.3 nN per interaction (Cell Example).

We can also linearly correlate mean inter-tension with **a** in scenario MT^{+}:

$$T_{mean} = 0.2567a + 0.0764 \text{ (Cell Example)}$$

$$R^2 = 0.9999$$

We found the same values of $\boldsymbol{T_{mean}}$ with the solved values of "$\boldsymbol{a}$":

$$a = 4.4 \text{ nN} \Rightarrow T_{mean} = 1.3 \text{ nN}$$

3.7. Cross-linear tension is a parameter that is more robust to nodal density

The problem at this time with the use of $\boldsymbol{T_{mean}}$ from an analysis perspective is that values given by the model depend on mechanical node density. We can thus conclude at this time that $\boldsymbol{T_{mean}}$ is simulation dependent rather than cell dependent. For instance, lowering the number of nodes would artificially decrease the number of interactions and increase the mean tension value per interaction. On the other hand, if the density of nodes increases, the value of mean tension per interaction would decrease. We can thus conclude that nodal density is directly linked to inter-tension magnitude. For this reason, we considered cross-linear tension, i.e., interaction tension divided by the distance between two nodes (d0 = 0.58 μm), so that our results could be viewed as being independent from nodal density.

$$T_{mean-cl} = \frac{T_{mean}}{d_0}$$

For instance, in the case of our cell example, when focal adhesion force magnitudes of the model correspond with the ones measured experimentally, we obtain a mean cross-linear tension value of $T_{mean\text{-}cl} = 2.3$ nN/μm (Cell Example).

3.8. Cross-linear tension forces within the Cell Example

c_i shade of gray			K_i (nN/µm) for a=4.4 nN		T_{cl-i} Cross-linear Tension (nN/µm) for a=4.4 nN		Actin expression
C	Shade	I	Min	Max	Min	Max	
[0.0; 0.1]		1	0	4.4	0	0.7	
[0.1; 0.2]		2	4.4	8.8	0.7	1.5	
[0.2; 0.3]		3	8.8	13.2	1.5	2.2	
[0.3; 0.4]		4	13.2	17.6	2.2	2.9	
[0.4; 0.5]		5	17.6	22	2.9	3.7	
[0.5; 0.6]		6	22	26.4	3.7	4.4	
[0.6; 0.7]		7	26.4	30.8	4.4	5.1	
[0.7; 0.8]		8	30.8	35.2	5.1	5.9	
[0.8; 0.9]		9	35.2	39.6	5.9	6.6	
[0.9; 1.0]		10	39.6	44	6.6	7.3	

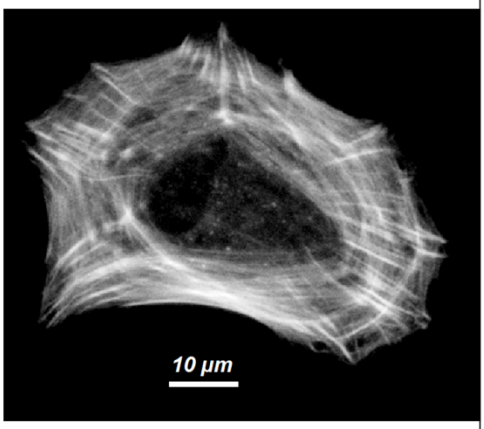

Figure 41: Cross-linear tension forces within the cell.

Cell Example: For a=4.4 nN, in the above table, we have the domain max and min values of K_i *&* T_{cl-i} *in correspondence to gray values, each of which is labeled by a value "i". For each label value "i" corresponds an interval of possible cross-linear tensions* T_{cl-i}*, ranging from* $T_{cl-max-i}$ *to* $T_{cl-min-i}$*. Since the amount of actin detected increase as a pixel gets brighter, i.e., as the label value "i" increases,* K_i *&* T_{cl} *increase as well. When we refer to* T_{cl-max} *we in fact refer to* $T_{cl-max-10}$*, the highest cross-linear tension value.*

The highest cross-linear tension T_{cl-max} may reach 7.3 nN/µm while highest cross-linear rigidity may be as high as 44 nN/µm² (Figure 41). Cross-linear tension is not limited to the model, so it allows direct tension measurement from the actin image. We can therefore directly measure the tension crossing a segment, i.e., the tension transiting through one or several stress fibers, on the image. All we need is the mean gray value and the width of the fiber or fibers we are considering.

Yet, since the resolution of our model is limited to 0.58 µm and since the number of gray value considered in the model is limited, we turned our attention back to the image which has a greater spatial definition and more precise tones of gray (256 compared to 10).

We recommend that this method should only be applicable to cross sections equal or greater than the definition of the model, meaning in this case anything larger than 0.6 µm. Even if this approach can also interpolate tension trough smaller cross sections, it may under estimate tension values due to diffraction and low resolution, for which both phenomena tend to average the local gray values.

3.9. Cross-linear tension forces within the cell population

Cross linear tension values within the cell population were calculated using the same solving method as used for the Cell Example. Nonetheless, we noticed that cross-linear tension values range from 7.3 nN/µm (Cell Example) to 42.3 nN/µm (see Table 4). On the other hand the cross-linear tension values average 24.1 µm/nN across the eight cells, with a standard deviation of 12.8 µm.

Table 4 : Cross-linear tension values of the cell population.

$T_{cl\text{-}max}$ (nN/µm)	
Average	24.1
SD dev	12.8
min	7.3
max	42.3

Maximal cross linear tension values within the cell population.

3.10. Tension within the stress fiber of the cell example

The amount of tension transiting in a stress fiber of the Cell Example was obtained by multiplying the mean gray value c_{mean} by the width of the stress fiber and the max cross-linear value ($T_{cl\text{-}max}$ = 7.3 nN/µm). Using this approach, we estimated intracellular tensions transiting across segments that we drew on the actin image (pink lines on actin images Figure 42–Figure 45). Pixel values were measured along the segment, while its length indicated the width of the fiber.

3.11. Tension within a stress fiber

The amount of tension transiting in a stress fiber was obtained by multiplying the mean gray value $\bar{c}$ by the width of the stress fiber and the max cross-linear value ($T_{cl\text{-}max}$=7.3 nN/µm). Using this approach we estimated intracellular tensions transiting across segments that we drew on the actin image (pink lines on actin images Figure 42–Figure 45). Pixel values were measured along the segment, while its length indicated the width of the fiber.

In Figure 42.a we thus found T=*9.2 n*N of tension transiting through the stress-fiber for a width of 1.58 µm (diffraction is not taken into account when mentioning the width of a stress fiber). We repeated the process for the same stress fiber, at a different location and found a tension value of 9.3 nN for a width of 1.75 µm (Figure 42.b). The force value remains very similar even though they have different grayscale histogram profiles. These results indicate that the same tension transit through the stress fiber without being redistributed elsewhere.

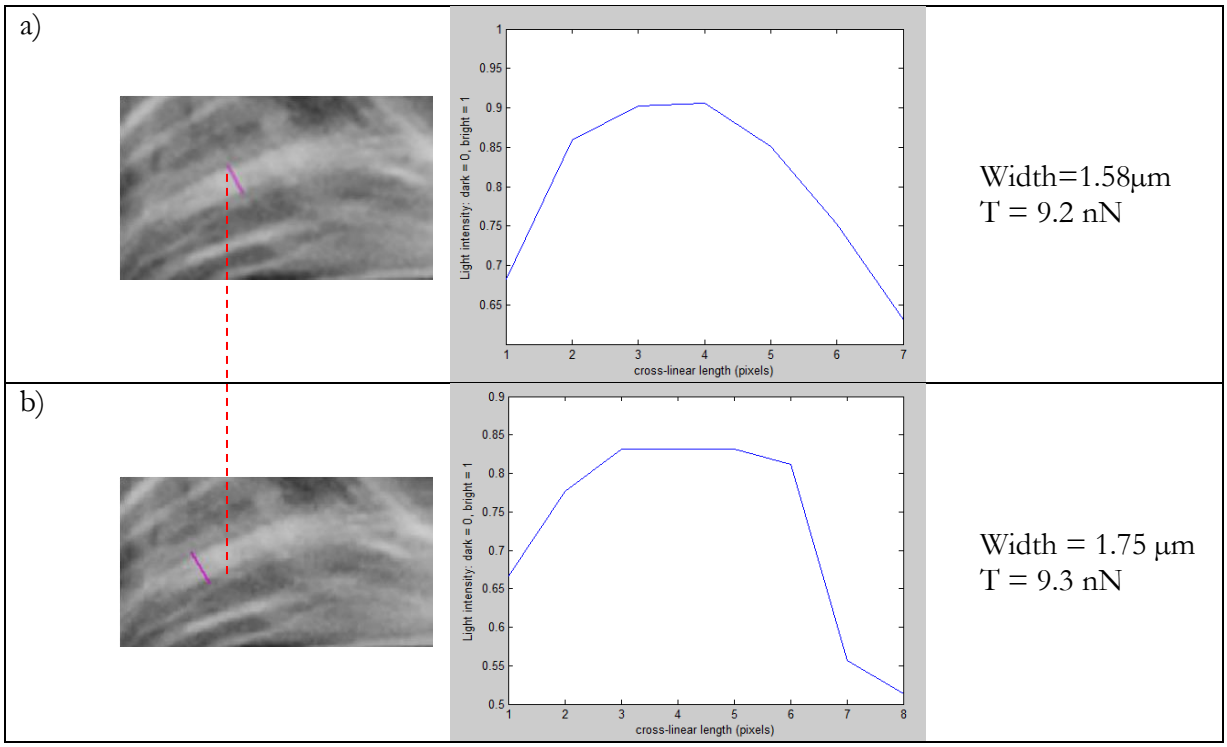

Figure 42: Measuring tension in a large stress fiber at different locations

Measuring tension in a large stress fiber at different locations (a & b). Photos in left column represent a partial view of the actin network. Gray values were measured along the straight pink line running across the considered stress fiber. Pixel gray values measured along each line were plotted on the corresponding graph located in the middle-column. From there the mean gray value was deduced, while the length of the pink line corresponds to the width of the stress fiber (right column). The width and mean gray values of the stress fiber was then used to calculate the amount of tension it is bearing.

Through a thinner stress fiber which we found to be 0.89 µm thick, we obtained 5.2 nN of tension (Figure 43 a). Similarly, a tension of 4.5 nN was found for another stress fiber which we measured to be 0.85 µm thick (Figure 43 b).

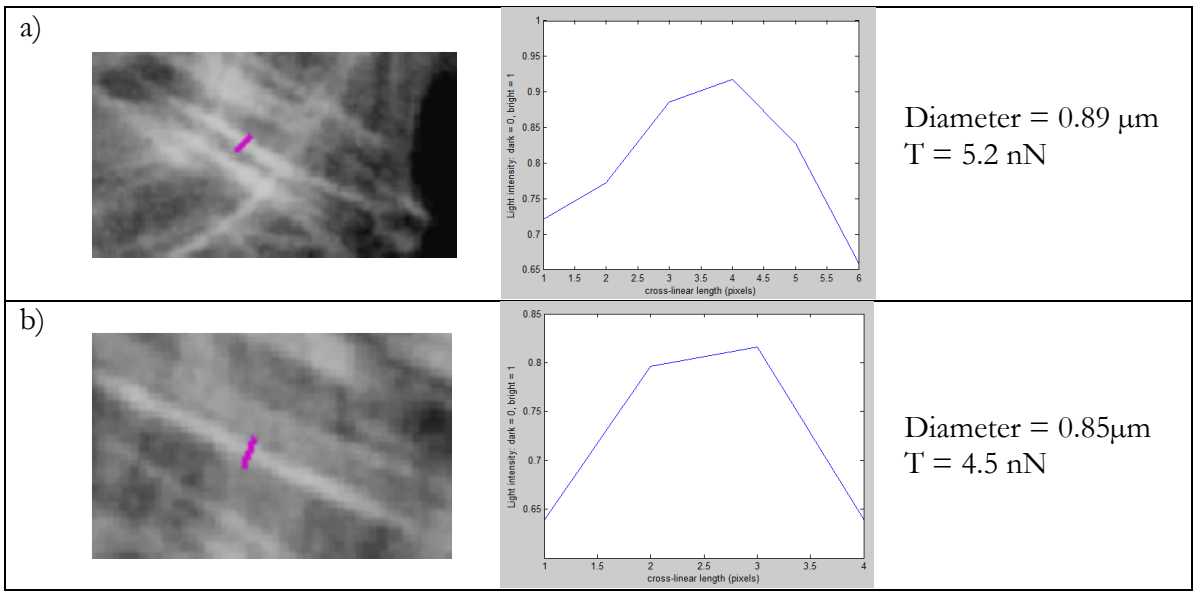

Figure 43: Measuring tension in two different thin stress fibers. (See Figure 42 for details).

An additional feature of this approach is that it allows the estimation of tension through radial stress fibers (Figure 44). We thus did force measurements within the circular actin network belt (Figure 44). We found equivalent tension magnitudes at different locations ranging from 39 nN to 55nN, with a mean value of 48 nN. These variations can be explained by the way the cytoskeleton belt is structured, because some of the tension might be distributed to other stress fibers linked to focal adhesions. Then again, if we look more closely on figure 10, we notice that cases a & b have very similar results. As could be expected, these are the same group of stress fibers and all additional stress fibers located between the two measurement lines are perpendicular and thus can't affect tension values significantly. The same principles apply to cases c, d & e. For all three cases we notice that the measurement error always remains below 10%. From these simple tests we can thus conclude that the random measurement error of this method should be below 10%.

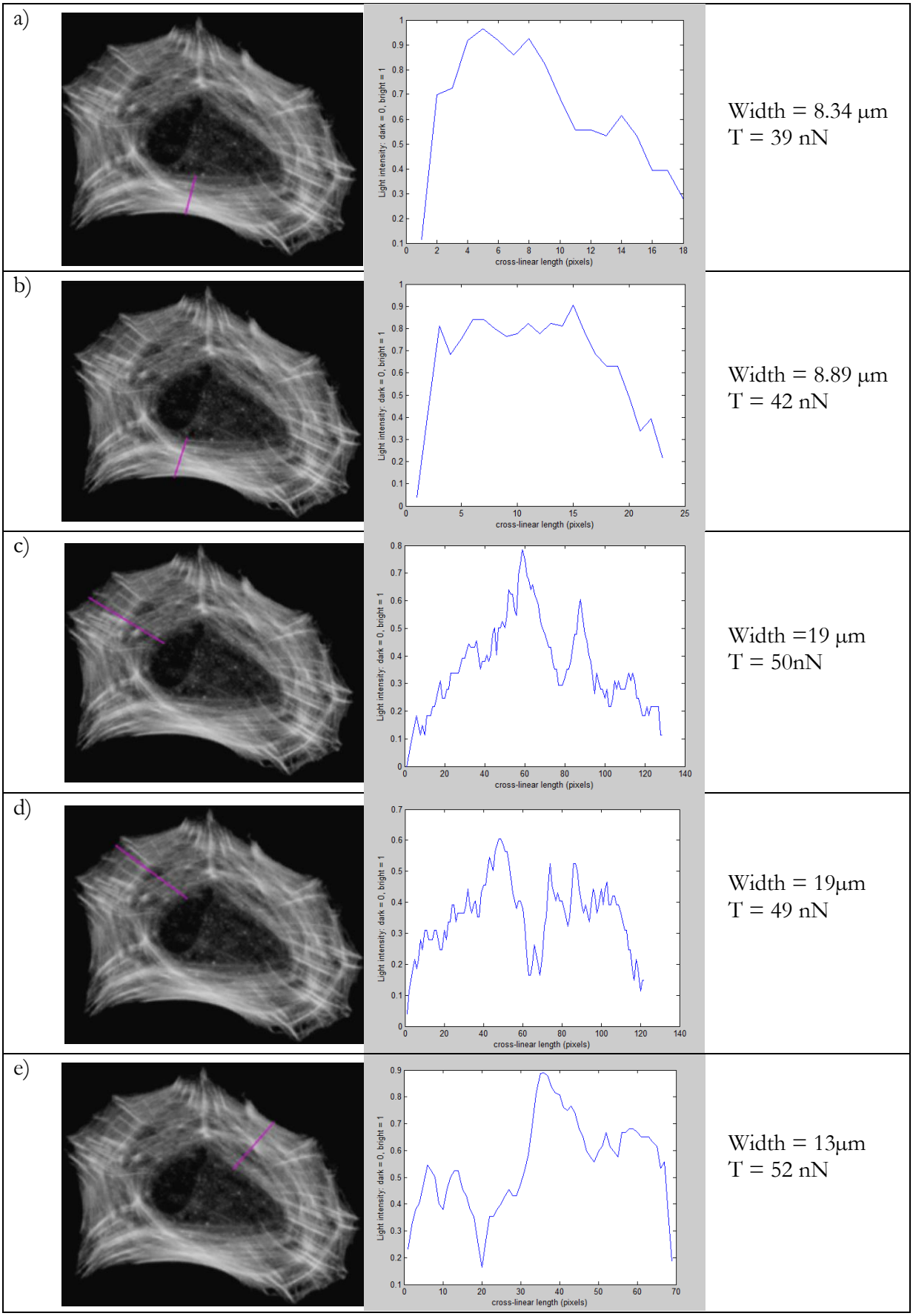

Figure 44 : Tension within circular actin network belt. (See Figure 42 for details).

To determine the overall intracellular tension, we respectively measured tension across the whole cell, on its short axis (35 µm) (Figure 45.a) and long axis (62µm) (Figure 45.b), and found 107 nN and 126 nN of tension transiting through each designated section (Figure 45).

This respectively equates to 32 % and 38% to the value of the sum of focal adhesion force magnitudes. If we consider this cell to be almost polarized along its long axis, we would thus expect to measure the highest cellular tonus along its long axis, i.e., across the short axis of the cell (Figure 45.a). On the contrary, results from Figure 45.a and Figure 45.b show that the morphological polarization of the cell is not necessarily linked to a polarization of mechanical tensile forces within the cell.

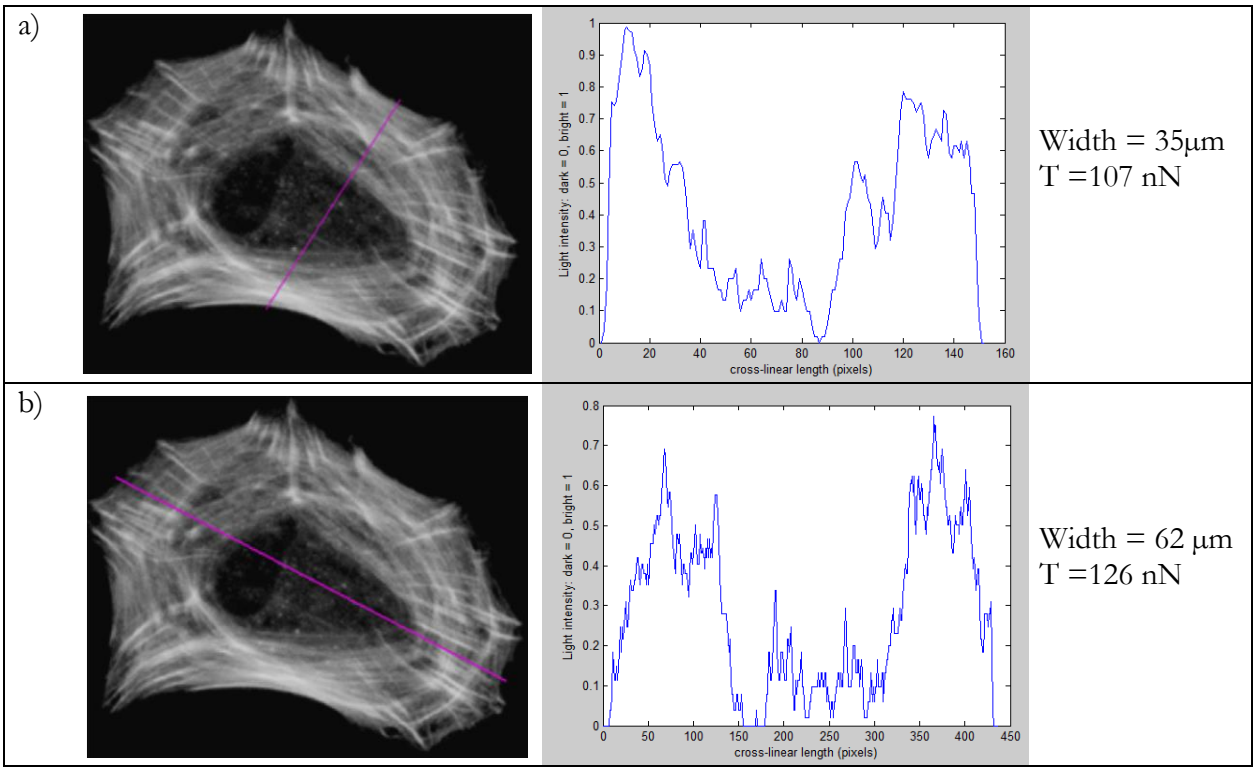

Figure 45: Tension across the whole cell. (See Figure 42 for details).

4. Discussion (an image based model)

4.1. Actin network, a network of tensions

A part from the choice of the mechanical theory (continuous, finite elements, divided or fluid mediums) used to model the cell, modeling intracellular structural elements may be essential to understand how mechanical forces are transmitted within the cell. Based on this simple assumption biofidelic and imaging based models may have a significant advantage compared to other types of models [93,95,92,109,110,111,112,9].

In our approach, actin amounts were transcribed into tensions within the model. This hypothesis is consistent with experiments which show that stress fiber creation and reinforcement result in an increase in tension. This suggests that the amount of force transiting through a stress fiber could be proportional to its thickness.

4.2. Modeling actin fibers by using pre-stressed elastic interactions

In our model, stress fibers act as purely linear rubber bands with a constant stiffness value and an almost constant strain of 0.2. When we measure tension within stress fibers on actin images, the calculation of force is inherited from the tensile interaction network composing our model. In the following we discuss the consistency of the representation of stress fiber in the model in terms of mechanical and material properties such as the Young's modulus. For instance, if we consider the stress fiber analyzed on Figure 43b (Cell Example), which possesses a diameter of 0.25 µm, and resulting tension value of 4.5nN combined with a default pre-strain value of 0.2, the equivalent Young's modulus is equal to 459kPa. Experimental results found in the literature statistically determined a parabolic relationship between stress and strain to characterize the hyperplastic property of stress fibers[106]; using this relationship for a stress fiber of 0.25 µm in diameter and strained by 20%, we found a Young Modulus equal to 322 kPa. We thus find a relative difference of 42% between both results. Furthermore, it is worth noticing that this difference could be encompassed by the standard deviation of the experimental results of the study cited above. Considering the fact that neither the level of strain, nor the diameter of the stress fiber could either be measured with accuracy, we thus consider these results to be very coherent.

When we consider $\boldsymbol{T}_{cl\text{-}max}$ which ranges in the cell population from 7.3 to 42.3 nN/µm, we may assume that the minimal value is not so significant since $\boldsymbol{T}_{cl\text{-}max}$ would be lower in cells at their initial stage of adhesion. What would be more relevant is to consider the average value (24.1 nN/µm) in relation with the maximal one. There is less than a factor 2. This means that from one cell to another the stiffness of stress fibers may only differ by a factor 2. Furthermore, in the case of a 1µm-diameter stress fiber pulling on a single focal adhesion, it could exert a traction force of 42.3 nN, which is consistent with force magnitude an in vitro cell could exert on a single micropost[16].

In this study, the mechanical state of the model results from the equilibrium between tensile interactions, only involving slight node displacements. Considering that tensile interactions did not strain further, modeling the hyperplastic properties of stress fibers would not significantly influence the global response of the model. Moreover the static nature of our current work does not require taking viscosity in to account. We can thus conclude that the model is valid to

compute intracellular forces within adherent cells. However, hyperelasticity, viscosity and plasticity could be valuable features during dynamic cell deformation or loading, such as oscillatory magnetic twisting cytometry[113].

4.3. Microtubules play a secondary role to ECM as compression bearing effector

Our results show that a significant increase of inter-tensions did not significantly impact inter-compression within the model. This result is in accord with the experimental results found by other research groups[44,43]. Furthermore the model shows that disabling inter-compression forces increased tug on focal adhesions. This is similar to experimental results found by another group when using chemical agents to depolymerize microtubules[44]. We can therefore conclude that the compression bearing elements of the model counteract actin tension in a similar manner as microtubules would.

As we increased inter-tension magnitudes, the cell model remained stable only involving slight inter-compression variations. In fact, in the model, internal tension is mainly balanced by the ECM compared to microtubules. Experiments have also shown that the ECM is the main counteracting effector to intracellular-tension, especially for cases of elevated intracellular-tension while microtubules tend to play a secondary role as compression bearing elements[44,43]. We can therefore conclude that in a static scenario, the intracellular compression bearing elements used in our model behaved in accordance with previously published experimental results. It thus appears that sphere/sphere interactions have valuable modeling features that include a qualitatively coherent behavior while requiring minimal information input.

4.4. Tension magnitudes given by the model.

The model computed stress fiber tensions ranging between 4.5 and 9.3 nN which is similar to the FA force magnitude measured by Balaban et al. (2001), who measured FA force magnitudes around 10 nN [16]. As the tensile interaction network exerted realistic amounts of force on FA, we can argue that consistent tension magnitudes were generated within the cell model. The model thus yields a coherent relationship between actin density and mechanical force. This allows quantitatively measurements of the amount of tension transiting through the observed stress fibers.

An intracellular tonus index was previously introduced by Milan et al. (2013) as the sum of all stress fiber forces crossing the mid-section of the cell. Based on this definition we found an intracellular tonus of 126 nN which corresponds to 35% of the sum of all FA force magnitudes. In a pre-stressed structure where internal compression is marginal, internal tension cannot be higher than half of overall peripheral forces. It is important to notice that the ratio we found is similar as the one found by Milan et al. (2013).

As mentioned previously, a linear relation exists[16] between the size and force magnitude of FA larger than 1 μm2. However, this linear relationship does not apply to sub-micro squared focal adhesion; this is the reason why we decided to only consider large FA in the present study. However, despite their small size, sub-micrometer squared FA have been reported to support high force magnitudes generally averaging about 15 nN and up to 60 nN [15]. For instance, in the adherent cell we studied here, 40 FAs were in the 0.5 to 1μm2 size category and were possibly

submitted each to a traction force of 15 nN in average (not published). If we take into account these additional focal adhesions, we can thus conclude that we ought to add another 600 nN to the sum of focal force magnitudes. In this case the sum of all FA forces would be equal to 936 nN, yielding a $T_{cl\text{-}max}$ value equal to 21 nN/µm instead of the 7.3 nN/µm found previously. This difference represents a factor of 2.9 between tension results, which is much more significant than the slight difference observed between scenarios MT+ and MT-. We can thus safely assume that an accurate measurement of FA forces is mechanically more significant than modeling compression bearing agents, such as microtubules.

Improving measurements of FA forces based on FA size, would significantly increase the accuracy of the model results. A potential improvement would be to use of super-resolution microscopy to estimate focal adhesion size, because what appears as a single adhesion in conventional microscopy, can be viewed with a super-resolution microscope as a group of elongated adhesions, between 100 to 280 nm in length. The coefficient of correlation between, focal adhesion size and the pulling forces is significantly higher with super-resolution ($R^2 = 0.711$) than with conventional microscopy ($R^2 = 0.459$). [20]

4.5. Limits and future perspectives

The representation of tension stress transiting through individual stress fibers would require overcoming the diffraction barrier to better measure their diameter. Super-resolution could be used to fulfill this purpose[75,114,76]. In addition, it would facilitate visual texture recognition to discriminate tension-bearing stress fibers from compression-bearing dendritic actin, which has a woven visual aspect; dendritic network and stress fibers may be represented as different materials with specific mechanical properties. Actin fibers could be modeled as tension interactions between nodes attached to different parts of the dendritic actin network, while dendritic actin could be modeled as a continuous material with compressive stiffness. However, the approach presented herein may not be extended to "mechanically" represent the cytoskeleton down to the molecular interaction scale, for it is bound by the limitations of classical mechanics.

3D acquisition of the cellular structure would allow 3D computation of mechanical stress within the cell[11], and thus help identification of overlaying mechanical pathways which would otherwise appear to be merged when observed in 2D [80]. 3D acquisition would also yield to the estimation of vertical forces exerted on the nucleus[11,68] which influence gene expression[11,115]. As a matter of fact, 3D confocal microscopy allows us to discriminate between ventral and dorsal actin networks. While dual-objective STORM microscopy, allows 3D visualization down to individual microfilaments[75].

5. Conclusion

Measuring intracellular forces within cells using this simple image based method seems to yield coherent tension values. Its advantage is that it is simple and straightforward. Yet, measuring forces transiting via individual stress fiber may be of limited use. Instead, what would be valuable would be to measure the mechanical state of the whole actin network for each cell. Which leads us to the following question: "How can we use the current model to analyze the whole actin network of a cell in a meaningful manner?"

CHAPTER 3
THE CONSEQUENCE OF LARGE SCALE RIGIDITY ON ACTIN NETWORK TENSION

1. Introduction

In Chapter 1, we developed a model able to compute a possible and valid cytoskeleton of an isolated cell cultured in vitro on a flat surface. The modeled cytoskeletal structure used the measurement of adhesion pulling forces generated by the observed cell on its focal adhesions. In Chapter 2, we developed a model closer to the real structure of the cytoskeleton. Indeed, this 2D model represents the cytoskeletal structure based on the image of the actin network. The contractility of the modeled actin network was computed so as to match the level of traction forces the cell applied on its focal adhesions. Yet part of the limit of this study, was that the traction forces on focal adhesions were only estimated depending on focal adhesion size and were not measured as precisely as we were able to do in Chapter 1. While this study served as a proof of concept for the image based modeling method, it also allowed us to better conceptualize how the cell is structured. In Chapter 3, we decided to combine the experimental methods used in Chapter 1 with the image based model developed in Chapter 2 (Figure 46). Our objective was to find a possible relationship between the tensile properties of the actin network, cell size, and the substrate stiffness.

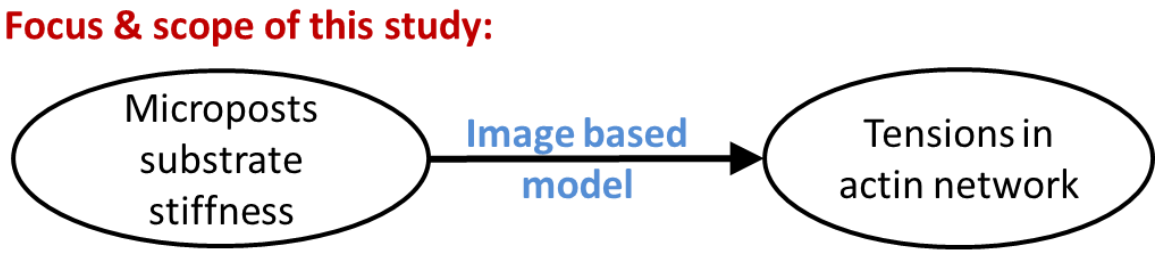

Figure 46: Scope and focus of this study

In this study, we used 4 types of micropost substrates which varied only in terms of micropost lengths. We therefore refer to these substrates, based on the bending stiffness of their microposts, as Very soft, Soft, Hard, Very hard (Figure 47A).

A) *Substrate dimensions*

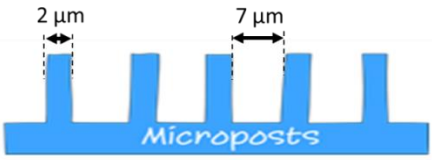

(cross-sectional side view)

B) Substrates microposts bending stiffness:

- Very soft (11.0 nN/µm)
- Soft (15.5 nN/µm)
- Hard (31.0 nN/µm)
- Very hard (47.8 nN/µm)

C) Deflection is proportional to force

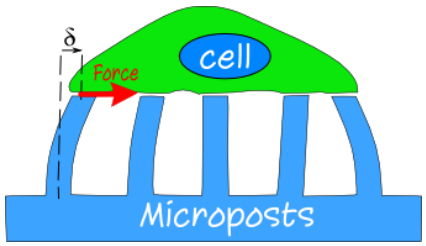

Figure 47 : Mircopost substrates used in this study

A) Micropost bending stiffness is based on its designated height (also referred to as length). Substrates with shorter microposts are harder to bend, i.e., stiffer, while longer microposts lead to the appearance of a softer substrate, although the material and its mechanical properties remain the same.

B) As cells are attached to the top of the micropost, they are not able to distinguish differences between the various types of substrate other than the apparent rigidity. Furthermore, the 7 µm spacing between posts is assumed to prevent contractile units from being able to perceive micropost bending stiffness.

C) Individual post deflection is a direct quantitative indication of the force being applied to it by the cell.

We therefore had 4 rigidity conditions, yet all the microposts were 2 µm in diameter, 9 µm form center to center and made of the same material (Figure 47A). It is important to note that the size and spacing (7 µm) of the micropost matters for this experiment. Indeed, adherent cells are known to measure substrate stiffness by the use of 2 µm long contractile units (CU) located right against their focal adhesions[39]. The way these contractile units work is by periodically contracting so as to measure local substrate stiffness. In other words, these contractile units can be considered as tools that allow the cell to pinch its surroundings so as to estimate how hard it is[39]. The microposts were therefore sufficiently large for contractile units to form on top of them so as to measure the mechanical properties of the material that was identical for all conditions.

In addition, there was a gap of 7 µm between microposts. The microposts were consequently too far apart for contractile units to bridge two microposts. This suggests that the contractile units were not be able to distinguish differences between the various substrates. If cells are affected by the micropost bending stiffness would therefore hint the idea that the cell can be influenced by stiffness of the substrate independently of the contractile unit.

2. Methods (intracellular tension vs rigidity)

The methods used in this study are largely inspired from the two previous ones; we therefore mainly focus on the specificities.

2.1. Biological protocol and adhesion force measurement

Human pulmonary artery endothelial cells (HPAECs, Lonza) were cultured on PDMS micropost substrates. In this study, we used 4 different types of micropost bending stiffness (Figure 47), which we will refer to with the following designations: Very Soft, Soft, Hard, and Very hard.

All 4 types of substrates were made of the same PDMS with a Young's modulus of 2.5MPa measured according to ASTM standard D412. All microposts in this experiment had a cylindrical shape with a diameter ranging between 2.14μm and 2.42μm. Microposts were evenly spaced in a grid like fashion, 9 μm from center to center. The gap between microposts was therefore 7μm.

The cells were permeabilized using Triton-extraction protocol after being allowed to spread for 14 hours on the micropost arrays. Cells were then stained with Hoechst 33342 (Invitrogen), phalloidin (Invitrogen), IgG anti-vinculin (hVin1, Sigma Aldrich), and anti-IgG antibodies (Invitrogen). Images of the cells and microposts were obtained via fluorescence microscopy (Nikon TiE, 60× oil objective, 1.4 NA).

Micropost deflection of was used to measure the pulling force exerted by the cell on each post (Lemmon 2005). Micropost deflection was measured by comparing the position of the center of the top of each micropost to position of the bottom. The planar difference in position allowed us to calculate the corresponding deflection vector, therefore indicating both the magnitude and directionality of the pulling force exerted by the cell on each post. The spread area of a cell on an array was measured from an outline of its actin image.

2.2. Image treatment

An image treatment was applied to all images before they were used to generate the model. Images of the micropost tops were manually binarized to represent equivalent bright disks with a diameter of 2 μm. Actin images with a bright spot that were considered to be due to staining artefacts were dimed down to match the brightness of their surrounding neighbors. The actin networks gray value of the image was then reset to a scale ranging from 0 to 1. 1 being the brightest point in the actin network image, while 0 was attributed to pixels below a threshold value attributed to the brightness of the background. An automated script also outlined the cell within the image. We then visually inspected the outlined image. In some instances, final minor touches were made manually.

2.3. Experimental adhesion force measurement

We used almost the exact same mechanical modeling protocol as in Chapter 2. Similar to before, this protocol allowed us to use an image of the actin network and external forces external to map internal tension forces transiting via the actin network. The image of the cell was converted into mechanical nodes allowed to interact via tensile interactions. All cells were identical nodal density, unless stated otherwise.

Micopost-tops in contact with the cell were used to represent focal adhesions. Each micropost top was therefore modeled as a cluster of nodes, therefore forming an adhesion cluster. Adhesion clusters were used so as to easily measure the net adhesion force exerted on each of them focal adhesion, i.e., micropost. These node-clusters where also fully constrained to model the anchoring properties of focal adhesions. In addition, the nodes contained within each cluster were allowed to form tensile interactions with direct neighboring nodes that represented the actin network.

Exactly as presented before, bright pixels of the actin network image were considered to represent a pronounced actin network, while dark areas were considered to represent an area with less actin. Bright areas with more actin were therefore allowed to interact with stronger tensile interactions then darker areas. It is important to consider that at this point the "strength" of the interactions were only defined relatively to one another, while their absolute quantitative value of the required parameters were determined later on. In addition, similarly to the previous study, the "strength" of an interaction was linearly proportional to the gray value of the corresponding pixel, while the interaction between two nodes was always defined by the weakest node of the two nodes, i.e., the node with the darkest parent pixel.

In this study, we assigned each actin network nodes with a color label. The color label for each node was assigned based on the gray value of its parent pixel. The label was then used by the mechanical solver to deterministically assign interactions between nodes during computation.

Based on the results of the previous study (Chapter 2), we decided to allow the formation of a passive compression network. The methodology was once again identical; each actin network node was decorated with a spherical contactor. A mechanical contact law prevented interpenetration between spherical contactors, therefore allowing a passive compression network to emerge.

2.4. Inversed mechanical solving

Once again we used the same inversed mechanics solving method as presented in Chapter 2. The main difference is that this time the method used to measure adhesion forces was much more accurate.

To recapitulate, this inverse solving method uses external adhesion forces to solve for the "strength" of the tensile interactions that connect all the actin network nodes. The idea is quite simple, since there is a linearity coefficient between interaction stiffness and the brightness of a pixel gray value, we need to solve for slope coefficient alpha and the slope constant beta. Since a fully dark pixel indicates that there is no actin, we thus conclude that there is not tension, we can therefore approximate that our slope goes through the origin (0,0). We therefore approximate beta to be equal to 0, leaving us only to solve for alpha.

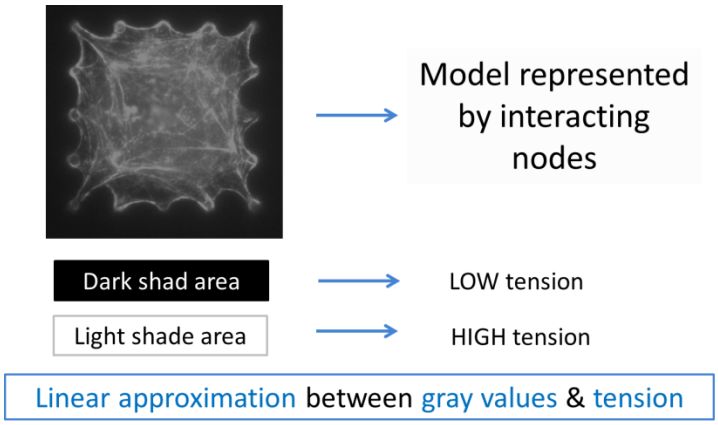

At this point we can iteratively solve for alpha. When alpha increases, the modeled cell pulls more on its adhesions, and vice-versa. We therefore use the sum of adhesion force magnitudes as a common metric to compare how the modeled cell pulls on its surrounding compared to the real cell. We can then iteratively increase or decrease the value of alpha until the modeled cell pulls as much as the real cell. The results from the previous study indicated that we could use an interpolation method to reduce the number of iterations, which we implemented in our automated iterative solver. We nonetheless added a few constraints to ensure the convergence of the solver. We considered that the cell model was mechanically "equivalent" to the real cell once the sum of adhesion forces magnitude matched what we measured experimentally with a relative error lower than 0.1%.

2.5. Max tension within an interaction

To resume, the iterative solving process tuned the rigidity of the elastic interaction until the tensions were appropriate. Knowing that the pre-strain is equal to 20%, we can estimate the tension generated by a tensile interaction as:

Equation 18

$$Tension = Stiffness * Strain$$

The "Stiffness" is expressed in nN per strain.

After optimization, the model can yield the stiffness value of the strongest interactions. Therefore enabling us to estimate highest tension value within the cell by using the following equation:

Equation 19

$$Tension_{max} = Stiffness_{max} * Strain$$

2.6. A simple method to calculate the maximal cross-linear tension

The previous study informed us that we can use the model to estimate tensions within the cell. It also, allowed us to use results from the model to go back to the image. But to untie our results from nodal density, we used cross-linear tension values (see Chapter 2 for details), which is equivalent to:

Equation 20

$$T_{cl} = Stiffness * Strain \ / \ Width_{interaction}$$

The "$Width_{interaction}$" depends on nodal density; it is equivalent to the spacing between nodes.

Similarly we can calculate the highest cross linear tension value:

Equation 21

$$T_{cl\text{-}max} = Stiffness_{max} * Strain \ / \ Width_{interaction}$$

2.7. An image based method to calculate mean cross-linear tension

Pixel gray values of our actin network image range between 0 (dark) and 1 (white). Furthermore, the tension is highest between nodes with a common brightness value of 1 (white). Yet we also assumed in our model that tension is proportional the gray value. We can therefore use the gray values of all the pixels of the cell to calculate an average gray value. The average gray value of the cell can consequently be used as an approximation factor to calculate the mean cross-linear tension value based on the value of the highest cross-linear tension, such that:

Equation 22

$$T_{cl\text{-}mean} = g_{mean} * T_{cl\text{-}max}$$

NB: *In this chapter we calculated cross linear tension values in a different way than we did in Chapter 2. The same results can be obtained using "coefficient a" mention in Chapter 2, but we thought that explaining it differently might allow some readers to better understand how we can obtain these values.*

On the other hand, it may be worth noting that Tcl-mean is not rigorously the same between this chapter and Chapter 2. In this chapter we calculated Tcl-mean using the mean gray values of the pixels that represent the cell. While, in Chapter 2, Tcl-mean was defined by calculating the mean value of all interactions of the model.

3. Results

3.1. Visual results

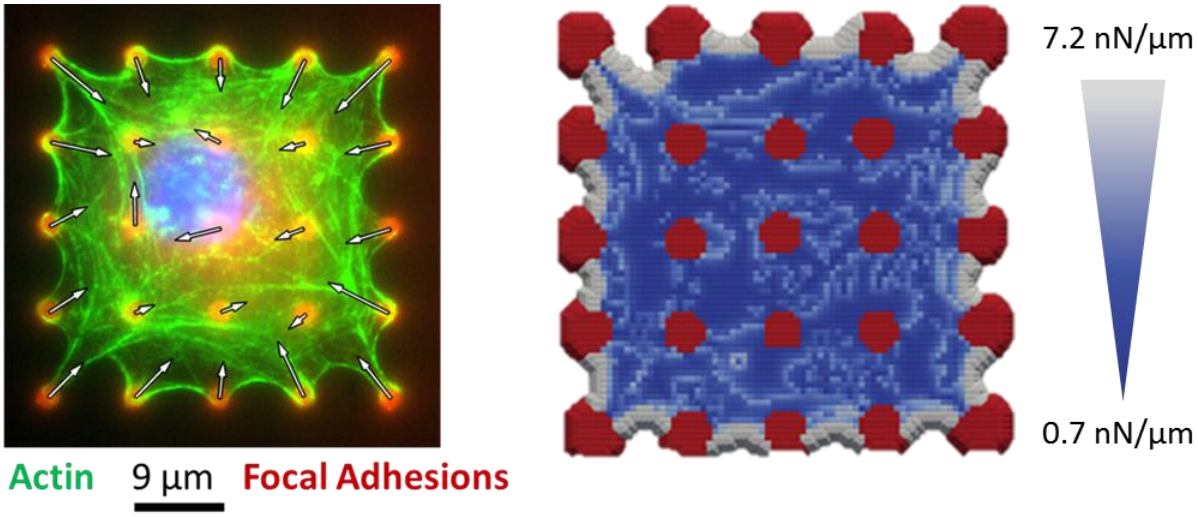

Figure 48 : Visual results:

> *Left) Fluorescence image adhering cell: actin in green, adhesion (vinculin & top of microposts) in red, adhesion force drawn as white arrows. Peripheral adhesion forces are directed inward. Adhesion force intensities are stronger at the periphery than at the center. Similarly to micropost based adhesion force measurements, the direction central adhesion forces are not necessarily directed inward (left image).*
>
> *Right) View of the model: adhesions are labeled in red, strong actin in white-gray and weaker actin in blue. The modeled cell maintains its initial shape.*
>
> *NB: microposts centers are 9 µm apart from each other*

A quick visual inspection (Figure 48) indicates that the cell model has an equivalent shape to that of the real cell. The visualizer also enables us to verify that tensile interactions form between all the nodes (Figure 48). Furthermore, we can also observe that peripheral adhesion forces output value of the model are oriented toward the center of the cell, as is the case with the real cell. In addition, peripheral forces appear to be more significant than the ones at the center, as it was experimentally observed. This quick visual observation, allows us to assume that the model behaves as expected. It should, nonetheless, be noted that adhesion forces calculated by the model are not rigorously the same as the ones expressed by the cell. The image based cell model tends to even out adhesion force intensities compared to what can be observed experimentally. Similarly we find that the directionalities of each adhesion force is not rigorously aligned with its experimentally observed counterpart.

A similar visual analysis was made on the other cells (results not shown), leading to the same conclusions. Based on these preliminary visual observations we can therefore conclude that image based cell model behaves coherently though it may lack precision to accurately represent individual adhesion forces.

3.2. How are adhesion forces and intracellular tension related?

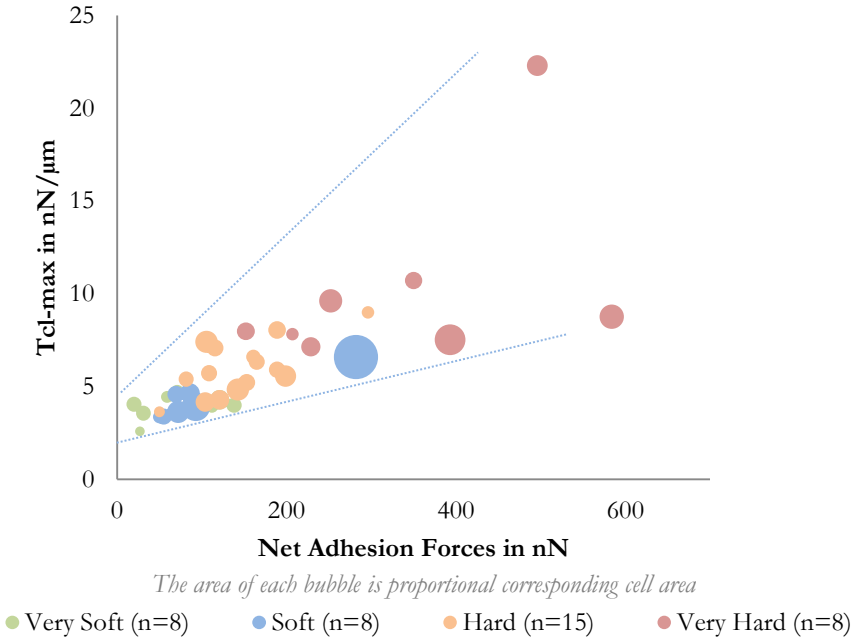

Figure 49 : Max cell tension in function of net adhesion force. Highest intracellular tension is expressed as a function of the adhesion forces generated by each cell. The highest intracellular tension is a cross-linear tension value expressed in nN/µm. Adhesion forces are in fact the sum of adhesion force magnitudes, therefore expressed in nN. The size of each bubble is proportional to the size of each cell.

Adhesion forces and max intracellular tension are positively correlated (R= 0.76, above 95% statistical chance), independently of cell size. As adhesion forces increase so does intracellular tension and vice versa. On the other hand, graphical and statistical linear regression analyses show a non-null intersect. We can consequently deduce that the model indicates that when adhesion forces tend to decrease toward zero, there is still residual tension within the actin network.

3.3. What is the relation between cell area and max tension?

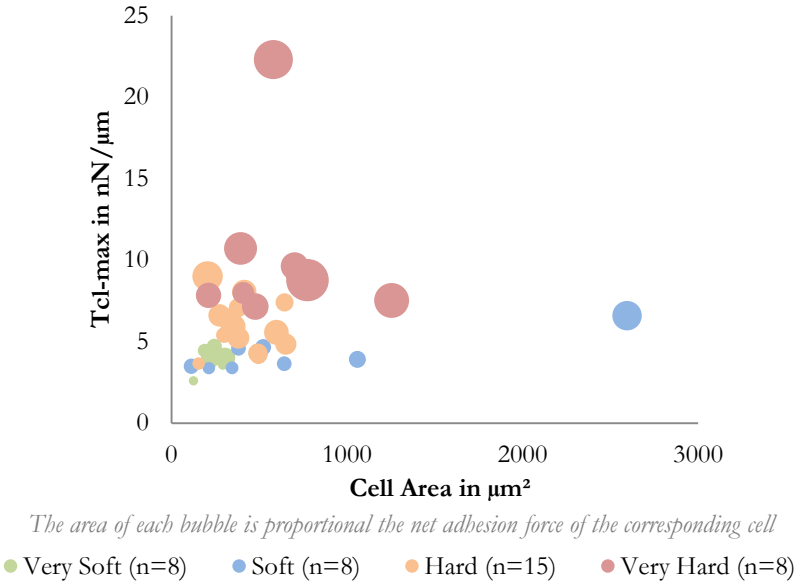

Figure 50 : Max cellular tension vs cell area. Projected cell area in abscise, highest whole cell intracellular tension, i.e., Tcl-max in ordinate. The highest intracellular tension value is a cross-linear tension value expressed in nN/µm. Each bubble represents a cell, and the size of the bubble is proportional to the sum adhesion force magnitudes exerted by each cell. In other words the size of the bubble is proportional to how much a cell pulls on its surrounding.

A Pearson correlation analysis of the results indicates that neither max cross-linear tension nor mean cross-linear tension values are correlated to cell size. Figure 50 graphically represents max intracellular tension in comparison to cell area, allowing us to graphically intuit the lack of correlation between the two parameters. We may thus conclude that cell size does not impact "contractility".

3.4. How does micropost bending stiffness affect tension within cells?

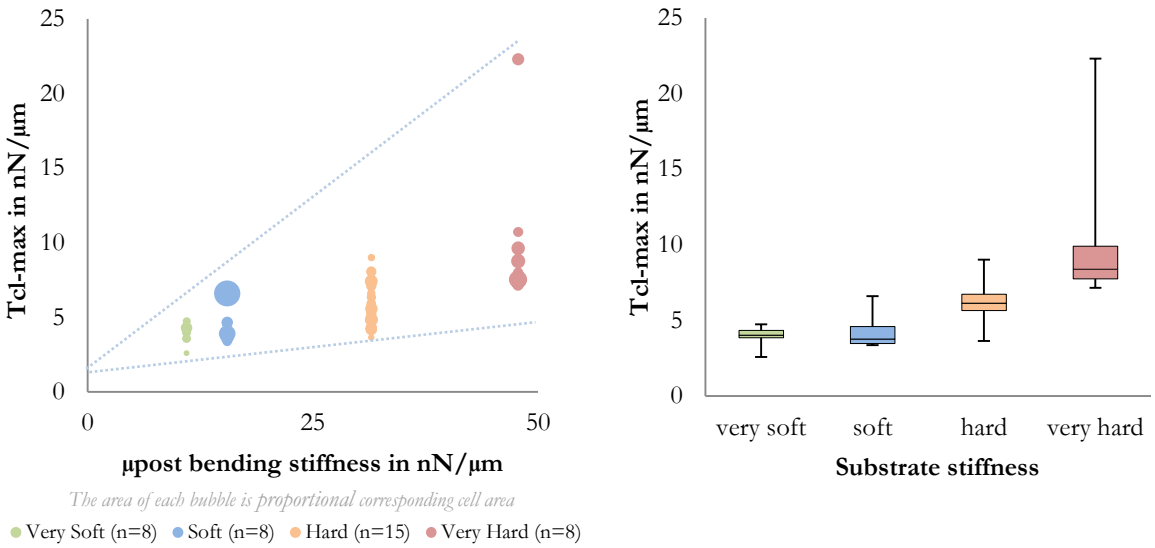

Figure 51 : Max cell tension in function of micropost bending stiffness. Highest intracellular tension is expressed as a function to the bending stiffness of the microposts. The highest intracellular tension value is a cross-linear tension value expressed in nN/µm. Micropost bending stiffness is expressed in nN/µm and can be assimilated to substrate rigidity. The size of each bubble is proportional to the size of each cell.

Table 5: A one-way ANOVA test showed significant variation between the 4 groups. We completed our analysis by conducting post-hoc t-tests with a Bonferroni multiple-significance-test correction. Labels: identical (=), statistically different (≠), not statistically different (~).

$T_{cl\text{-}max}$	very soft	soft	hard	very hard
very soft	=	~	≠	≠
soft	~	=	≠	≠
hard	≠	≠	=	≠
very hard	≠	≠	≠	=

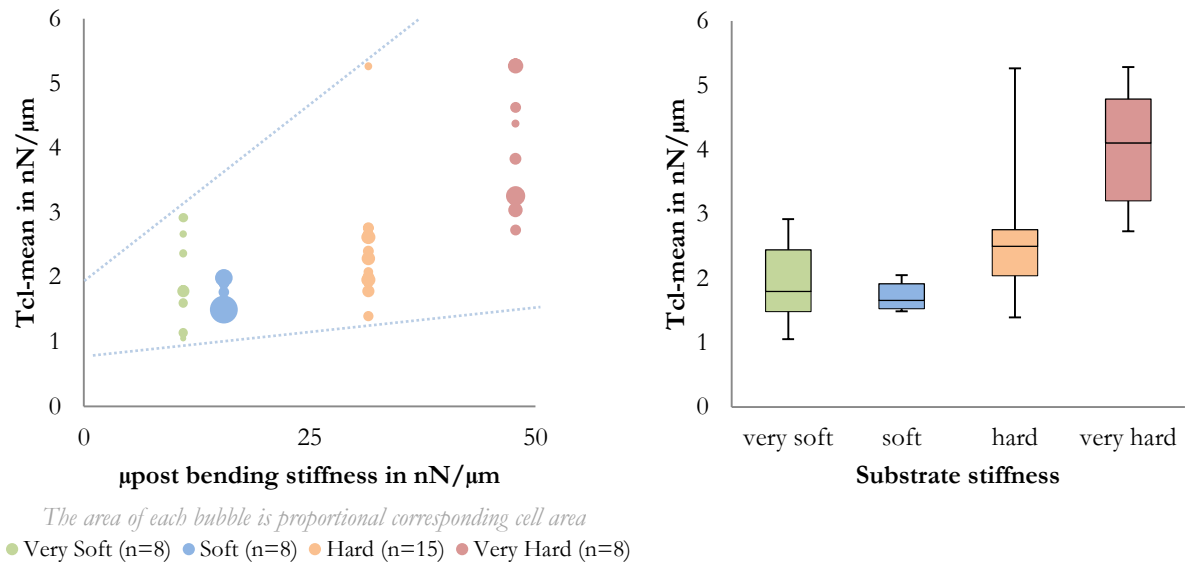

Figure 52 : The mean intracellular tension value is expressed in function to the bending stiffness of the microposts. The mean intracellular tension value is a cross-linear tension value expressed in nN/µm. Mirco-post bending stiffness is expressed in nN/µm and can be assimilated to substrate rigidity. The size of each bubble is proportional to the size of each cell.

Table 6: A one-way ANOVA test showed significant variation between the 4 groups. We completed our analysis by conducting post-hoc t-tests with a Bonferroni multiple-significance-test correction. Labels: identical (=), statistically different (≠), not statistically different (~), p-value indicates at least 95% chance but does not pass Bonferroni multiple-significance-test criteria (~).*

$T_{cl\text{-}mean}$	very soft	soft	hard	very hard
very soft	=	~	~	≠
soft	~	=	~*	≠
hard	~	~*	=	≠
very hard	≠	≠	≠	=

As previously explained in the introduction, micropost spacing should prevent contractile units from being affected by micropost bending stiffness, yet the model indicates that max and mean cross-linear tension increase in the case of the "Very Hard" substrate. The model therefore indicates (Figure 51, Figure 52, Table 5, Table 6) that the actin network is tension is influenced by the bending stiffness of the microposts.

A Pearson correlation analysis reveals that adhesion forces, the maximal cross-linear value, and the substrate rigidity seem to be correlated with the mean cross linear value within the whole cell. Yet, only the net adhesion force parameter verifies a 95% chance of correlation, the other parameters are therefore rejected as they only ensure an 80% to 95% percent chance of correlation.

Interestingly, the model may indicate that lowering micropost bending stiffness down to zero (blue lines Figure 51 & Figure 52) would still allow for internal contractility.

4. Discussion

4.1. How relevant is cross-linear tension as a mechanical indicator to study tensile loads within the cell's actin network?

When studying the tensile loads within a structure, one would generally use common mechanical indicators such as forces, pressure, stress, strain. Mechanical forces are generally relevant to study a given reoccurring and well defined mechanical structure, such as the pulling force needed to unfold a talin protein[41,4,49]. Measuring forces within the cytoskeleton can in some instances be an extremely valuable method. On the other hand, in this study, due to limited imaging resolution we are unable to tell individual filaments apart. With our current experimental setup, it is not feasible to calculate the amount of force transiting via each individual filament. Even though FRET tension sensors can be used to generate a tension map at a pN force resolution, at this time they cannot be used to quantify the amount of force transiting through a filamentous sub-structure of the cell. The resulting image can only indicate whether these molecular scale tension sensors are individually being stretched or not. Using this technique to measure forces transiting via a filament bundle or a substructure of the cell would require counting the number of stretched tension sensors and knowing how they are mechanically coupled with each other[116].

We may thus be tempted to use tensile stress as an indicator. Yet such use of tensile stress as a mechanical indicator may need further consideration. First, calculating mechanical stress requires knowing the cross sectional area through which the pulling force transits. Assessing the cross sectional area would require a 3D visualization of the cellular structure, while we only have a 2D top view of the cell at our disposal. Assessing height measurements (vertical cell thickness), is therefore not possible with the current experimental setup, which would require a confocal microscope. The inability to measure intracellular tensile stress is why cross-linear tension was introduced.

Secondly, the actin network is made of separate, yet intertwined filaments. While conventional microscopy imaging can express relative filament density in terms of gray values, unless it is a well-defined stress fiber, the directionality of filamentary substructures cannot clearly be identified. We may therefore conclude that pixel gray values are relative indicators of the net amount of tensile force transiting through the corresponding cell volume, which is proportional to the number of actomyosin filaments. On the other hand, it is unable to clearly indicate the anisotropic nature of the tensile stress transiting through the corresponding cell volume. For these reasons, we therefore consider that cross-linear[I] tension values calculated from a collection of gray values are relevant.

In this study cross-linear tension is only based on adhesion forces and actin network imaging, yet, other parameters also determine tension. For instance an actin filament may passively resist and transmit a tensile load. In such a case the tension values expressed by the model might not be accurate. Moreover, myosin phosphorylation should also be taken into account. Therefore, cross-

[1] It should be noted that in the previous chapter "cross-linear tension" required selecting the corresponding pixels perpendicularly across to a stress fiber in order to asses directional force.

linear tension values expressed in this study are only quantitatively meaningful to compare whole cell tension, so as to compare cells cultured under similar condition.

4.2. Adhesion forces and intracellular forces

The model indicates that intracellular tension is proportional to the sum of adhesion force magnitudes. In other words the intracellular stress is correlated to how much a cell pulls on its surrounding.

Furthermore, it appears that larger cells have a tendency to pull more as a whole cell on their surroundings compared to their smaller counterpart. Interestingly, they appear to exert less force on each individual micropost[18].

4.3. No deflection does not always mean no force!

Micropost experiments seem to indicate that large cells appear to exert less force on each individual micropost. We would nonetheless like to state that such results may be misleading, because the deflection expressed by micropost is determined by the net adhesion force applied on that given post (Figure 53 B). Still, micropost deflection may be minimal as it may simultaneously be pulled in opposite directions. In such a case the net vector force would be null as these opposite pulling forces would cancel each other out, as it may be the case at the center of the cell. Yet in this case adhesion molecules, such as talin, vinculin and integrin may be mechanically stressed while the micropost is not being deflected.

A) All adhesion forces applied to each post *B) Net adhesion force applied on each force*

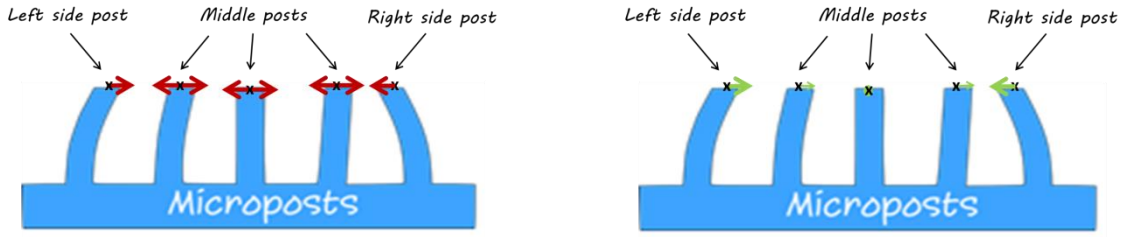

Figure 53 : No post deflection does not always mean no adhesion force!

A) Cartooned representation of all vector adhesion force applied to each post. In this example middle posts are subject to more adhesion forces. However they bend less, because opposing forces balance each other out. This is one of the reasons why central microposts appear to bend less.

B) Cartooned representation of the net adhesion force. Micropost bending is the direct consequence of the net adhesion force applied at its top end.

This balancing effect may be one of the reasons why it appears that adhesion forces (expressed in a horizontal plane) are lower near the center of the cell (Figure 53). Furthermore, it would explain why the average pulling force measured per micropost seems to decrease when we consider larger cells, while intracellular tension does not seem to do so. A second element of reflection is worth considering, which is that, adhesion forces at the periphery may also be more significant due to contribution of the dorsal actin network. This is because the dorsal part of the actin network, including dorsal stress fiber and the dorsal part of the actin cortex, can transmit tensile stress from opposite edges of the cell without interference from ventral adhesions located in the middle

of the cell. We therefore believe that it is because larger cells have more "middle" post that were previously reported to generate a lower adhesion force per post[18].

4.4. Adhesion forces and intracellular forces

While the substrate should in theory prevent contractile units from distinguishing the micropost bending stiffness[39], the results clearly show that the actin network generates more tensile stress on the more rigid substrate. We may therefore infer that the cell is sensible to the overall rigidity of its surrounding[117] in addition to being influenced by much more localized stiffness via its contractile units[39]. This conclusion therefore raises the following question: "How is 'cell scale' substrate stiffness able to influence cellular behavior?" [117]

4.5. Larger cells pull more on their surroundings because they are bigger!

Interestingly, experimental findings have time and time again expressed that larger cells pulled more on their surroundings. Yet, these experimental results failed to mention whether larger cells pulled more only because of their larger size or if they were also subject to higher internal tensile stress. Here, the model showed that there is no apparent link between intracellular tension and cell area. We therefore conclude that large cells pull more on their surroundings because they are bigger, and not because of an increased internal stress.

4.6. Bonus Results: Default tension

Interestingly, as substrate rigidity reduces intracellular the overall data profile seems to indicate that tension would be non-null if rigidity were at zero (Figure 51). Similarly, as net adhesion force tends to zero, it would seem that the cell remains contractile (Figure 49). We can therefore suppose that in addition to adhesion mediated cellular contractility; the cell is subject to default contractility. These supposed results seem consistent with cortical actin contractility, which does not require adhesion to take place.

4.7. A few words of caution concerning our analysis

While in this study we assume that contractile units are unable to bridge microposts between each other based on the literature, we did not verify this to be true. Other studies suggest that cells are influenced by large scale substrate rigidity[117]. Furthermore, while we believe that the model is sufficiently accurate to compare intracellular tension between cells when cultured, imaged, and modeled under the same conditions. In contrast, believe that quantitative cross-linear tension results expressed in this study should only be considered as estimates that may strongly depend on experimental and modeling parameters.

5. Conclusion

In this study we calculated intracellular cross-linear tension values. To do so we used a previously developed image based model to formulate a mechanical tension parameter. The objective here was not to arrive at absolute measurements. Instead, the objective of this study was to do a relative comparison of tension values between cells that were allowed to spread on microposts substrates of different rigidities. We reassuringly found that net adhesion force intensity and intracellular tension (internal stress) were positively correlated. Surprisingly, the model seems to indicate that tensile stress maybe be due to the superposition of at least two different phenomena. One seems to be mediated by adhesion while the other one seems to remain independent. We believe that the latter may be the reason why adherent cells are round when removed from their substrate.

In addition, our results indicate that large cells pull more on their surroundings because of their size and not due to significantly higher tensile stress within the actin network. It should also be borne in mind, that substrate stiffness does allow for higher tensile stress within cells, without necessarily acting as a promoter.

Moreover, in this study we presented a theoretical framework that links mechanical tensile stress within the actin network of an adherent to biochemical concentrations. We believe that this theoretical framework is an embryonic version of one of the tools needed to better understand the interplay between mechanics and biochemistry in respect to actin network contractility within human adherent cells.

GENERAL DISCUSSION

Our first objective was to use an existing model to estimate intracellular forces and their effect on the nucleus. For this we used the CDM model, which is based on divided medium mechanics. Similarly to a tensegrity structure, this modeling method allowed us to represent a tensile structure equilibrated by a passive internal compression network. To develop this interaction network, the model started from a default round configuration. It then gradually spread until it matched the observed cell's shape. Afterwards, the model went through an optimization phase. This phase required adhesion forces as an input, so that the model could successfully recreate the observed traction patterns. To experimentally measure adhesion forces, we used microposts substrates. The deflection of each micropost was a quantitative indicator of the pulling force generated by the cell. Furthermore, micropost substrates of different rigidities were used, which allowed us to analyze the effect of substrate rigidity on the cellular structure. The objective of the optimization phase was for the model to recreate an equivalent cytoskeleton. The results provided by the model showed that cytoskeletal tension and the amount of force applied to the nucleus are more important as rigidity increases. In addition, nuclear strain was also found to have increased in cells cultured on more rigid substrates. These results therefore, support the idea that the cytoskeleton is mechanically capable of deforming a stiffer nucleus. These results may have an implication on gene transcription due to nuclear deformation[11,58]. However, a visual comparison between an actin network image of the cell and that of the model, showed a lack of resemblance (page 61). While, such result does not invalidate those obtained from the model, it nonetheless weakens their credibility. Based on this conclusion, we wanted to represent the cytoskeleton with better bio-fidelity. To do so, in our second study, we used an image of the actin network to generate the structure of the model and then used inversed mechanics principle to generate an equivalent structure. In this part, based on Balaban et al., we used focal adhesion size to estimate adhesion forces[16]. The objective was to be able to measure forces on any type of flat substrate. In opposition to tensegrity theory, most of the compression force did not transit via the cell, but via the substrate instead. Furthermore, the forces ($\boldsymbol{T}_{cl}$) value provided by the model ranged from 1 to 50 nN/μm, i.e., per stress fiber, which is in line with what could have been expected, based on experimentally measured adhesion forces[16,15]. While, the results outputted by the model were coherent, we nonetheless concluded using focal adhesion size to derive adhesion force measurement, was too imprecise to generate meaningful results. Therefore, as in the first study, we once more turned our attention to micro post substrates to measure adhesion forces. But this time the model was designed to better represent the specificities of the adherent cell structures. Using the micropost substrates allowed for a well-controlled parametric study on the influence of rigidity. Moreover, the space between microposts is expected to have prevented focal adhesion contractile units form forming post to post bridges, therefore disabling their ability to differentiate micropost bending stiffness.

The results showed that the cells were influenced by substrate rigidity after being allowed to spread on top of microposts for a period of 14 hours. We noticed that an increase in rigidity allowed cells to pull more on their adhesions by generating a more tensed actin network. However, it is not because a cell was cultured on a harder substrate that it always really pulled more. For the Very-Soft, Soft and Hard conditions, it seems that an increase in substrate rigidity,

enabled the cytoskeleton to generate higher mechanical stress, rather than leading to its systematic increase. In the condition of the very hard substrate, however, we noticed that all of the cells were more contractile. Based on these results and our experimental conditions, we may assume that cells can still be influenced by substrate stiffness when the effects of contractile units are removed from the equation.

Interestingly, several studies have reported in the past that substrate rigidity, which is known to increase contractility, also promoted an increase in cell size (spreading area)[18,118]. Furthermore, larger cells were shown to generate a higher net adhesion pulling force. However, Han et al. experimentally found that mean adhesion force magnitude per post was reduced in large cells. We therefore wondered if internal tensile stresses in large cells would differ from those generated by their smaller counterparts. The results showed that under the same culture conditions, larger cells generated cross-linear tension values that were equivalent to their smaller counterparts. We conclude that larger cell size does not promote internal stresses (Figure 54).

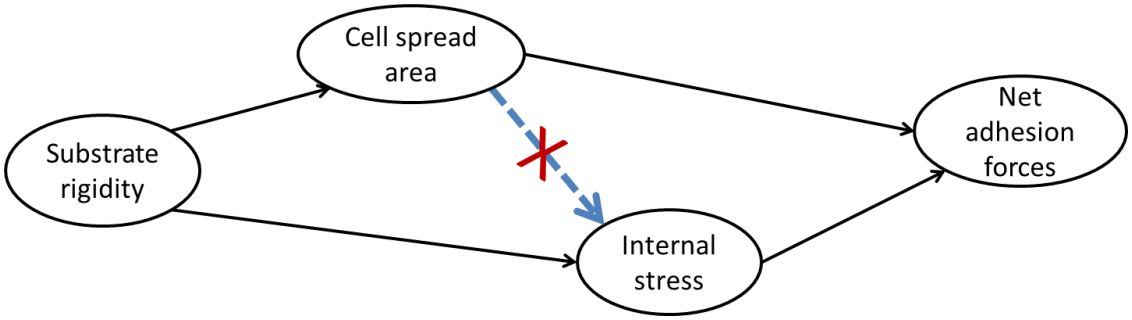

Figure 54: How different cellular parameters seem to influence one another.

Black arrows show how a parameter may promote another. We wondered if cell spread area could increase internal stresses in actin network (blue arrow), the model suggests that is not the case (red-cross).

A surprising result from the model was the fact that it seemed to indicate the presence of a "default tension" that does not seem to be influenced by adhesion conditions. Moreover, our analysis would suggest that this contractility takes place, even without adhesion. Logically, were the cells not adhering to the substrate or during early stages of adhesions, the image based model would not have been able to perceive this non adhesion mediated tension. Instead, we believe that the model was able to perceive this superimposed tension because the cells were already fully adhering to the substrate. We can consequently suppose that the cross-linear tension values expressed by the model overestimate tension forces in stress fibers.

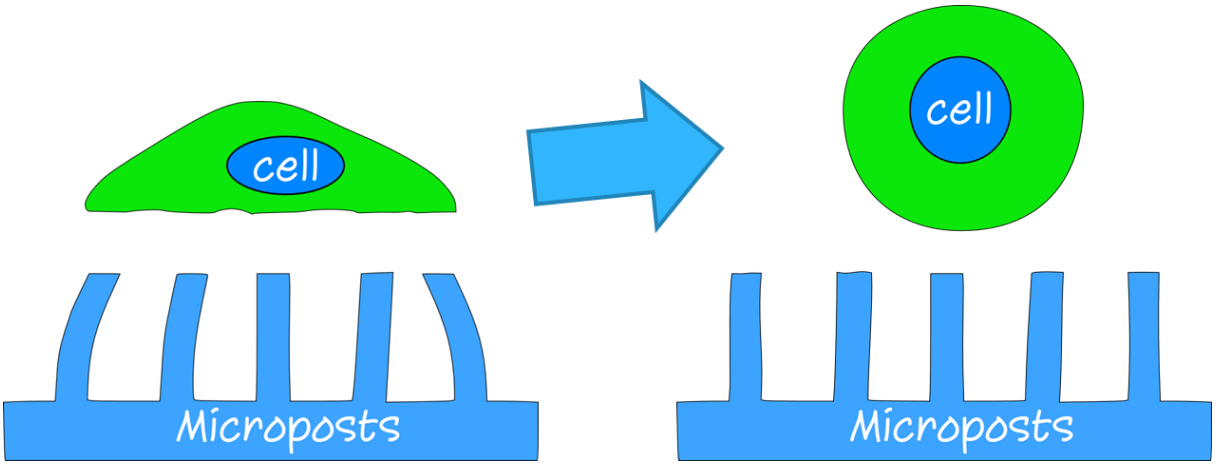

Figure 55: The cell becomes round when it is in suspension. We hypothesize that this may be due to cortical actin contractility

Assuming that this analysis is correct, we may therefore, wonder what this "default tension" corresponds to. We therefore have to consider what source of cytoskeletal contractility may be in play when the cell does not adhere. In such case the cell becomes round, and the actin cortex remains (Figure 55). We therefore, sugest that this "default tension" is the manifestation of super imposed contractility generated by the cortical actin nework, which is also responsible for cytoplasmic fluid pressure and subsequent cell blebs.

Interestingly, the cortical actin network does not seem to be affected by adhesion conditions. However, it is not the case for integrin mediated actin network components such as the stress fibers, the lamellipodium and lamella, which dissolve completely. This means that, unlike what may be the case in a typical contractile structure, the cytoskeleton dissolves and then regenerates during spreading. Even though we understand how individual cytoskeletal structures are formed, the fact that the cytoskeleton self-assembles and reassembles is hard to fathom. It is especially true when we try to understand how all these sub-cytoskeletal structures and molecular cytoplasmic components interact with one another to form a complex system[119]. Thus, the basic principles enabling complex inter-molecular self-organization still remain unexplained.

1. A conceptual model of adherent cell mechanics

1.1. Using our results to provide a better understanding of cell mechanics

Our model seems to indicate a "default cross linear tension", $\boldsymbol{T_{cl-def}}$ of about 1 nN/µm, i.e., in an adherent cells, every section of 1 µm diameter is crossed by an average tensile force of 1nN. We would like to know, if this "default" tension could be responsible for intracellular hydrostatic fluid pressure.

If we consider $\boldsymbol{T_{cl-def}}$ to be equivalent to the super imposed cross-linear tension of the ventral and dorsal actin cortex, we can calculate the theoretical intracellular pressure it should generate if the cell were round (Figure 56) and compare it with values found in the literature.

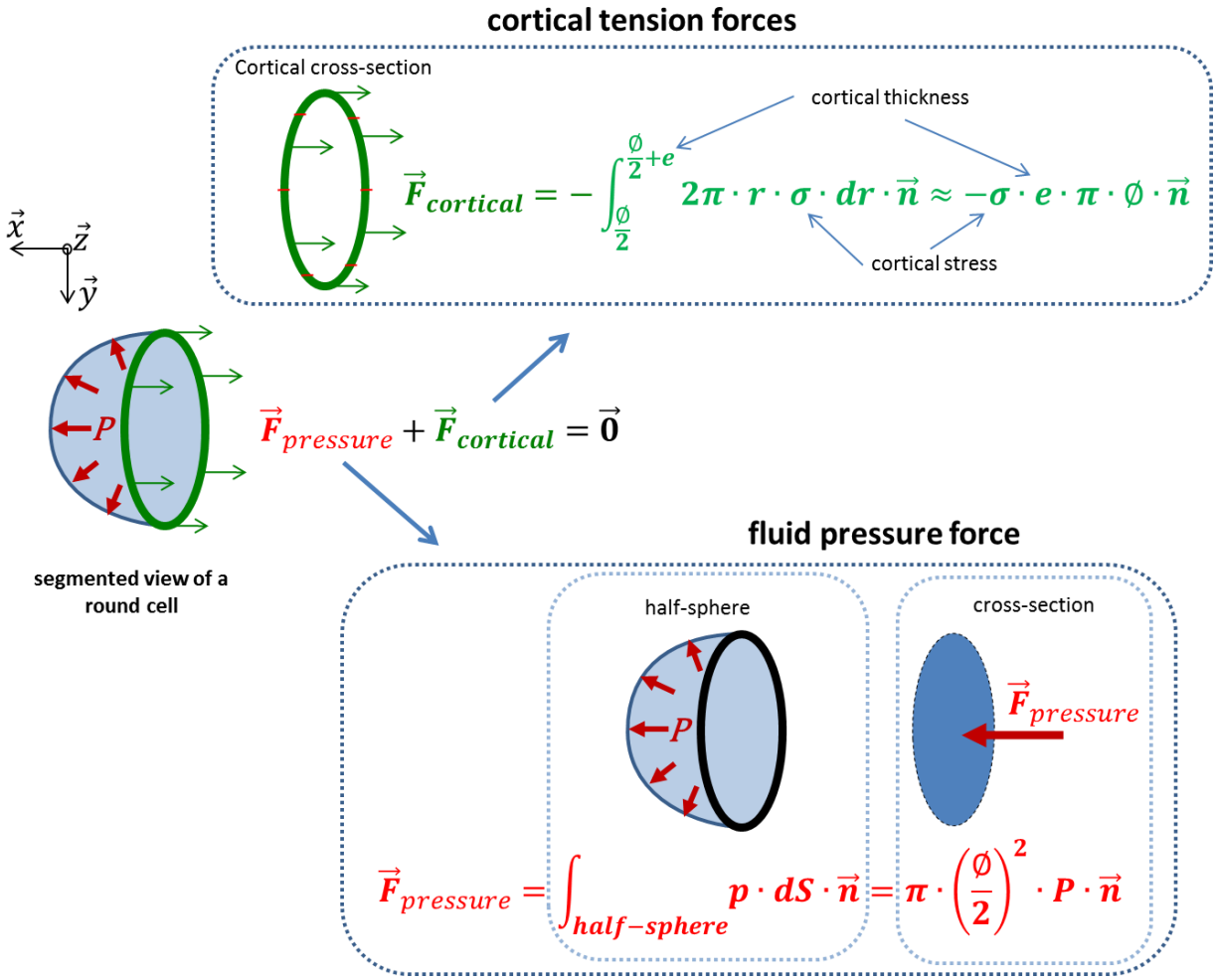

Figure 56: Illustration of cross-sectional forces generated by the actin cortex and the intracytoplasmic fluid pressure of a round cell.

To calculate the intracellular cytoplasmic pressure inside a round cell, we use the following reasoning. We can consider that if we take a cross section of the cell going straight through its center, we can assume that the peripheral force generated by the thin actin cortex ($\vec{F}_{cortical}$) is counter balanced by the fluid pressure (P), and therefore equal and opposite to the fluid pressure force ($\vec{F}_{pressure}$) exerted on the half-sphere (Figure 56).

Equation 23

$$\vec{F}_{pressure} + \vec{F}_{cortical} = \vec{0}$$

In other words, since the actin cortex is 'thin', we can consider that its internal stress (σ) is constant. Furthermore, the internal stress multiplied by the thickness (e) of the actin cortex is equal to half the default cross linear-tension (T_{cl-def}), since this cross-linear tension value accounts for the dorsal and ventral layer of the actin cortex.

Equation 24

$$\sigma \cdot e = \frac{T_{cl-def}}{2}$$

Equation 25

$$\vec{F}_{cortical} \approx -\sigma \cdot e \cdot \pi \cdot \emptyset \cdot \vec{n} = -\frac{T_{cl-def} \cdot \pi \cdot \emptyset}{2} \cdot \vec{n} \quad with\ \emptyset = diameter\ of\ the\ round\ cell$$

Equation 26

$$\vec{F}_{pressure} = \pi \cdot \left(\frac{\emptyset}{2}\right)^2 \cdot P \cdot \vec{n} \quad with\ \vec{n}:\ unitery\ vector$$

Equation 27

$$\vec{F}_{pressure} + \vec{F}_{cortical} = \vec{0} \quad \rightarrow \quad P = \left|\frac{2 \cdot T_{cl-def}}{\emptyset}\right|$$

Based on our calculations using Equation 27, for $\boldsymbol{T_{cl-def}}$ equal to ~1 nN/μm and a diameter (∅) of 15 μm, we obtain a theoretical[I] hydrostatic pressure (***P***) of 133 Pa. This value is in accordance with internal hydrostatic pressure values found in the literature, which range between 40 to 400 Pa[120]. We can therefore conclude that it would not only be qualitatively coherent, but also quantitatively coherent to assume that the "default" tension found by the image based model corresponds to cortical actin contraction.

Therefore, based on these results and those found in Chapters 2 & 3, we conclude that in a spread cell inward intracellular forces, i.e., tension, are largely counterbalanced by hydrostatic pressure and the ECM. In addition, when the cell is no longer bound to a substrate, the actin cortex maintains hydrostatic pressure, consequently minimizing external area and making the cell round. We conclude that unlike what the tensegrity theory predicted, the cell does not largely balance internal compressions forces based on a compression network, nor does it round due to stress fibers. Therefore, the compression network found in Figure 29 on page 59 of Chapter 1, represents, mostly fluid pressure. However, it has been stated that microtubules do bear compression loads and buckle[83]. Yet, these forces have been found to be marginal, and unable to sustain the contraction load generated by the actin network[43]. In addition, microtubules and actin filaments are interconnected, consequently creating a reticulated pre-stressed network of tensed actin cables and compression bearing microtubules that may help stabilize the nucleus and organelles inside the cell. While this may appear to be the mechanical properties of a tensegrity structure, strictly speaking, it is not the case, since the compression bearing agents only counteract a marginal part of the tensile stress[44,43,105]. We consequently conclude, that the tensegrity theory is a confusing and misleading concept that is unable[96] to correctly describe the mechanical structure of adherent cells[121,44,43,105]. Nevertheless, this theory has been most valuable to highlight the notion of intracellular pre-stress and from an external point of view, tensegrity cell models can still be useful to describe the elastic behaviors of the cytoskeleton in static conditions[81] and a modified version developed by Canadas et al. can also be used to model the viscoelastic properties of the cell[122].

[I] The expressed pressure value equates to relative pressure, ambient pressure must be added to obtain absolute pressure.

Yet, when trying to conceptually understand the cell structure or model intracellular forces, it may be more appropriate to use another modeling strategy. Since the cell is surrounded by a contractile actin cortex the viscous cytoplasmic fluid is pressurized. This leads us to conclude that adherent cells may best be viewed as a hybrid hydrostatic skeleton that includes a pre-stressed filamentous network. Furthermore, adherent cells are pinned to the substrate via their adhesions and stress fibers[121]. The viscous cytosol and the elastic filamentous components which compose the cytoplasm may consequently explain the viscoelastic behavior of the cell structure.

Additionally, the high viscosity of the cytosol interacts with the various filamentous elements of the cytoskeleton as the cytosol has to seep between the filaments as if it were to navigate in a porous network. In that regard Charras et al. state that the observed mechanical behavior resembles that of a poro-elastic medium[123]. Charras et al.'s proposal therefore explains why hydrostatic pressure differences between different parts of the cell require an unexpectedly long periods of time to equilibrate. But once again, a poro-elastic model does not represent the authentic structure of the cell which includes a hybrid mechanical structure that combines a pre-stressed fibrous and hydrostatic skeleton.

1.2. The hydrostatic skeleton model is in accord with early spreading dynamics

Interestingly, the initial spreading stage (before stress fiber formation) of various cell types was experimentally shown to follow a set of universal power laws[124]. This phenomenon can be explained by a mechanical model that includes an actin cortex and a viscoelastic cytoplasmic fluid[124,125]. At the very initial spreading stage, the radius of the contact area increases proportionally to the square root of time since spreading started. This rate is due to a purely geometrical phenomenon involving contact dissipation without requiring irreversible deformation of the actin cortex[124,125]. Afterward, as spreading further progresses, its rate slows down and follows another power law ($\sim t^{1/4}$) due to increasing tension and dissipation within the cell's cortex[125]. The hybrid hydrostatic cytoskeleton is therefore in accord with early spreading stages. Still, the mechanical purpose of stress fibers needs to be discussed.

1.3. Adherent cell mechanics and stress fibers

In the introduction, we specified the type of stress fibers and the way they formed (pages 24-27), but their mechanical role was not clearly stated. We nonetheless stated that on a 2D substrate stress fibers may either stabilize as ventral or cap stress fibers. The only difference being that cap stress fibers go over the nucleus, consequently contributing to its overall deformation. In contrast, ventral stress fibers run along the cell membrane directly connecting two focal adhesions, which are bound to the substrate. The primary role of ventral stress fiber might therefore not be as a primary internal structural element, instead, it is used as a way to mechanically connect the cell to its environment, to partially or totally immobilize it, while shielding other internal structural components from high mechanical stresses induced by significant substrate stretching. This hypothesis is furthermore supported by the fact that stress fibers will align perpendicularly to the direction of cyclic substrate deformation[126]. In addition, stress fibers and the focal adhesions they pull on have a regulatory purpose, such as inhibiting lamellipodium formation, consequently contributing to cell immobilization both mechanically and chemically[127].

PERSPECTIVES

1. A lot more to learn

While using our model we were able to show that spreading could mechanically induce nuclear deformation. Linkage between the cell and the nucleus is known to involve various LINK proteins[58]. The way these connections are organized still remains unclear as they also involve the nucleus and intermediate filaments. Furthermore, while we know that nuclear deformation impacts gene activation, there is still a lack of understanding of how these processes take place[11,58].

In addition, the concept of cell motility has hardly been discussed in this manuscript, yet it is an important concept that may allow us to develop a clearer understanding of the cytoskeletal structure.

1.1. Migration: a way to better understand the cell, including during spreading

1.1.1. Migration vs spreading

Cell migration and spreading are generally presented in the literature as segregated processes, so it may be confusing to notice that the spreading process and adherent cell migration may resemble one another in many ways as they involve common sub-processes, such as lamellipodium, lamella, stress fiber formation, and so on. From a conceptual perspective it may thus be easier to think of both processes as two sides of the same coin. On the other hand, in many cases it is clear that a cell is either adhering or migrating[128], while at other times things might not be so clear.

During cell motility or spreading, the actomyosin network contracts, and consequently generates internal fluid pressure. At the leading edge, internal fluid pressure, and lamellipodium polymerization push the membrane forward and to the side (Figure 57, thick black arrows). At this point, the actomyosin network contraction is mechanically unstable, creating an actin flow (Figure 57, red arrows)[129].

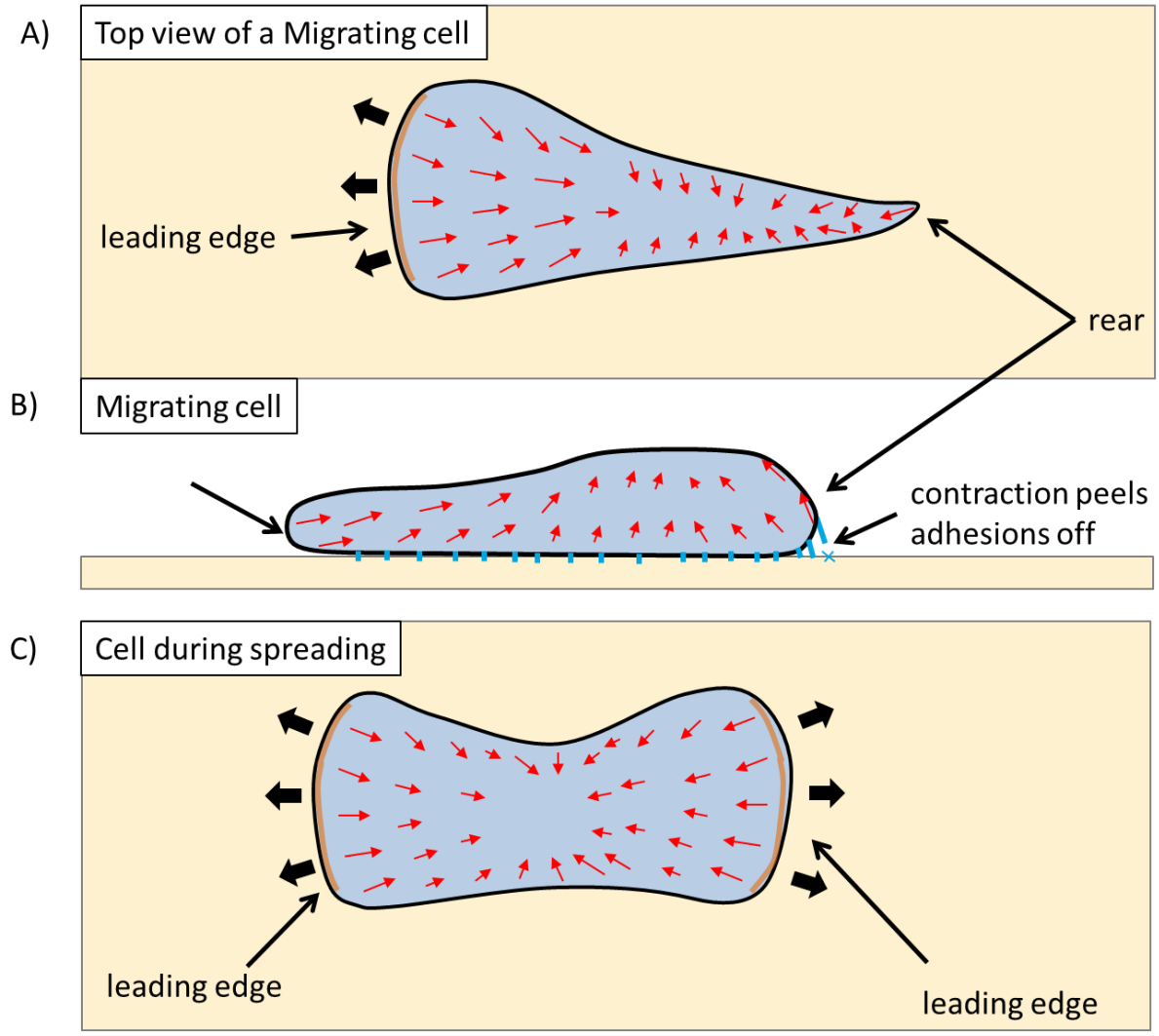

Figure 57: Actin flow (red arrows), lamellipodium pushes cell membrane forward (thick black arrows)

A) Top view of a migrating cell. The sides and the rear of the cell retract inward due to actomyosin contractility, therefore becoming thinner over time. As the cell body retracts on itself , the cytosol is consequently displaced towards the front of the cell forming and filling a forward moving protrusion that may also expand to the side, either making the cell long and narrow or allowing a large cell front.

B) Side view of a migrating cell. In highly contracted cells, integrin molecules can be left behind, suggesting a rear adhesion peel off mechanism[122]*. On the other hand, focal adhesions are believed to partially disassemble at the rear of the cell*[122]*.*

C) The cell is spreading, it has two lamellipodium running in opposite directions, allowing it to flatten, but not migrate.

The actomyosin flow may locally converge in one or more points, thus increasing local actomyosin density, which leads to actomyosin disassembly, allowing the monomers to be reused in another location for reassembly[130]. As the cell migrates (Figure 57A), the newest part of the network is located at the front of the cell, but as time passes, continuous contraction reduces the width of the cell, making the rear thinner since it is older (Figure 57A). The cytoplasmic fluid is consequently squeezed to the front of the cell, the only place where volume increases. This intracytoplasmic fluid movement and osmosis allows for the necessary monomers to be moved

forward for assembly to continue. As actin filaments assemble, they form the new actin cortex, lamella, and stress fibers. In some cases, as the cell moves forward, the actin cortex contraction may even forcefully rip a stress fiber that was previously trailing behind off from its focal adhesion. More generally, as the actin cortex contracts it is able to peel of adhesions at rear of the cell (Figure 57B), leading to corresponding integrin mediated structures to disassemble[131].

Similarly, cell spreading involves many of these steps (Figure 57C), lamellipodium protrusions, fluid pressure, F-actin flow and disassembly, except that the cell does not move over a large distance. Instead, large stress fibers stabilize and thicken, until the cell is fully spreads. Interestingly, the same thinning effects may be observed on a cell as it spread, as is illustrated at the middle of the cell Figure 57C. Therefore, while there are some differences between cell motility and cell spreading, the two are, nonetheless, extremely similar.

1.1.2. The cell is an unstoppable freak machine

Cells have this amazing capacity to squeeze through small holes. The process is similar to that of cell blebbing, it may also involve lamellipodium protrusion to help push the cell membrane down the hole. Everything that is inside the cell is squished and squeezed through the hole by fluid pressure, itself generated by actin cortex contraction (Figure 58). This process requires the cell to assemble and repair its structure, which still remains elusive phenomena.

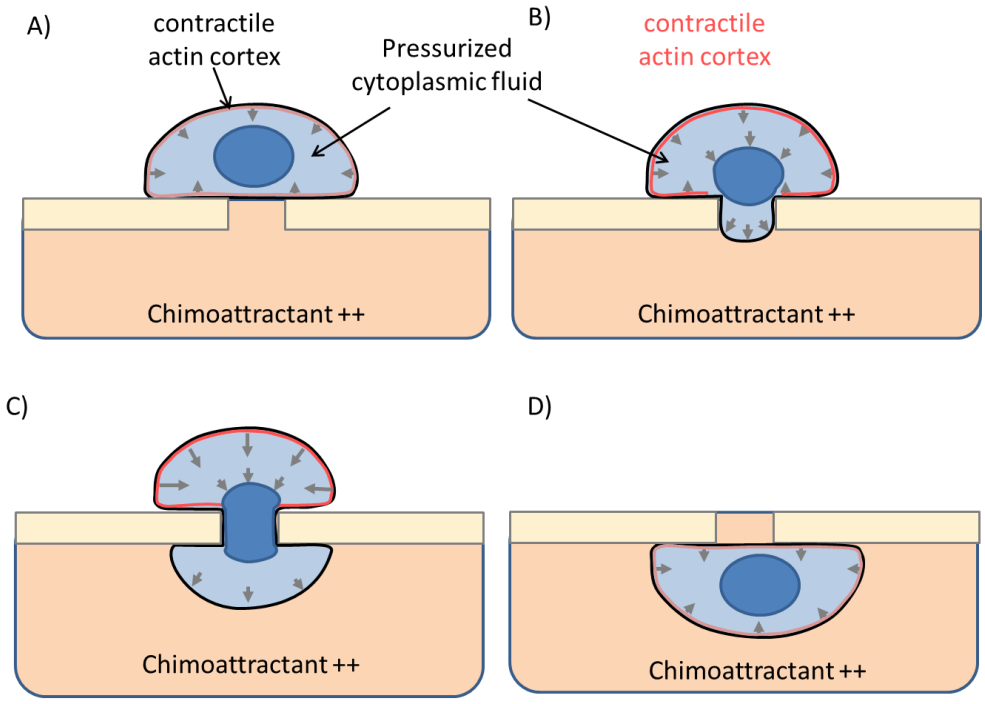

Figure 58: Cell going through small hole.

A) The cell is on the other side of the chemical gradient.

B) Actin cortex contraction generates cytoplasmic fluid pressure, which pushes the weaker membrane down through the hole.

C) The nucleus is also being pushed and squeezed through the hole.

D) The cell is on the other side.

2. Understanding cell mechanics will require a change in perspective

2.1. Understanding a cell requires understanding how it interacts with its neighbors

Studying collective cell migration allows us to understand that trying to study the behavior of an isolated cell is not sufficient to get the full picture[132]. Similarly, at high cell culture density, fibroblast cells align with each other at the bottom of a culture flask, forming a sheet of well aligned similarly shaped cells. Be that as it may, isolated adherent cells usually take erratic shapes, therefore hinting the idea that such cells are not able to fully control their shapes by themselves and require interactions with other cells to do so. This would in part explain why in Chapter 3, we found significant variability of size and contractility between cells cultured in identical conditions. This idea is further supported by the literature which states that multicellular clusters are able to fully regulate tensional homeostasis, whereas isolated cells are not.[133]

In some way, an analogy between the structural variability of isolated cells and a double pendulum's chaotic motion can be made, if we consider that unpredictability is due to "a lack of constraints".

2.2. Correlating intracellular mechanical stresses with biological behavior

While this project enabled us to assess the mechanical behavior of the cell, it would be interesting to correlate these findings with a biochemical response of the cell. For instance, to see if there is a positive relationship between gene activation and cytoskeletal stresses. Moreover, we could use a FRET tension sensor adapted to LINK complex proteins, to see if overall tensile stresses generated by the actin network are correlated to the forces that are directly transmitted to the nucleus.

2.3. Continuing in the same direction has its limitations

A way to deepen our understanding of the subject might be to pursue and improve our current research strategy by developing a 3D cell model from confocal images. In addition, we could also significantly increase accuracy by using super resolution microscopy[75,114,76]. This would allow us to accurately model individual stress fibers. We could also include additional information, such as images of myosin phosphorylation to better specify the mechanical stresses inside the cytoskeleton. Imaging other cytoskeletal components such as the microtubules and intermediate filaments would also complete our current partial view of the subject, as both of these structural components have their importance. Yet, sometimes more information and more accuracy does not remove important barriers. For instance, such improved models would not be able model dynamic cellular behaviors such as the actual spreading process or cell motility, as this technique is currently limited to taking snap shots of the cell. Therefore, formulating a model that may gradually evolve over time requires a change in strategy. A cellular structure self-assembles and is extremely dynamic, but these phenomena rely on different principles than those we have discussed in this manuscript.

3. Understanding the role of complexity in cellular self-assembly

While there are still a lot of missing details on cytoskeleton self-assembly, the formation of many structures, such as ventral stress fiber, are largely explainable, at least in theory (pages 24-26).[17] For instance, we now know that arc stress fiber assembly involves polymerization of polar filaments, cross-link and motor proteins, as well as the clever use of boundary conditions to enable the emergence of such structures. Similarly, lamellum formation could theoretically be explained based on arc filament formation (page 20).[17] A similar descriptive analogy could be made about how cortical actin forms during cell blebbing (page 24).[1] This descriptive analysis could include a significant number of molecules, i.e., proteins, that are involved in the formation of such structures[1,17,116,50,134,100]. Furthermore, we would almost be able to describe step by step how these structures are self-assembled[1,17]. In addition, many regulation pathways and molecules interactions are known. Yet, we only have a partial understanding of the way these molecules interact to make a coherent system. This subsequently prevents us from designing a functional in silico model. In addition, creating such a complex model at the molecular level goes beyond our current computational capabilities. What is more striking and fundamentally more important, however, is that we are currently unable to simplify such mechanibiological systems. This is mostly because we still do not understand the fundamental principles used by the cell to generate a coherent self-assembling structure.

There are several theories concerning the subject of self-assembly[135] and self-organization[136,119,137]. Yet, there currently is no explanation as to how a set of molecules, i.e., proteins, are able to collectively form and maintain a dynamically changing structure, such as the cytoskeleton. Moreover, there is currently no theory able to formally explain how the cellular system is able to cope with massive stresses and extensive disruptions, such as a cellular passage, that abruptly dissolve major and much needed structural elements of the cytoskeleton. While the cell does mechanically collapse on itself, as it rounds, it is still able to robustly and resiliently reorganize its internal structure without dying. In other words:

"We currently do not understand the strategy used by the cell to manage internal chaos."

Understanding the basis of this strategy will require an understanding of how all the components interact to form a coherent system that can be interrupted at any time or submitted to unpredictable chaos while still being able to self-restart and self-reorganize.

The field of Complexity Science may provide a useful strategy. This recent scientific field has gradually been able explain and model various phenomena involving the emergence of self-organization within pseudo chaotic systems (Figure 59). This is why it may be relevant in that domain. It involves the idea that a system whose components interact in multiple ways and follow local rules may allow the emergence of a supra-organized state.[136,138] The cytoskeleton and complex systems have several behavioral attributes in common. Both of them do not rely on individual components, they are able to adapt to change, they behave in a non-deterministic fashion, consequently allowing significant variability while still remaining coherent over time[139].

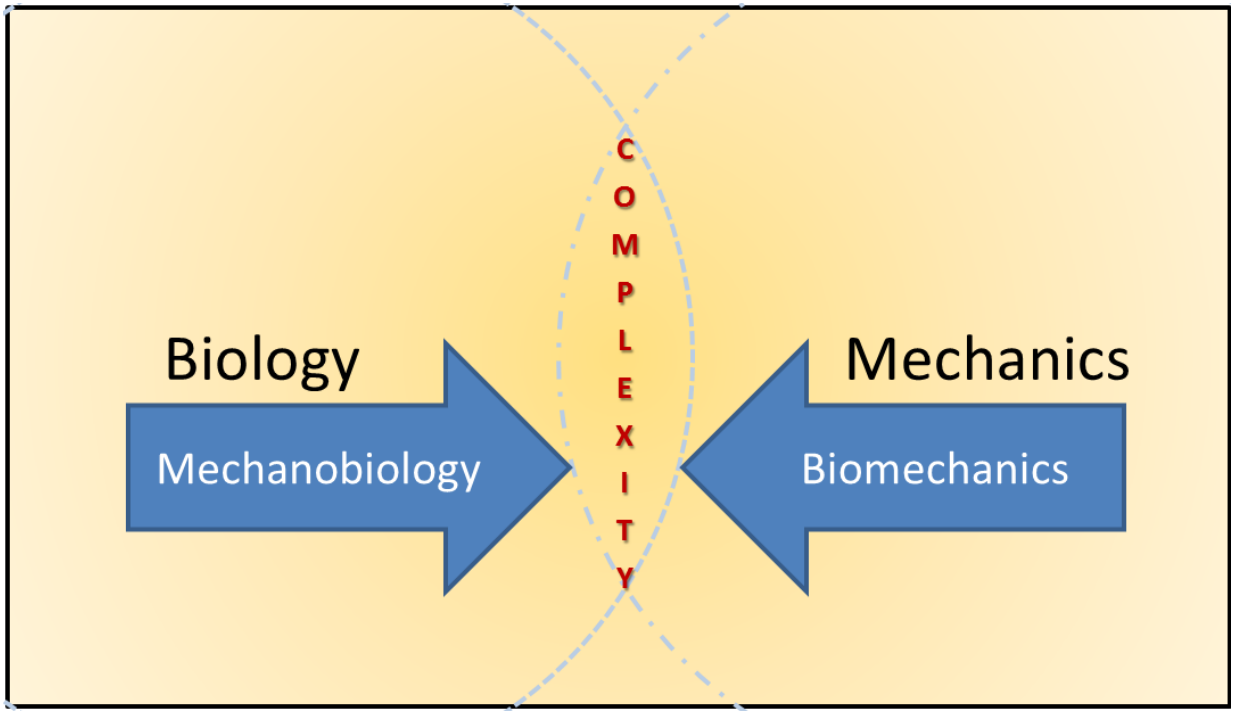

Figure 59: Complexity is a promising way to bridge mechanobiology and biomechanics, so as to enable a better phenomenological understanding of mechanostransduction and the emergence the cytoskeleton structure.

While there is a limited number of publications that have considered the involvement of complexity in cytoskeleton dynamics, it is nonetheless a promising approach[138]. Complexity has allowed researchers from other subfields of biology to understand hard to model problems such as the formation of bird swarms and schools of fish.[136,140] But to model complexity will first force us to understand the fundamental concepts of cytoskeletal self-assembly.

GENERAL CONCLUSION:

We used two distinct computational models, to better understand how the cell is structured and how forces are distributed within the cell. The CDM model showed that the cytoskeleton is able to mechanically deform the nucleus and that mechanical load applied on the nucleus increases due to substrate rigidity, consequently further increasing mechanical deformation. Yet we felt that there must be a different approach to model the cell, to better take into account the specificity of each cell. We consequently developed an image based model. This model allowed us to focus on the mechanical properties of the actin network.

Larger cells had been reported to pull more on their surroundingss[7,18]. In addition, cells cultured on Hard+ substrate were also reported to pull more on their surroundings, while their projected cell area had increased as well[18]. We therefore wondered if cell size could promote intracellular tension. The image based model showed that larger cells do not generate higher intracellular stresses then their smaller counterparts allowed to spread under the same conditions. In addition, our results indicate that adherent cells are sensitive to large scale rigidity properties, while also being able to generate a "default tension", which we identify as cortical actin contraction.

The lack of a consensus concerning a conceptual basis of adherent cell mechanics in the literature made it difficult to grasp basic principles that would enable cell spreading and migration without contradictions. Yet, based on the bibliographic analysis presented in the introduction and our own results, we have excluded ideas and models that did not correspond to experimental observations.

While microtubule compression load bearing does exist, their mechanical role is marginal as it only supports only about 10% of the total compression load[44,43]. Moreover, our results show that the ECM or the substrate counter balance a significant amount of the compression load generated by the actin cortex, lamella and stress fibers. While the lamellipodium is able to push the cell membrane, it only represents a temporary and localized phenomenon that does not contribute to the mechanical stability of the overall cell structure. Our conclusion is that the cell structure resembles that of a stretched visco-elastic water balloon, filed with a meshwork of pre-stressed filaments. In addition, this "balloon" is pinned to a substrate via its focal adhesions. The latter are inter-connected via actin stress fibers, that act as pre-stress self-tightening belts that either ultimately stabilizes as ventral or actin cap stress fibers (page 27). Moreover, cap stress fibers go over the nucleus and press it against the substrate[17]. In other word, the conceptual model of the cellular structure involves a hydrostatic skeleton filled with a viscoelastic cytosol and an internal meshwork of pre-stressed filaments.

This conceptual model allows us to understand how the cytoskeleton, the cell membrane, the cytoplasm, and the nucleus interact with one another to form a coherent system that seems to agree with experimental findings. Furthermore, this conceptual model explains the inherent contractile nature found in both adherent and non-adherent cells. It is also both compatible with cell spreading and during more extreme events such as cell passage. In addition, we were able to understand how cells could pass through small holes. Regrettably, many important details, such as a clear understanding of the mechanical coupling between the nucleus and substrate, are still

missing. Yet, maybe from a mechanical perspective, the most important missing detail is a way to understand the basic principles behind self-assembly as it prevents us from designing similar systems to either study the cell or build entirely new systems.

ACKNOWLEDGEMENTS:

I would like to formerly acknowledge the people that are listed below. While some where official participants to my research project and were therefore mentioned as co-authors in our publications, others did not benefit from such recognition but where nonetheless work colleagues and friends I could always turn to for help and advice.

Institut des Sciences du Mouvements (Aix Marseille Université & CNRS), Marseille, France:

- Jean-Louis Milan Ph.D – Associate Professor, biomechanics
- Patrick Chabrand Ph.D – Professor & Head of Giboc Research Team, biomechanics
- Sophie Séguinel - Lab Clerk
- Charlotte Janneau Ph.D - Associate Professor, biology
- Imad About Ph.D - Professor, biology
- Patrick Laurent Ph.D - Associate Professor & Dentist
- Thomas Soler Dr. - Dental Teaching Assistant
- Jean-Baptiste Renault, Ph.D candidate, biomechanics
- Mathias Donnez, Ph.D candidate, biomechanics
- Yassine Saadlaoui, Ph.D candidate, mechanics
- Cécile Baron, Ph.D, Associate Research Professor, biomechanics
- Martine Pithioux, Associate Research Professor, biomechanics
- Sophie Lecann, Ph.D, biomechanics
- Maxime Vasseaux, Ph.D, biomechanics
- Martin Seyres, Ms., biomechanics
- Fanny Chimeleski, Ph.D, biology
- Victoria Spartacus, Ph.D candidate, biomechanics
- Pascal Chavet, Associate Professor, biomechanics
- Pierre Rufas, Ph.D candidate, biologist
- Flavy Roseren, Ph.D candidate, biomechanics

Washington State University, Seattle, USA

- Nathan Sniadecki, Ph.D, Associate Professor, mechanobiology
- Kevin Beussman, Ph.D candidate, mechanobiology
- Sangyoon Han, Ph.D, mechanobiology

Université de St-Etienne, St-Etienne, France

- Alain Guignandon, Professor, mechanobiology

Université de Valencienne, Valencienne, France:

- Maxence Bigerelle, Professor, material science

Institut de Science des Materiaux de Mulhouse, Mulhouse France:

- Karine Anselme, Research Professor, mechanobiology
- Tatiana Bourgade, Research Lab Engineer, biology

I would like to give a special thank you to:

- Jean-Louis Milan for attempting to teach me his positive critical thinking skills
- Imad About for his never ending patience and support
- Patrick Chabrand for his kindness and being the first to welcome me into the lab
- Charlotte Jeanneau for tutoring me during my first cell culture manipulations
- Sophie Séguinel for everything she did to enabling us to focus and not focus on our work
- Martine Pithioux for never giving up
- Sophie Le Cann for preparing classes together in the ups and downs
- Pascal Sommer for your never ending open mildness
- Jean-Marie Rossi for your skeptical mind towards my ideas and your resulting humor
- Cécile Baron for kindly agreeing to disagree
- Maxime Vassaux for your bluntness
- Martin Seyres for allowing me to witness the unpredictable effects of your programming skills
- Alain Guignandon for your open mildness and curiosity
- Marie Semann, Jean Baptiste Renault, Yassine Saadlaoui and Mathias Donnez for accepting to share their office with me. You and your better halves Audrey, Cecilia and Julie were great.
- My parents, Kathryn Trulsen and Gerard Manifacier for their unconditional love and support.

I would also like to thank Colette Manifacier, Marie-Louise Achard, Lorie Ringering, Phyllis Barbour, Michael Manifacier, Justin Owsely and Ourson En Pelluche for their kindness and support. And Carmen Deghan, Béatrice Pivet, Colette Faravel for their support.

Lastly, my warmest and greatest thank you goes to Jeanne Manifacier, without whom I would not be who I am today.

But most importantly, the things I am most thankful for are, the good moments of laughter we all shared together. As well as, the moments of indulgence as new ideas arose, that nonetheless included laughter and kind mockery.

So while the subject was, and still is fascinating, working with all of you is what made it worth it.

Institutional partners

REFERENCES:

1. Charras, G. T., Hu, C.-K., Coughlin, M. & Mitchison, T. J. Reassembly of contractile actin cortex in cell blebs. *J Cell Biol* **175,** 477–490 (2006).
2. Jiu, Y. *et al.* Bidirectional Interplay between Vimentin Intermediate Filaments and Contractile Actin Stress Fibers. *Cell Reports* **11,** 1511–1518 (2015).
3. Mitchison, T. & Kirschner, M. Dynamic instability of microtubule growth. *Nature* **312,** 237–242 (1984).
4. Hirata, H., Tatsumi, H., Lim, C. T. & Sokabe, M. Force-dependent vinculin binding to talin in live cells: a crucial step in anchoring the actin cytoskeleton to focal adhesions. *American Journal of Physiology - Cell Physiology* **306,** C607–C620 (2014).
5. Ujihara, Y., Nakamura, M. & W, S. in *Biomedical Engineering - From Theory to Applications* (ed. Fazel, R.) (InTech, 2011).
6. Huang, S. & Ingber, D. E. The structural and mechanical complexity of cell-growth control. *Nat Cell Biol* **1,** E131–E138 (1999).
7. Fu, J. *et al.* Mechanical regulation of cell function with geometrically modulated elastomeric substrates. *Nature Methods* **7,** 733–736 (2010).
8. Tee, S.-Y., Fu, J., Chen, C. S. & Janmey, P. A. Cell Shape and Substrate Rigidity Both Regulate Cell Stiffness. *Biophysical Journal* **100,** L25–L27 (2011).
9. Dokukina, I. V. & Gracheva, M. E. A model of fibroblast motility on substrates with different rigidities. *Biophys. J.* **98,** 2794–2803 (2010).
10. Shieh, A. C. & Athanasiou, K. A. Dynamic compression of single cells. *Osteoarthr. Cartil.* **15,** 328–334 (2007).
11. Itano, N., Okamoto, S., Zhang, D., Lipton, S. A. & Ruoslahti, E. Cell spreading controls endoplasmic and nuclear calcium: a physical gene regulation pathway from the cell surface to the nucleus. *Proc. Natl. Acad. Sci. U.S.A.* **100,** 5181–5186 (2003).

12. Titushkin, I. & Cho, M. Modulation of cellular mechanics during osteogenic differentiation of human mesenchymal stem cells. *Biophys. J.* **93,** 3693–3702 (2007).
13. Sangaletti, S. & Colombo, M. P. Matricellular proteins at the crossroad of inflammation and cancer. *Cancer Letters* **267,** 245–253 (2008).
14. Tozluoğlu, M. *et al.* Matrix geometry determines optimal cancer cell migration strategy and modulates response to interventions. *Nature Cell Biology* **15,** 751–762 (2013).
15. Tan, J. L. *et al.* Cells lying on a bed of microneedles: An approach to isolate mechanical force. *Proceedings of the National Academy of Sciences* **100,** 1484–1489 (2003).
16. Balaban, N. Q. *et al.* Force and focal adhesion assembly: a close relationship studied using elastic micropatterned substrates. *Nat Cell Biol* **3,** 466–472 (2001).
17. Tojkander, S., Gateva, G. & Lappalainen, P. Actin stress fibers - assembly, dynamics and biological roles. *Journal of Cell Science* **125,** 1855–1864 (2012).
18. Han, S. J., Bielawski, K. S., Ting, L. H., Rodriguez, M. L. & Sniadecki, N. J. Decoupling Substrate Stiffness, Spread Area, and Micropost Density: A Close Spatial Relationship between Traction Forces and Focal Adhesions. *Biophysical Journal* **103,** 640–648 (2012).
19. Meacci, G. *et al.* α-actinin links ECM rigidity sensing contractile units with periodic cell edge retractions. *Mol. Biol. Cell* (2016). doi:10.1091/mbc.E16-02-0107
20. van Hoorn, H. *et al.* The Nanoscale Architecture of Force-Bearing Focal Adhesions. *Nano Lett.* (2014). doi:10.1021/nl5008773
21. Loosli, Y., Luginbuehl, R. & Snedeker, J. G. Cytoskeleton reorganization of spreading cells on micro-patterned islands: a functional model. *Philosophical Transactions of the Royal Society A: Mathematical, Physical and Engineering Sciences* **368,** 2629–2652 (2010).
22. Alon, U. Network motifs: theory and experimental approaches. *Nat Rev Genet* **8,** 450–461 (2007).
23. Kaverina, I., Krylyshkina, O. & Small, J. V. Microtubule Targeting of Substrate Contacts Promotes Their Relaxation and Dissociation. *J Cell Biol* **146,** 1033–1044 (1999).

24. Wolfenson, H., Lavelin, I. & Geiger, B. Dynamic Regulation of the Structure and Functions of Integrin Adhesions. *Developmental Cell* **24,** 447–458 (2013).

25. Simons, K. & Ikonen, E. Functional rafts in cell membranes. *Nature* **387,** 569–572 (1997).

26. Galbraith, C. G., Yamada, K. M. & Sheetz, M. P. The relationship between force and focal complex development. *J. Cell Biol.* **159,** 695–705 (2002).

27. Amann, K. J. & Pollard, T. D. Cellular regulation of actin network assembly. *Current Biology* **10,** R728–R730 (2000).

28. Svitkina, T. M. & Borisy, G. G. Arp2/3 Complex and Actin Depolymerizing Factor/Cofilin in Dendritic Organization and Treadmilling of Actin Filament Array in Lamellipodia. *J Cell Biol* **145,** 1009–1026 (1999).

29. Le Clainche, C. & Carlier, M.-F. Regulation of Actin Assembly Associated With Protrusion and Adhesion in Cell Migration. *Physiological Reviews* **88,** 489–513 (2008).

30. Ponti, A. *et al.* Periodic Patterns of Actin Turnover in Lamellipodia and Lamellae of Migrating Epithelial Cells Analyzed by Quantitative Fluorescent Speckle Microscopy. *Biophys J* **89,** 3456–3469 (2005).

31. Hotulainen, P. Stress fibers are generated by two distinct actin assembly mechanisms in motile cells. *The Journal of Cell Biology* **173,** 383–394 (2006).

32. Vallotton, P. & Small, J. V. Shifting views on the leading role of the lamellipodium in cell migration: speckle tracking revisited. *J. Cell. Sci.* **122,** 1955–1958 (2009).

33. Ydenberg, C. A., Smith, B. A., Breitsprecher, D., Gelles, J. & Goode, B. L. Cease-fire at the leading edge: New perspectives on actin filament branching, debranching, and cross-linking. *Cytoskeleton* **68,** 596–602 (2011).

34. Hotulainen, P. & Lappalainen, P. Stress fibers are generated by two distinct actin assembly mechanisms in motile cells. *J. Cell Biol.* **173,** 383–394 (2006).

35. Tojkander, S. *et al.* A Molecular Pathway for Myosin II Recruitment to Stress Fibers. *Current Biology* **21,** 539–550 (2011).

36. DesMarais, V., Ichetovkin, I., Condeelis, J. & Hitchcock-DeGregori, S. E. Spatial regulation of actin dynamics: a tropomyosin-free, actin-rich compartment at the leading edge. *Journal of Cell Science* **115,** 4649–4660 (2002).

37. Burnette, D. T. *et al.* A role for actin arcs in the leading-edge advance of migrating cells. *Nat Cell Biol* **13,** 371–382 (2011).

38. Choquet, D., Felsenfeld, D. P. & Sheetz, M. P. Extracellular Matrix Rigidity Causes Strengthening of Integrin–Cytoskeleton Linkages. *Cell* **88,** 39–48 (1997).

39. Meacci, G. *et al.* α-actinin links ECM rigidity sensing contractile units with periodic cell edge retractions. *Mol. Biol. Cell* mbc.E16-02-0107 (2016). doi:10.1091/mbc.E16-02-0107

40. Kuo, J.-C., Han, X., Hsiao, C.-T., Yates Iii, J. R. & Waterman, C. M. Analysis of the myosin-II-responsive focal adhesion proteome reveals a role for β-Pix in negative regulation of focal adhesion maturation. *Nat Cell Biol* **13,** 383–393 (2011).

41. Gingras, A. R. *et al.* Mapping and Consensus Sequence Identification for Multiple Vinculin Binding Sites within the Talin Rod. *J. Biol. Chem.* **280,** 37217–37224 (2005).

42. Stehbens, S. & Wittmann, T. Targeting and transport: How microtubules control focal adhesion dynamics. *J Cell Biol* **198,** 481–489 (2012).

43. Ketene, A. N., Roberts, P. C., Shea, A. A., Schmelz, E. M. & Agah, M. Actin filaments play a primary role for structural integrity and viscoelastic response in cells. *Integr. Biol.* **4,** 540–549 (2012).

44. Hu, S., Chen, J. & Wang, N. Cell spreading controls balance of prestress by microtubules and extracellular matrix. *Front. Biosci.* **9,** 2177–2182 (2004).

45. Lodish, H. *et al.* Myosin: The Actin Motor Protein. (2000).

46. Hamill, O. P. & Martinac, B. Molecular basis of mechanotransduction in living cells. *Physiol. Rev.* **81,** 685–740 (2001).

47. Bray, D. & White, J. G. Cortical flow in animal cells. *Science* **239,** 883–888 (1988).

48. Fackler, O. T. & Grosse, R. Cell motility through plasma membrane blebbing. *The Journal of Cell Biology* **181,** 879–884 (2008).

49. Ciobanasu, C., Faivre, B. & Le Clainche, C. Actomyosin-dependent formation of the mechanosensitive talin–vinculin complex reinforces actin anchoring. *Nature Communications* **5,** (2014).

50. Yao, M. *et al.* Mechanical activation of vinculin binding to talin locks talin in an unfolded conformation. *Scientific Reports* **4,** (2014).

51. Direct observation of microtubule treadmilling by electron microscopy. *J Cell Biol* **101,** 1637–1642 (1985).

52. Enomoto, T. Microtubule disruption induces the formation of actin stress fibers and focal adhesions in cultured cells: possible involvement of the rho signal cascade. *Cell Struct. Funct.* **21,** 317–326 (1996).

53. Gardel, M. L., Kasza, K. E., Brangwynne, C. P., Liu, J. & Weitz, D. A. in *Methods in Cell Biology* **89,** 487–519 (Elsevier, 2008).

54. Dogterom, M. & Yurke, B. Measurement of the force-velocity relation for growing microtubules. *Science* **278,** 856–860 (1997).

55. Mizushima-Sugano, J., Maeda, T. & Miki-Noumura, T. Flexural rigidity of singlet microtubules estimated from statistical analysis of their contour lengths and end-to-end distances. *Biochim. Biophys. Acta* **755,** 257–262 (1983).

56. Hu, S., Chen, J., Butler, J. P. & Wang, N. Prestress mediates force propagation into the nucleus. *Biochem. Biophys. Res. Commun.* **329,** 423–428 (2005).

57. Potthoff, M. J. & Olson, E. N. MEF2: a central regulator of diverse developmental programs. *Development* **134,** 4131–4140 (2007).

58. Ihalainen, T. O. *et al.* Differential basal-to-apical accessibility of lamin A/C epitopes in the nuclear lamina regulated by changes in cytoskeletal tension. *Nat Mater* **14,** 1252–1261 (2015).

59. Versaevel, M. *et al.* Super-resolution microscopy reveals LINC complex recruitment at nuclear indentation sites. *Scientific Reports* **4,** 7362 (2014).

60. Coyer, S. R. *et al.* Nanopatterning reveals an ECM area threshold for focal adhesion assembly and force transmission that is regulated by integrin activation and cytoskeleton tension. *Journal of Cell Science* **125,** 5110–5123 (2012).

61. Lullo, G. A. D., Sweeney, S. M., Körkkö, J., Ala-Kokko, L. & Antonio, J. D. S. Mapping the Ligand-binding Sites and Disease-associated Mutations on the Most Abundant Protein in the Human, Type I Collagen. *J. Biol. Chem.* **277,** 4223–4231 (2002).

62. Sherman, V. R., Yang, W. & Meyers, M. A. The materials science of collagen. *Journal of the Mechanical Behavior of Biomedical Materials* **52,** 22–50 (2015).

63. Pezet, M. *et al.* Elastin Haploinsufficiency Induces Alternative Aging Processes in the Aorta. *Rejuvenation Research* **11,** 97–112 (2008).

64. Behmoaras, J. *et al.* Differential Expression of Lysyl Oxidases LOXL1 and LOX During Growth and Aging Suggests Specific Roles in Elastin and Collagen Fiber Remodeling in Rat Aorta. *Rejuvenation Research* **11,** 883–889 (2008).

65. Hadj-Rabia, S. *et al.* Twenty patients including 7 probands with autosomal dominant cutis laxa confirm clinical and molecular homogeneity. *Orphanet Journal of Rare Diseases* **8,** 36 (2013).

66. Brennan, J. R. & Hocking, D. C. Cooperative effects of fibronectin matrix assembly and initial cell–substrate adhesion strength in cellular self-assembly. *Acta Biomaterialia* **32,** 198–209 (2016).

67. Yeh, W.-C. *et al.* Elastic modulus measurements of human liver and correlation with pathology. *Ultrasound in Medicine and Biology* **28,** 467–474 (2002).

68. Hersen P et Ladoux B Nature 2011. Push it, pull it.

69. Li, B. *et al.* Development of micropost force sensor array with culture experiments for determination of cell traction forces. *Cell Motil. Cytoskeleton* **64,** 509–518 (2007).

70. Berney, C. & Danuser, G. FRET or No FRET: A Quantitative Comparison. *Biophys J* **84,** 3992–4010 (2003).

71. Grashoff, C. *et al.* Measuring mechanical tension across vinculin reveals regulation of focal adhesion dynamics. *Nature* **466,** 263–266 (2010).

72. Haga, H. *et al.* Time-lapse viscoelastic imaging of living fibroblasts using force modulation mode in AFM. *J Electron Microsc (Tokyo)* **49,** 473–481 (2000).

73. Wang, N., Butler, J. P. & Ingber, D. E. Mechanotransduction across the cell surface and through the cytoskeleton. *Science* **260,** 1124–1127 (1993).

74. le Digabel, J. *et al.* Magnetic micropillars as a tool to govern substrate deformations. *Lab Chip* **11,** 2630–2636 (2011).

75. Xu, K., Babcock, H. P. & Zhuang, X. Dual-objective STORM reveals three-dimensional filament organization in the actin cytoskeleton. *Nat Methods* **9,** 185–188 (2012).

76. Metcalf, D. J., Edwards, R., Kumarswami, N. & Knight, A. E. Test Samples for Optimizing STORM Super-Resolution Microscopy. *Journal of Visualized Experiments* (2013). doi:10.3791/50579

77. Olivier, N., Keller, D., Gönczy, P. & Manley, S. Resolution Doubling in 3D-STORM Imaging through Improved Buffers. *PLoS ONE* **8,** e69004 (2013).

78. Mendoza, M. C., Besson, S. & Danuser, G. Quantitative Fluorescent Speckle Microscopy (QFSM) to Measure Actin Dynamics. *Curr Protoc Cytom* **0 2,** Unit2.18 (2012).

79. Wang, N. & Ingber, D. E. Control of cytoskeletal mechanics by extracellular matrix, cell shape, and mechanical tension. *Biophys J* **66,** 2181–2189 (1994).

80. Wang, N. *et al.* Mechanical behavior in living cells consistent with the tensegrity model. *Proceedings of the National Academy of Sciences* **98,** 7765–7770 (2001).

81. Stamenović, D., Fredberg, J. J., Wang, N., Butler, J. P. & Ingber, D. E. A microstructural approach to cytoskeletal mechanics based on tensegrity. *J. Theor. Biol.* **181,** 125–136 (1996).

82. Gómez Jáuregui, V. *Tensegrity structures and their application to architecture*. (PUbliCan- Ediciones Universidad de Cantabria, 2010).

83. Ingber, D. E., Wang, N. & Stamenović, D. Tensegrity, cellular biophysics, and the mechanics of living systems. *Rep Prog Phys* **77,** 46603 (2014).

84. Ingber, D. E. Tensegrity I. Cell structure and hierarchical systems biology. *Journal of Cell Science* **116,** 1157–1173 (2003).

85. Ingber, D. E. Tensegrity II. How structural networks influence cellular information processing networks. *J. Cell. Sci.* **116,** 1397–1408 (2003).

86. Laurent, V. M. *et al.* Tensegrity Behaviour of Cortical and Cytosolic Cytoskeletal Components in Twisted Living Adherent Cells. *Acta Biotheor* **50,** 331–356

87. Karcher, H. *et al.* A three-dimensional viscoelastic model for cell deformation with experimental verification. *Biophys. J.* **85,** 3336–3349 (2003).

88. Vaziri, A. & Mofrad, M. R. K. Mechanics and deformation of the nucleus in micropipette aspiration experiment. *J Biomech* **40,** 2053–2062 (2007).

89. eCM - eCells & Materials Journal - Manuscript - A three-dimensional finite element model of an adherent eukaryotic cell - True Open Access. Available at: http://www.ecmjournal.org/journal/papers/vol007/vol007a03.php. (Accessed: 16th September 2016)

90. Gladilin, E. *et al.* 3D finite element analysis of uniaxial cell stretching: from image to insight. *Phys. Biol.* **4,** 104 (2007).

91. Milner, J. S., Grol, M. W., Beaucage, K. L., Dixon, S. J. & Holdsworth, D. W. Finite-Element Modeling of Viscoelastic Cells During High-Frequency Cyclic Strain. *Journal of Functional Biomaterials* **3,** 209–224 (2012).

92. Milan, J.-L. *et al.* Computational model combined with in vitro experiments to analyse mechanotransduction during mesenchymal stem cell adhesion. *Eur Cell Mater* **25,** 97–113 (2013).

93. Milan, J. L., Wendling-Mansuy, S., Jean, M. & Chabrand, P. Divided medium-based model for analyzing the dynamic reorganization of the cytoskeleton during cell deformation. *Biomech Model Mechanobiol* **6,** 373–390 (2007).

94. Yoann CHÉLIN *, Julien AVERSENG, Patrick CAÑADAS, Bernard MAURIN. Modèle granulaire de morphogenèse tissulaire.

95. Maurin, B., Cañadas, P., Baudriller, H., Montcourrier, P. & Bettache, N. Mechanical model of cytoskeleton structuration during cell adhesion and spreading. *Journal of Biomechanics* **41,** 2036–2041 (2008).

96. Ujihara, Y., Nakamura, M., Miyazaki, H. & Wada, S. Proposed Spring Network Cell Model Based on a Minimum Energy Concept. *Ann Biomed Eng* **38,** 1530–1538 (2010).

97. Milan, J.-L. *et al.* In silico CDM model sheds light on force transmission in cell from focal adhesions to nucleus. *J Biomech* (2016). doi:10.1016/j.jbiomech.2016.05.031

98. Dubois, F. & Jean, M. in *Analysis and Simulation of Contact Problems* (eds. Dr, P. W. P. & Dr, U. N. P.) 375–378 (Springer Berlin Heidelberg, 2006).

99. Jean, M. The non-smooth contact dynamics method. *Computer Methods in Applied Mechanics and Engineering* **177,** 235–257 (1999).

100. McBeath, R., Pirone, D. M., Nelson, C. M., Bhadriraju, K. & Chen, C. S. Cell shape, cytoskeletal tension, and RhoA regulate stem cell lineage commitment. *Dev. Cell* **6,** 483–495 (2004).

101. Dahl, K. N., Ribeiro, A. J. S. & Lammerding, J. Nuclear shape, mechanics, and mechanotransduction. *Circ. Res.* **102,** 1307–1318 (2008).

102. Nathan, A. S., Baker, B. M., Nerurkar, N. L. & Mauck, R. L. Mechano-topographic modulation of stem cell nuclear shape on nanofibrous scaffolds. *Acta Biomater* **7,** 57–66 (2011).

103. Yang, M. T., Fu, J., Wang, Y.-K., Desai, R. A. & Chen, C. S. Assaying stem cell mechanobiology on microfabricated elastomeric substrates with geometrically modulated rigidity. *Nature Protocols* **6,** 187–213 (2011).

104. Yang, M. T., Reich, D. H. & Chen, C. S. Measurement and analysis of traction force dynamics in response to vasoactive agonists. *Integr. Biol.* **3,** 663–674 (2011).

105. Manifacier, I. *et al.* Computational Tension Mapping of Adherent Cells Based on Actin Imaging. *PLoS ONE* **11,** e0146863 (2016).

106. Deguchi, S., Ohashi, T. & Sato, M. Tensile properties of single stress fibers isolated from cultured vascular smooth muscle cells. *J Biomech* **39,** 2603–2610 (2006).

107. Abramoff, M. D., Magalhães, P. J. & Ram, S. J. Image processing with ImageJ. *Biophotonics international* **11,** 36–42 (2004).

108. Collins, T. J. ImageJ for microscopy. *BioTechniques* **43,** 25–30 (2007).

109. Colombelli, J. *et al.* Mechanosensing in actin stress fibers revealed by a close correlation between force and protein localization. *Journal of Cell Science* **122,** 1928–1928 (2009).

110. Besser, A. & Schwarz, U. S. Coupling biochemistry and mechanics in cell adhesion: a model for inhomogeneous stress fiber contraction. *New J. Phys.* **9,** 425 (2007).

111. Han, S. J. & Sniadecki, N. J. Simulations of the contractile cycle in cell migration using a bio-chemical–mechanical model. *Computer Methods in Biomechanics and Biomedical Engineering* **14,** 459–468 (2011).

112. DiMilla, P. A., Barbee, K. & Lauffenburger, D. A. Mathematical model for the effects of adhesion and mechanics on cell migration speed. *Biophys J* **60,** 15–37 (1991).

113. Wang, N. *et al.* Cell prestress. I. Stiffness and prestress are closely associated in adherent contractile cells. *American Journal of Physiology - Cell Physiology* **282,** C606–C616 (2002).

114. Huang, B., Babcock, H. & Zhuang, X. Breaking the Diffraction Barrier: Super-Resolution Imaging of Cells. *Cell* **143,** 1047–1058 (2010).

115. Wang, N., Tytell, J. D. & Ingber, D. E. Mechanotransduction at a distance: mechanically coupling the extracellular matrix with the nucleus. *Nature Reviews Molecular Cell Biology* **10,** 75–82 (2009).

116. Grashoff, C. *et al.* Measuring mechanical tension across vinculin reveals regulation of focal adhesion dynamics. *Nature* **466,** 263–266 (2010).

117. Trichet, L. *et al.* Evidence of a large-scale mechanosensing mechanism for cellular adaptation to substrate stiffness. *Proceedings of the National Academy of Sciences* **109,** 6933–6938 (2012).

118. Ghibaudo, M. *et al.* Traction forces and rigidity sensing regulate cell functions. *Soft Matter* **4,** 1836–1843 (2008).

119. Huber, F. *et al.* Emergent complexity of the cytoskeleton: from single filaments to tissue. *Adv Phys* **62,** 1–112 (2013).

120. Fischer-Friedrich, E., Hyman, A. A., Jülicher, F., Müller, D. J. & Helenius, J. Quantification of surface tension and internal pressure generated by single mitotic cells. *Scientific Reports* **4,** 6213 (2014).

121. McGarry, J. G. & Prendergast, P. J. A three-dimensional finite element model of an adherent eukaryotic cell. *Eur Cell Mater* **7,** 27-33-34 (2004).

122. Cañadas, P., Laurent, V. M., Oddou, C., Isabey, D. & Wendling, S. A cellular tensegrity model to analyse the structural viscoelasticity of the cytoskeleton. *J. Theor. Biol.* **218,** 155–173 (2002).

123. Charras, G. T., Yarrow, J. C., Horton, M. A., Mahadevan, L. & Mitchison, T. J. Non-equilibration of hydrostatic pressure in blebbing cells. *Nature* **435,** 365–369 (2005).

124. Cuvelier, D. *et al.* The Universal Dynamics of Cell Spreading. *Current Biology* **17,** 694–699 (2007).

125. Odenthal, T. *et al.* Analysis of Initial Cell Spreading Using Mechanistic Contact Formulations for a Deformable Cell Model. *PLOS Comput Biol* **9,** e1003267 (2013).

126. Yoshigi, M., Hoffman, L. M., Jensen, C. C., Yost, H. J. & Beckerle, M. C. Mechanical force mobilizes zyxin from focal adhesions to actin filaments and regulates cytoskeletal reinforcement. *J Cell Biol* **171,** 209–215 (2005).

127. Alexandrova, A. Y. *et al.* Comparative dynamics of retrograde actin flow and focal adhesions: formation of nascent adhesions triggers transition from fast to slow flow. *PLoS ONE* **3,** e3234 (2008).

128. McGrath, J. L. Cell Spreading: The Power to Simplify. *Current Biology* **17,** R357–R358 (2007).

129. Gardel, M. L. *et al.* Traction stress in focal adhesions correlates biphasically with actin retrograde flow speed. *J Cell Biol* **183,** 999–1005 (2008).

130. Wilson, C. A. *et al.* Myosin II contributes to cell-scale actin network treadmilling via network disassembly. *Nature* **465,** 373–377 (2010).

131. Hodges, S. R. & Jensen, O. E. Spreading and peeling dynamics in a model of cell adhesion. *Journal of Fluid Mechanics* **460,** 381–409 (2002).

132. Scarpa, E. & Mayor, R. Collective cell migration in development. *J Cell Biol* **212,** 143–155 (2016).

133. Tam, S. N., Smith, M. L. & Stamenović, D. Modeling tensional homeostasis in multicellular clusters. *Int. J. Numer. Meth. Biomed. Engng.* n/a-n/a (2016). doi:10.1002/cnm.2801

134. Huang, B. *et al.* The three-way switch operation of Rac1/RhoA GTPase-based circuit controlling amoeboid-hybrid-mesenchymal transition. *Scientific Reports* **4,** 6449 (2014).

135. Doty, D. Theory of algorithmic self-assembly. *Communications of the ACM* **55,** 78 (2012).

136. The Nature of Code. Available at: http://natureofcode.com/book/chapter-10-neural-networks/. (Accessed: 5th September 2016)

137. Batty, M. & Torrens, P. M. Modeling Complexity : The Limits to Prediction. *Cybergeo : European Journal of Geography* (2001). doi:10.4000/cybergeo.1035

138. Huber, F. *et al.* Emergent complexity of the cytoskeleton: from single filaments to tissue. *Adv Phys* **62,** 1–112 (2013).

139. Allen, P. M. & Strathern, M. Models, knowledge creation and their limits. *Futures* **37,** 729–744 (2005).

140. Hinchey, M. G., Sterritt, R. & Rouff, C. Swarms and Swarm Intelligence. *Computer* **40,** 111–113 (2007).

141. Burridge, K. & Guilluy, C. Focal adhesions, stress fibers and mechanical tension. *Experimental Cell Research* doi:10.1016/j.yexcr.2015.10.029

SUMMARY (ENGLISH):

Tissue engineering is based on utilizing cells and scaffolds to regenerate missing tissues, requiring interaction with the surrounding biomaterial to be successful. Yet for healthy tissue to form, a precise ballet of intertwined interactions must take place for individual cells to respond appropriately. In addition to chemical reactions, the cell interacts mechanically with its environment by sensing its rigidity. Here, I developed several computational models to understand how substrate rigidity mechanically affects a cell's structure as the cell adheres and spreads on it. In simpler terms, we tried to understand how a cell senses the softness or hardness of its surroundings, how that affects its internal structure, and the forces that transit within the cell. In addition, instead of focusing on mechanical properties, I developed a simplified, yet coherent conceptual understanding of the cellular structure.

In Chapter 1, we cultured cells on microposts substrates of various rigidities. The tensegrity based model showed that cells were influenced by the substrate rigidity. This model shows that the cytoskeleton is capable of deforming the nucleus. Furthermore, the model shows an increase in the amount of force transmitted from the cytoskeleton to the nucleus, which may have an impact on gene synthesis.

Then in Chapter 2, I used microscope images of the actin network to generate a more representative mechanical model of the cell. This model showed that most of the compression load does not transit through the compression network of the cell, but rather via the substrate.

In Chapter 3, I combined the experimental methods based on microposts of diverse rigidities with the image based model developed in Chapter 2 to analyze the influence of substrate rigidity on a large number of adherent cells. We used micropost substrates of various distinct rigidities. The model showed that cells were influenced by substrate rigidity after being allowed to spread on a bed of microposts for a period of 14 hours. On average, cells cultured on harder substrates generated higher internal tensile stress. Furthermore, the literature states that adherent cells are equipped with contractile units located near focal adhesions that pinch the substrate to measure local stiffness and consequently mediate cell contractility. In theory, the spacing of 7μm we used between the microposts prevented contractile units from distinguishing micropost bending stiffness. Yet, our results indicate that cells were affected by substrate stiffness. This may suggest that another cell rigidity sensing mechanism is in play, allowing cells to evaluate surroundings rigidity at a cellular scale.

The literature repeatedly indicates that an increase in substrate stiffness promotes cells spread area and contractility, as well. This suggests a tight relationship between cell size and contractility. In addition, the model indicates that, under similar culture conditions, the cell size does not seem to significantly impact its contractility.

Surprisingly, the model also delivered an unexpected result, hinting at the idea of two superimposed sources of actin network contractility. One appeared to be adhesion mediated while the other did not. We supposed that the non-adhesion based tension was due to actin cortex contractility. A simple calculation showed that the resulting fluid pressure would be equivalent to intracellular pressure values found in the literature, thus supporting the idea that

this non-adhesion mediated contractility is provoked by the actin cortex. My own findings along with those of others expressed in the literature, brought me to conceptually model the cell structure as a hybrid hydrostatic skeleton.

Thus, cells behave as complex biomechanical structures that can be mechanically influenced by the rigidity of their environment and affect it in return.

SUMMARY (FRENCH):

L'ingénierie tissulaire est une stratégie médicale largement utilisée et qui repose sur la formation de tissu par les cellules associées à un support. Pour maîtriser cette synthèse, il faut comprendre la cellule comme une part intégrante du tissu. Hormis les relations biochimiques, la cellule interagit également mécaniquement avec son environnement. Elle s'accroche à son support et évalue sa dureté pour adapter sa réponse biologique. Dans cette étude, j'ai développé des modèles numériques pour analyser l'influence de la rigidité du substrat sur le comportement mécanique de la cellule, sur sa structure contractile interne et les efforts qu'elle génère. En d'autres termes, j'ai essayé de comprendre comment la cellule ressent la rigidité de son environnement. De plus, au lieu de me focaliser sur les propriétés mécaniques quantitatives, j'ai cherché à développer un modèle conceptuel simplifié plus proche de la structure cellulaire.

Les différents modèles développés montrent que les cellules étudiées sont capables de percevoir leur environnement et d'adapter leur structure en fonction de la rigidité du substrat. La littérature montre qu'une augmentation de la rigidité peut favoriser une augmentation de la taille de la cellule, ainsi que la contractilité de cette dernière. Ceci sous-entend un lien possible entre la taille d'une cellule et sa contractilité. En revanche, le modèle montre que dans des conditions de culture identique, la taille cellulaire ne semble pas impacter la contractilité de manière importante.

Il est intéressant de noter, qu'en vertu des conditions expérimentales et d'un espacement entre micro-plots de 7µm, l'adaptation de la structure cellulaire à la rigidité du substrat, indique que les cellules étudiées sont capables de ressentir la rigidité du substrat à une échelle de plus de 7µm. Ceci implique un mécanisme de palpation fonctionnant à une échelle quasi cellulaire, ce qui ne semble pas correspondre aux organes de palpation connus à ce jour.

De plus, j'ai obtenu un résultat inattendu. Le modèle semble capable de percevoir la superposition de la contractilité induite respectivement par les conditions d'adhésions et le cortex actinien. Ce qui m'a en partie orienté vers un modèle conceptuel de la structure cellulaire basé sur une architecture d'hydrosquelette hybride.

On peut donc déduire de cette étude que la cellule est un système biomécanique complexe qui perçoit les stimuli mécaniques de son environnement, telle que la rigidité du substrat et peut également agir mécaniquement sur ce dernier.

EXTENDED SUMMARY (FRENCH):

Aux Etats Unis, 22 personnes meurent chaque jour en attente d'une greffe d'organe, alors que toutes les 10 minutes une nouvelle personne est mise sur la liste des demandeurs[1]. Cette liste est longue de près 120 000 personnes[1]. A titre d'exemple, la durée d'attente pour un rein est de 3.6 ans en moyenne aux USA. Cela conduit chaque année à des milliers de décès et un nombre comparable de personnes qui deviennent trop malades pour pouvoir recevoir un organe[1]. Ces statistiques américaines montrent en creux l'ampleur du problème à l'échelle planétaire, la population américaine représentant moins de 5% de la population mondiale.

Pour répondre à cette écrasante demande mondiale, l'ingénierie tissulaire espère bientôt être en mesure de régénérer ou fabriquer de nouveaux organes. Pour cela diverses méthodes sont utilisées ou en cours de développement, telles que l'impression 3D d'organes, des techniques de régénération in vivo ou encore l'utilisation de biomatériaux inducteurs. Bien que ce domaine soit ponctué de succès, la réalité est qu'un organe représente un système complexe régi par des interactions cellulaires et moléculaires. A l'heure actuelle, le fonctionnement à la fois global et local d'un tel système est difficile à conceptualiser. D'autant plus, que les phénomènes sous-jacents ne se limitent pas à des réactions purement biochimiques, mais incluent aussi des facteurs mécaniques. En effet, les tissus sont avant tout des structures anatomiques répondant à un besoin mécanique : l'os pour soutenir, le muscle pour contracter et le cartilage pour favoriser le glissement des surfaces articulaires. Les facteurs mécaniques jouent donc un rôle essentiel et nécessaire pour la constitution même des tissus. Les tissus étant synthétisés par les cellules, celles-ci sont donc capables de ressentir ces facteurs mécaniques. De ce fait une cellule est en perpétuelle interaction mécanique avec son environnement, ce qui influe de manière très significative sur son comportement[2,3,4,5], et lui permet de jouer un rôle biologique adapté au sein de la matrice extracellulaire, du tissu et de l'organe[6].

Pouvoir expliquer la manière dont une cellule interagit mécaniquement avec son environnement est donc crucial pour développer et maitriser des processus de régénération capables d'être en adéquation avec une telle complexité. C'est d'abord par le processus d'adhésion que la cellule éprouve mécaniquement son environnement. La phase d'adhésion conditionne également la première réponse biologique de la cellule qui est déterminante. Dans ce sens, j'ai souhaité m'intéresser à la manière dont une cellule adhère et s'étalepour devenir une part intégrante de son tissu. Cela nécessite, entre autres, de comprendre comment une cellule s'étale contre les parois des matériaux qui l'environnent, s'accroche, tire dessus et en ressent les propriétés mécaniques. L'adhésion cellulaire est, par conséquent, un sujet grandement étudié. De plus, l'adhésion conditionne la formation du cytosquelette, la sécrétion de certaines protéines, l'activation de certains gènes, voire une différentiation cellulaire complète. L'adhésion est de plus, une condition de survie des cellules adhérentes[7,4].

Le processus d'adhésion module l'étalement cellulaire, au cours duquel une cellule assemble son cytosquelette pour s'arrimer fermement à son substrat via ses points focaux d'adhésion[3,] en créant des fibres de tension[8]. Le processus d'adhésion cellulaire se déroule sur plusieurs étapes successives. Tout d'abord des molécules d'intégrines transmembranaires s'attachent au substrat via leur extrémité extérieure. Cette attache primaire, induit un changement de conformation sur

l'extrémité intérieure de l'intégrine ce qui dévoile un nouveau site réactionnel déclenchant ainsi une réaction en chaîne. Tout d'abord un lamellipode se forme et pousse la membrane cellulaire. Puis des fibres de stress et des points focaux d'adhésion s'assemblent le long de la membrane cellulaire. Une fois formées, les fibres de tension commencent à s'auto-contracter et se lient aux points focaux et se tendent. Lorsque la cellule adhère à un substrat 2D, une fibre de stress peut être ventrale ou apicale, si elle fait partie de la dernière catégorie, elle peut appuyer sur le noyau et le déformer en le plaquant contre le substrat. Les fibres de stress apicales peuvent également être mécaniquement liées aux lamines intranucléaire via les protéines du complexe LINK[9,10].

A ce jour plusieurs études ont essayé de modéliser la mécanique cellulaire, parfois pour des raisons différentes. Cela va de la modélisation des propriétés mécaniques de la cellule[11,12,13,14] jusqu' à essayer d'identifier des stimuli mécaniques qui pourraient s'inscrire dans un processus de mécanotransduction[15,16]. Ces divers modèles reposent sur des représentations conceptuelles de la cellule qui sont différentes. Ceci peut s'expliquer par le fait qu'ils s'intéressent à des phénomènes particulier. En revanche, il est étonnant de remarquer qu'il n'y a toujours pas de consensus autour d'un seul modèle conceptuel capable d'expliquer la structure cellulaire. Certaines publications soutiennent l'idée selon laquelle la cellule est une structure de tenségrité[14,17,18,19,20], alors que d'autres remettent cette hypothèse en question[21,22]. Un autre modèle conceptuel considère la cellule comme un fluide viscoélastique entouré d'une enveloppe contractile[23], ou bien comme un milieu poro-élastique[24]. Le manque de consensus montre que la structure cellulaire n'est pas encore clairement comprise. Ceci est d'autant plus vrai car les composants qui la constituent s'auto-contraignent[25], s'auto-assemblent[8,26] et se désassemblent dynamiquement[27,28]. Ceci permet à la cellule de changer de forme de manière dynamique pour s'étaler par exemple[29], en réponse à un stimuli mécanique[30,31], ou encore pour migrer[32].

Entre autres raisons, la structure des cellules adhérentes est influencée par la rigidité des substrats sur lesquels elles s'étalent. Une cellule, en cours d'adhésion, est en général, plus étalée et tire plus sur un substrat rigide[33,34] que sur un substrat mou. De plus une cellule plus étalée tirera en générale plus qu'une autre de ses consœurs. On peut de ce fait, se demander si la contrainte interne en tension augmente lorsque la cellule est plus étalée.

Lors de l'adhésion, le noyau se déforme, entraînant un changement de l'expression des gènes[4].

« Est-ce qu'une telle déformation du noyau peut s'expliquer par des sollicitations purement mécaniques ? Ou est-il nécessaire qu'un changement des propriétés mécaniques du noyau ait lieu avant de pouvoir envisager une déformation notable de ce dernier? »

Enfin : « Est-ce que les conditions d'adhésion changent les efforts mécaniques appliqués au noyau, ce qui pourrait en partie expliquer un changement d'expression des gènes ? »

Pour répondre à ces questions j'ai décidé d'utiliser des modèles numériques permettant de simuler la mécanique cellulaire.

Chapitre 1 - Utilisation du modèle CDM

Je me suis donc inspiré du 'Cytoskeleton Divided Medium (CDM) model'. Ce modèle mécano-numérique, introduit par Milan et al., utilise la mécanique des milieux divisés pour modéliser un ensemble mécaniquement 'équivalent' au cytosquelette d'une cellule[16,15]. L'avantage notable de

l'utilisation de cette théorie mécanique est que l'on peut considérer les interactions entre les différents éléments du modèle comme des composants filamentaires du cytosquelette. De ce fait, la gestion de la simulation est grandement facilitée car la création et la disparition d'interactions mécaniques entre les composants du modèle suivent des lois prédéterminées. L'autre avantage de cette approche, est que l'on peut considérer que ces interactions imitent en grande partie la réorganisation dynamique du cytosquelette. Ainsi, le CDM nous donne la possibilité de représenter la majeure partie des composants du cytosquelette. Ce qui inclut les microfilaments d'actine, les fibres de stress, les microtubules, les filaments intermédiaires cytoplasmiques (vimentine), ainsi que leurs homologues intranucléaires principalement composés de lamine.

Phase étalement

Afin de pouvoir adapter le modèle à la diversité des géométries cellulaires observées expérimentalement, chaque simulation démarre depuis une configuration de référence pour arriver en fin de calcul à la configuration observée. Cette procédure a l'avantage de commencer la simulation avec un modèle anatomiquement comparable à une structure cellulaire connue. La configuration de référence choisie est celle d'une cellule ronde avant étalement. Le modèle cellulaire est ensuite graduellement déformé jusqu'à obtenir sa forme finale. Ce processus de déformation a lieu tout en conservant la cohérence de l'organisation interne du modèle, ce qui imite par conséquent le processus d'étalement de la cellule. Pendant ce temps, de nouvelles interactions se forment permettant de connecter les différents composants du modèle. Ceci représente ainsi la restructuration dynamique du cytosquelette au cours de l'adhésion.

Phase optimisation

Après 'l'étalement', nous obtenons un modèle géométriquement 'équivalent' à la cellule observée. En revanche, ce modèle ne l'est pas encore mécaniquement. A ce stade, il est nécessaire de poursuivre la simulation. C'est là où l'amélioration la plus notable du modèle intervient. Les interactions en tension des fibres de stress sont ajustées pour que le modèle cellulaire exerce des efforts d'adhésions d'une intensité équivalente aux efforts mesurés expérimentalement. Ce processus d'ajustement se déroule de manière itérative, tel un processus d'optimisation. Une fois le processus d'ajustement terminé la simulation numérique s'arrête. On considère à ce stade que la structure du modèle est équivalente à celle de la cellule.

Micro-plots et culture cellulaire

Avec cette version améliorée du CDM model, nous avons étudié 25 cellules en adhésion sur des micro-plots. La longueur des plots ont permis de changer leur flexibilité sans impacter d'autres paramètres tels que le diamètre et le matériau des plots. La flexibilité d'un plot est donc assimilable à la rigidité apparente du substrat. Plus les plots sont flexibles, plus le substrat paraît mou et inversement. Un substrat composé de micro-plots, offre l'avantage de contrôler la rigidité apparente d'un substrat sans influencer la cellule via d'autres facteurs. La « flèche » autrement dit la déflection d'un plot nous a permis de déduire la composante horizontale de l'effort exercé par la cellule sur ce plot.

Parmi les 25 cellules étudiés, 10 étaient sur des substrats « mous », 10 sur des substrats « durs » et 5 sur des substrats « très durs ». Il est à noter que nous ne considèrerons que les conditions molles et dures comme statistiquement significatives.

Résultats expérimentaux pour modèle CDM

Une augmentation de la rigidité apparente a conduit à un accroissement moyen de : l'aire projetée de la cellule, de son diamètre moyen, du nombre de points focaux d'adhésions, de la tension à l'intérieur des fibres de stress modélisées. En revanche, l'augmentation de la rigidité était accompagnée d'une réduction de la circularité moyenne des cellules.

Résultats du modèle CDM & Analyse

Nous avons remarqué qu'entre la phase post-étalement et la phase post-optimisation, les résultats du calcul variaient de manière importante. Nous concluons que l'amélioration apportée au modèle, c'est-à-dire la phase d'optimisation est donc justifiée.

De plus, les résultats de la simulation indiquent qu'un accroissement de la rigidité entraine une augmentation moyenne de la somme de toutes les tensions des filaments d'actine et des fibres de stress. On constate également que la déformation verticale et horizontale moyenne du noyau augmente, ainsi que la tension appliquée à ce dernier.

Une analyse plus poussée dévoile que la déformation du noyau augmente avec la valeur de somme des tensions intra-cytosqueletique.

En revanche, il est à noter qu'une inspection visuelle du 'cytosquelette numérique' dévoile une organisation tout de même différente de celle de la cellule réelle. Alors que les résultats quantitatifs et qualitatifs du modèle sont cohérents, il n'est pas évident de conclure sur les mesures de forces au sein de la cellule et leur impact mécanobiologique. Par conséquent, j'ai décidé de développer un nouveau type de modèle numérique qui a pour but de mieux imiter la structure du cytosquelette.

Chapitre 2 – Développement d'un modèle mécanique de la cellule à partir d'images du réseau d'actine

Le fait que les cellules aient des formes géométriques et des structures très variées rend le sujet d'autant plus complexe. Alors :

« Comment caractériser mécaniquement le réseau d'actine malgré cette variété de formes et structures? »

Méthode : Pour répondre à cette question, nous avons développé une méthode alliant imagerie et mécanique. Elle permet de comparer les propriétés mécaniques de cellules adhérentes entre plusieurs conditions d'adhésions, indépendamment de leurs morphologies. Le principe de modélisation est relativement intuitif. Sachant que le réseau de filaments d'actine représente en grande majorité la structure cellulaire[43], nous avons utilisé des images microscope de ce réseau pour générer un modèle numérique. En d'autres termes, les pixels de l'image du réseau d'actine sont convertis en nœuds mécaniques. Ces nœuds sont mécaniquement liés de proche en proche par des interactions élastiques de rigidité **K** et d'un pre-stress[106] de 20%. Cette stratégie permet de

représenter les propriétés contractiles du réseau d'actine. De plus, chaque nœud est entouré d'un contacteur sphérique. Ce dernier permet de représenter un effort de compression qui se forme lorsqu'un déséquilibre mécanique local le met en contact avec un autre contacteur sphérique. Un réseau de compression passif peut ainsi se former lorsqu'un déséquilibre tasse les différents contacteurs les uns avec les autres. Ce réseau permet ainsi de stabiliser la structure cellulaire.

En revanche à ce stade, la rigidité **K** des interactions en tension n'est pas connue. Nous avons choisi de la considérer proportionnelle à la densité locale visible. Si la densité est élevée la rigidité **K** l'est aussi et inversement. A ce stade, il reste cependant nécessaire de connaître le coefficient de proportionnalité **a**, qui lie la densité d'actine et la rigidité **K**.

Pour déterminer **a**, l'idée est que le modèle doit exercer sur le substrat une traction similaire à celle de la cellule réelle, c'est-à-dire, qu'il doit générer des forces d'adhésion équivalentes à celles que la cellule génère. La détermination de ce coefficient **a** revient donc à utiliser des méthodes de mécanique inverse : déterminer les efforts internes en comparant les efforts externes. Premièrement nous avons cherché une manière simple d'estimer les efforts de tensions que la cellule exerce à ses points d'adhésion. En accord avec la littérature, ces efforts ont été définis comme étant proportionnels à la taille de ces derniers[15,16]. Ceci nous a permis de calculer la somme des intensités des forces d'adhésion, que nous avons nommée : **'force d'adhésion totale estimée'**. Pour obtenir les efforts exercés par le modèle au niveau de ses points d'adhésion, nous avons exécuté une première itération, en définissant le coefficient **a** de manière arbitraire. . Nous avons nommé la somme des intensités des forces résultantes au niveau des points d'adhésion du modèle : **'force d'adhésion totale calculée'**. En relançant plusieurs fois la simulation pour différentes valeurs de **a**, nous avons réalisé une analyse paramétrique du coefficient **a**. Cette analyse paramétrique couplée à une interpolation linéaire nous a permis de déterminer le coefficient **a** qui permet d'obtenir une force d'adhésion calculée qui est identique à celle **estimée**.

Le modèle a permis d'estimer les rigidités K du réseau de filaments d'actine quelle que soit la zone de la cellule considérée. Nous avons introduit une grandeur simple nommée tension cross-linéaire. Cette dernière définit la tension en nN transitant via une section de 1μm. Conceptuellement, cette tension cross-linéaire calculée en 2D est équivalente à la définition d'une contrainte en 3D. Cette nouvelle grandeur nous permet ainsi de quantifier la tension moyenne et la tension maximale au sein du cytosquelette.

Résultats : Cette procédure a été répétée sur un total de 8 cellules. Les résultats indiquent que cette méthode de modélisation donne des valeurs de tension raisonnables. De plus la tension moyenne et la tension maximale déterminées au sein du réseau d'actine à l'aide de la tension cross-linéaire suffisent à caractériser l'état de contraction mécanique de n'importe quelle cellule. De plus, le modèle a montré que le réseau de forces de compression passive représentant les microtubules, joue un rôle de stabilisateur. En accord avec les observations expérimentales décrites dans la littérature, les résultats du modèle indiquent également que les microtubules ne soutiennent qu'une partie marginale des efforts de compression.

En revanche, notre analyse soutient l'idée selon laquelle la méthode utilisée pour estimer les forces d'adhésion n'est pas suffisamment précise. Bien que quantatifs, ces résultats restent peu

concluants. Pour cette raison nous avons décidé de reconduire une étude similaire en utilisant des micro-plots pour mesurer les efforts d'adhésion.

Chapitre 3 – Influence de la rigidité du substrat sur la contractilité du réseau d'actine

Dans cette étude nous avons cherché à analyser la relation entre le niveau de tension intracellulaire et la rigidité du substrat, en s'appuyant d'une part sur le protocole expérimental développé au chapitre 1 et utilisant les substrats micro-plots et d'autre part sur le modèle basé sur l'image réelle du réseau d'actine développé dans le chapitre 2.

Méthode : Pour cette étude nous avons utilisé 4 substrats de rigidités différentes :

- très mous - 11.0 nN/µm (8 cellules)
- mous - 15.5 nN/µm (8 cellules)
- durs - 31.0 nN/µm (15 cellules)
- très durs 47.8 nN/µm (8 cellules)

La méthode de modélisation utilisée est quasi identique à celle décrite dans le chapitre 2. La différence, est qu'un algorithme a permis au modèle de converger seul vers la valeur de **a** la plus appropriée, sans nécessiter d'étude paramétrique ni d'interpolation.

Résultats :

Le modèle indique que, comme au chapitre 1 les cellules sont influencées par la rigidité de substrat. En effet, un substrat plus rigide permet aux cellules de générer un réseau d'actine plus tendu. Ceci a été visible via une tension cross-linéaire moyenne et max plus importante. En revanche, la distribution des valeurs de tension laisse supposer, que ce n'est pas parce qu'une cellule est placée sur un substrat plus rigide qu'elle va nécessairement développer un réseau actine plus tendu. Nous pouvons donc conclure qu'un substrat rigide tend à augmenter la tension intracellulaire, sans que ce soit forcément un facteur totalement suffisant.

Selon la littérature[15,18], les cellules très étalées sont capables d'exercer une force totale d'adhésion plus importante[18]. Nos résultats indiquent que pour des cellules cultivées dans des conditions d'adhésion identique, le stress contractile intracellulaire (tension cross-linéaire) n'est pas différent entre les cellules très étalée et celles qui le sont moins. On s'aperçoit également en interpolant les résultats du modèle vers les domaines de rigidités de substrat nulles, que la tension cross-linéaire ne s'annule pas et est égale à environ 1 nN/µm. Nous supposons que cette tension par défaut, indépendante des conditions d'adhésion, peut être due au réseau d'actine cortical. Dans le but de tester cette hypothèse, nous avons fait un calcul permettant d'estimer la pression hydrostatique que cette tension cross-linéaire pouvait générer si la cellule venait à se détacher. Nous avons obtenu une pression théorique de 133 Pa. Cette valeur est comprise dans la plage des valeurs de pression intracellulaire mesurées expérimentalement issues de la littérature. Par conséquent, ce résultat soutient l'idée que la structure cellulaire génère en permanence une pression hydrostatique au sein de la cellule.

Modèle conceptuel

D'après mon analyse de la littérature et les résultats des modèles numériques (chapitre 2&3), le modèle conceptuel le plus en adéquation avec la réalité semble être celui de ce que l'on pourrait appeler un hydrosquelette hybride. Ce modèle prend en compte la contractilité du cortex actinien, qui utilise la membrane cellulaire pour confiner et comprimer le cytoplasme. Ce dernier agit comme un liquide interstitiel incompressible. Ainsi le cortex génère une pression hydrostatique qui permet à la cellule de devenir une structure rigide. Le principe de base est identique à celui d'un ballon de baudruche qui devient dur quand il est gonflé, ou plus exactement une bombe à eau bien pleine. En revanche, la structure filamentaire du cytosquelette lui donne des propriétés mécanobiologiques supplémentaires. Par exemple, les efforts mécaniques peuvent transiter via les filaments du réseau d'actine[106], les microtubules[44] et les filaments intermédiaires. Ainsi un stimulus mécanique peut transiter de l'extérieur de la cellule jusqu'au noyau[115,11,38]. Il est également important de considérer que l'interaction mécanique entre le fluide cytoplasmique et le cytosquelette peut donner un comportement inattendu. Le cytoplasme est en effet, un fluide visqueux, mais lorsqu'il est en interaction avec le cytosquelette, le noyau et les organelles, les écarts de pression entre différentes zones cellulaires peuvent mettre un temps important pour se rééquilibrer[123]. Ceci d'après Charras et al. donne à cet ensemble un comportement de type poro-élastique[123].

De plus, le cytosquelette est capable de s'auto-contraindre. Des signes clairs de ce phénomène sont connus, le réseau d'actine est contractile[106,17,141] et les microtubules peuvent supporter des efforts de compression[44]. Le cytosquelette est donc bien une structure précontrainte. La majeure partie des efforts de tension sont générés par le couplage actine-myosine. En revanche, les efforts de compression sont largement contrebalancés par la pression cytoplasmique et la matrice extracellulaire ou le substrat, les microtubules ne supportant qu'une petite partie de la charge totale.

Il y a néanmoins un aspect du cytosquelette que je ne fais que survoler dans ce manuscrit, et qui est la capacité du cytosquelette à s'assembler, se désassembler et à se préparer au fil de l'activité biologique de la cellule. Bien que ce sujet soit très étudié, les principes fondamentaux de ce phénomène restent encore mal compris à ce jour. Comprendre ces principes de base devrait nous donner une meilleure compréhension des raisons pour lesquelles une cellule peut avoir un tel pouvoir de remodelage de sa structure et de son organisation.

Conclusion

Les cellules adhérentes sont capables de percevoir leur environnement et d'adapter leur structure à cet effet. Les différents modèles que nous avons mis en place montrent que les cellules étudiées sont capables de percevoir leur environnement et d'adapter leur structure en fonction de la rigidité du substrat. La littérature indique qu'un substrat rigide tend à augmenter l'étalement cellulaire et la tension intracellulaire. En revanche, l'analyse que j'ai développée dans le chapitre 3 montre que dans des conditions de culture identique, la tension intracellulaire ne semble pas être influencée de manière significative par taille de la cellule. De surcroît, nous avons obtenu un résultat inattendu. Après analyse, il serait possible de distinguer dans le calcul de la tension intracellulaire donné par le modèle, la contribution des fibres de tension, créées au cours de l'adhésion, de celle du cortex actinien. Ceci m'a en partie orienté vers un modèle conceptuel de la structure cellulaire basé sur une architecture d'hydrosquelette hybride.